CONNEXIN EXPRESSION AND THE ROLE OF GAP JUNCTIONS IN AIRWAY SMOOTH MUSCLE CONTRACTION

A Thesis

Presented to the

Faculty of Graduate Studies

of the

University of Manitoba

in partial fulfillment of the requirements

for the degree

Master of Science

In

Physiology

by

Alexander Vörös

March, 2004

THE UNIVERSITY OF MANITOBA

FACULTY OF GRADUATE STUDIES

*****

COPYRIGHT PERMISSION PAGE

Connexin Expression and the Role of Gap Junctions in Airway Smooth Muscle Contraction

BY

Alexander Vörös

A Thesis/Practicum submitted to the Faculty of Graduate Studies of The University of Manitoba in partial fulfillment of the requirements of the degree of

MASTER OF SCIENCE

TABLE OF CONTENTS

ACNOWLEDGEMENTS

I would like to thank to everybody who helped me to complete my theses over the past couple of years. First of all to Dr Andrew Halayko who invested a lot of his time and effort well beyond expected and helped me to enter the world of science on his own way. I will always remember how we sat in the culture hood for hours and he was going through the basics of cell culture with me over and over and showed me the patient side of his nature. He was a starting professor at that time and I was brand new to science. Since than 5 years passed by and we went through a lot of highs and lows, but in a sum we managed to finish my work successfully. . . Andrew thanks for everything again. ...

I want to thank to all my committee members: Dr Newman Stephens, Dr Judy Anderson and Dr Elissavet Kardami, who each participated in my work and development on their own way.

I also want to thank you Dr Nagy, HongWei, Kam, Craig, Lu, Gerry, Mohini, Cheng, Lynn, Carol, Gail, Judy, and to all those people, who I forgot to list here but contributed to my work.

ABBREVIATIONS

ACh	Acetylcholine
AMP	Adenosine monophosphate
ATP	Adenosine triphosphate
BK	Bradykinin
[Ca2+]i	Intracellular free calcium
Cx	Connexin
Cyto TBS	Cytoskeleton-preserving Tris-buffered saline
Cyto TBST	Cytoskeleton-preserving Tris-buffered saline with 0.01% Tween-20
Da	Dalton
DMEM	Dulbecco's modified Eagle's medium
DMSO	Dimethylsulphoxide
EDTA	Ethylenediaminetetraacetic acid
EFS	Electrical field stimulation
EGTA	Ethylene glycol-0,0'-bis-[2-amino-ethyl]-N,N,N',N',-tetraacetic acid
FBS	Fetal bovine serum
GJ	Gap junction
HASMC	Human airway smooth muscle cells
IP3	Inositol-1,4,5-triphosphate
LY	Lucifer yellow
M3R	Muscarinic M3 receptor
NEAA	Non-essential amino acids

PBS	Phosphate buffered saline
PCR	Polymerase chain reaction
Pen-Strep	Penicillin streptomycin
PMSF	Phenylmethylsulfonylfluoride
RIPA	Radioimmuno-precipitation assay
SDS	Sodium dodecyl sulphate
TAE	Tris acetate buffer
TEA	Tetraethylamonium

ABSTRACT

Rationale:

Though increased airway reactivity is a feature of asthma, little is known about the role of myocyte-myocyte interactions in altering responses to contractile agonists. This study builds from an in vitro observation that though only 25% of human airway smooth muscle cells (HASMC) express functional muscarinic M3 receptors (M3R) for the contractile agonist acetylcholine (ACh); paradoxically, in confluent primary HASMC cultures exposed to ACh, virtually all myocytes mobilize intracellular free Ca^{2+} ([Ca2+]i), which is required to initiate smooth muscle contraction. A possible explanation for this phenomenon might be the presence of myocyte-myocyte communication, thus enabling signals induced by cells expressing M3R to spread to neighboring cells, causing release of calcium from intracellular stores. As gap junctions (GJ) are aqueous channels that form a conduit for molecules <1kD to diffuse between cells, the studies for this project were designed to characterize the expression of connexins (protein building blocks of GJs) and their functional role in responses of airway smooth muscle to contractile agonists.

Hypothesis:

Airway smooth muscle cells express a range of connexins that form gap junctions *in vivo* and *in vitro*, and these gap junctions integrate and amplify the response of airway smooth muscle to contractile agonists.

Specific Aims:

1. Establish HASM cell cultures and characterize their M3R expression pattern and responsiveness to ACh.

2. Characterize the expression of connexins and distribution of GJs in HASM in vitro, and determine their role in cell-cell coupling and in integrating mobilization of [Ca2+]i in response to contractile agonists.
3. Characterize the expression of connexins in intact airway smooth muscle and determine their functional role in isometric contraction induced by contractile agonists.

Results:

1. We showed the presence of functional GJ and hemichannels in confluent and subconfluent cultures respectively.
2. Using western blot, immunocytochemistry and or reverse transcriptase polymerase chain reaction (RT-PCR) we demonstrated that connexins (Cx) 40, 43, and 47 are expressed by cultured HASM cells and Cx 40, 43 and 57 in intact bronchial smooth muscle.
3. We observed that GJ are required for ACh-induced mobilization of $[Ca^{2+}]i$ in HASM cells that do not express muscarinic M3 receptors.
4. Using intact equine tracheal smooth muscle strips we observed that GJ are required for the development of maximum isometric force in response to ACh.

Significance:

This is the first study to characterize the profile of connexins expressed by human airway smooth muscle cells *in vitro* or *in vivo*. In addition our studies using cultured HASM cells and intact equine trachealis are the first to demonstrate that GJ play a significant role in determining responses to contracile agonists. These observations are

significant, as they imply that the development of specific inhibitors of GJ as therapeutic agents to reduce bronchospasm in asthma patients may be of merit. The development of novel new therapies for the treatment of asthma is necessary because despite the increasing use of current anti-asthma medications (eg. bronchodilators and/or anti-inflammatory agents) disease prevalence, morbidity and mortality are increasing steadily.

INTRODUCTION AND LITERATURE REVIEW:

Smooth muscle

1. Tissue organisation:

Smooth muscle is found in the walls of blood vessels [1], airways [2], hollow organs such as the stomach and uterus, the iris [3], or associated with the hair follicles. It is not under voluntary control, but displays automaticity. In *multiunit smooth muscle* each cell exists as a discreet independent unit that is innervated by a single nerve ending (e.g. iris in the eye) [3]. Smooth muscle of visceral embryologic origin, such as that found in the circular and longitudinal muscles of the large intestine, is categorized as being *single unit smooth muscle*, as it exists as a sheet or bundle of fibers connected by cell-cell junctions that allow ions and electrical signals to flow freely [4]. Single unit smooth muscles perform as a syncytium, so that when one portion of the smooth muscle is stimulated a biochemical or electrical signal spreads to all other fibers, resulting in an amplification of contractile responses. Intact airway smooth muscle, which is of visceral origin, is of an intermediate phenotype, exhibiting characteristics of both single unit and multi unit smooth muscle.

2. Smooth muscle contraction (Figure 1):

One of the functions of differentiated smooth muscle cells is to contract when activated. Different types of smooth muscle in the body serve to create motion, maintain tone or stabilize shape. In the case of airway smooth muscle there is no clear-cut physiological requirement function; not a single disease state is known in which impairment of airway

smooth muscle contraction or degeneration of the muscle is the underlying cause. In contrast, the excessive contraction of airway smooth muscle is a principal cause of acute bronchoconstriction associated with asthma [5]. Indeed the primary target for reversing an asthma "attack" is to use bronchodilators that target β-adrenergic receptors on airway myocytes leading to relaxation of the muscle. As in skeletal muscle, the basic contractile unit of airway smooth muscle is the cross bridge, which is composed of myosin II and accessory proteins, and its interaction with filamentous smooth muscle actin. The contractile unit has to operate within a cytoskeletal framework that is extensible [6-9], under a continuous state of remodelling [10-15], and is exposed to an extremely unstable and fluctuating load [16-19]. Figure 1 summarizes the primary signaling pathways and proteins involved in the regulation of smooth muscle contraction. Interaction between actin and myosin with the subsequent hydrolysis of ATP by the myosin head is the basic chemical reaction leading to muscle contraction [20].

The first event involved with pharmaco-mechanical coupling in airway smooth muscle is the interaction of a contractile agonist (eg. ACh released by parasympathetic nerve terminals) with its cognate receptor (eg. the M3R for ACh) [21]. Many receptors, such as M3R are coupled with signaling effectors via trimeric G-proteins composed of α, β, and γ subunits [22]. Upon ligand binding M3R, which is coupled to trimeric G-proteins of the $G\alpha_{q/11}$ sub-family, induces activity of phospholipase Cβ, which generates second messengers including IP_3 and diacylglycerol [22]. IP_3 binds to IP_3 receptors on the sarcoplasmic reticulum resulting in Ca^{2+}-activated release of Ca^{2+} from stores in the

sarcoplasmic reticulum [23]. Once $[Ca^{2+}]i$ increases above ~400nM sequential binding of calcium ions to each of four binding sites on the regulatory protein, calmodulin, occurs [24]. This calcium-calmodulin complex then binds to myosin light chain kinase (MLCK), which leads to catalytic activation of MLCK [20]. MLCK phosphorylates regulatory myosin light chains (MLC) near the myosin head, thereby evoking a conformational change in the head that increases the ability of actin to activate myosin-Mg^{++}-ATPase and causes the hydrolysis of ATP bound to the myosin head [25]. At the beginning of the cross bridge cycle the myosin head with ATP is detached or weakly attached to actin. ATP hydrolysis by Myosin (Mg.ATPase) leads to an intermediate with the products of hydrolysis still bound to it (myosin.ADP.Pi), which is detached or weakly attached to actin [25]. By releasing Pi from the myosin complex the binding between actin and myosin changes from weak to strong and the angle of the myosin head changes from 90 to 45°. The strain on the cross bridge caused by the angle is relieved when actin slides past cross bridge. ADP is slowly released, and then the myosin head rebinds ATP and reverts to 90° angle facing the next actin molecule [26].

Asthma

Asthma is one of the most prevalent chronic diseases affecting Canadians. It afflicts 6.3% of adults and 12.2% of children [27]. Asthma by the newest definition is: "a disorder of the airways characterized by paroxysmal or persistent symptoms (dyspnoea, chest tightness, wheeze and cough), with variable airflow limitation and airway hyperresponsiveness to a variety of stimuli" [28]. Asthma is a chronic disease in which airflow in and out of the lungs may be blocked by contraction of airway smooth muscle

that encircles the airways, airway wall swelling and excess mucus secretion. The exact cause of asthma is unknown, though there is a suspected interaction of three factors:

a) ***Predisposing factors*** such as atopy (higher tendency to respond to allergens), gender (young boys tend to develop asthma more often than young girls, with adulthood this imbalance reverses), genetics (asthma is more common in families where at least one parent has asthma) [28].

b) ***Causal factors***, which may sensitize the airways, such as indoor allergens (house dust containing domestic dust mites, animal denders of animals like cat and dog, cockroach allergen, and fungi), outdoor allergens (pollens and fungi), and occupational sensitizers (exposure to work-related agents) [28].

c) **Contributing factors** such as respiratory infections (viral respiratory infections do not cause asthma early in life, but may be an exacerbating factor), air pollution (it is not causing asthma by itself, but may trigger an asthma attack). Other contributing factors include outdoor pollutants as industrial and photochemical smog, indoor pollutants from cooking, heating sources, materials used in building construction and furnishings, and tobacco smoke. Passive smoking, (i.e. inhalation of second hand smoke) is especially irritating to the respiratory system. Socio-economic status is also related to asthma incidence (asthma is more prevalent in low-income adults over 35 years of age) [28].

The diagnosis of asthma is not straightforward, because the symptoms may mimic other respiratory diseases. According to the Canadian Asthma Consensus Conference Guidelines for Asthma Management, diagnosis should be based on: 1) the presence of

typical symptoms (coughing, sneezing, chest tightness, shortness of breath) that improve with asthma medication, 2) objective evidence of variable airflow limitation and/or obstruction (low peak readings, taken with a peak flow meter), and 3) evidence of hyperresponsiveness of the airways using a provocative challenge. Patients with asthma may respond to factors in the environment, called triggers, which do not affect non-asthmatics. This is defined as hyperresponsiveness. Hyperresponsiveness leads to a state of reversible increases in bronchial smooth muscle contraction, and variable amounts of inflammation of the bronchial mucosa. In response to a trigger, an asthmatic's airways become narrowed and inflamed, resulting in wheezing and/or coughing symptoms. During an acute asthma attack, the already-inflamed airways narrow further due to bronchospasm, which leads to increased airway resistance. Because of the increased smooth muscle tone during an asthma attack, the airways also tend to close at abnormally high lung volumes, trapping air behind occluded or narrowed small airways. Thus the acute asthmatic will breathe at high lung volumes, his functional residual capacity will be elevated, and he will inspire close to total lung capacity. The accessory muscles of respiration are often used to maintain the lungs in a hyperinflated state.

There are a number of hypotheses for the development of airway hyperresponsiveness. One hypothesis is that airway remodelling due to chronic airway inflammation may contribute to progression of airways hyperresponsiveness [29-31]. This hypothesis suggests, that no change in the intrinsic properties of airway smooth muscle is required, in particular relating to the responses to contractile agonists and to bronchodilating

agents. Airways remodelling is characterized by airway wall thickening associated with epithelial damage, submucosal fibrosis with increased numbers of submucosal myofibroblasts, mucous gland metaplasia, and increased smooth muscle mass [32-37]. Other hypotheses suggest that airways inflammation can affects airway responses to spasmogens responses directly [38]. In addition it has been suggested that there is abnormal beta-adrenergic receptor adenylate-cyclase function with decreased adrenergic responsiveness [39], and/or that increased cholinergic activity in the airway is the fundamental defect in asthma [40]. Based on these diverse hypotheses it is likely that for a given asthma phenotype multiple biological factors contribute to disease development and severity.

The changes noted above that occur in the airways are directly or indirectly related to the focus of the present project. Increased amount of smooth muscle is a well-known feature of the remodeling process in asthma. It is not entirely clear what causes this increase in smooth muscle mass but both cellular hypertrophy and hyperplasia have been proposed [41, 42]. In one study [42] morphometry revealed that structural changes in the airways of asthmatics are characterized by two different patterns of airway smooth muscle growth. In "type I" asthma there was an increased smooth muscle mass mostly in central airways that was attributable to hyperplasia of smooth muscle cells. In "type II" asthma there was a diffuse airway smooth muscle mass increase throughout the airways due to hypertrophy of smooth muscle cells. In these "type II" patients the hypertrophy was mostly localized to the smaller bronchi, but there was no clinically detectable difference between the two groups of patients.

Myofibroblasts have features of both fibroblasts and myocytes. They possess both, the synthetic apparatus of fibroblasts and the contractile apparatus of smooth muscle cells. It is well known that in tissues undergoing reparative processes the number of myofibroblasts is increased [43-45]. As one would expect under the chronic airway inflammation associated with asthma, the number of myofibroblasts is greatly increased in the submucosa. This increase correlates with the increased thickness of the lamina reticularis [46, 47]. From where these cells are derived is not known [48]. Appearance of myofibroblasts is very fast after antigen challenge, with up to 40-fold greater number of the cells appearing within 24 hours of allergen challenge in human asthmatics [49]. This suggests the possibility for the existence of a quiescent precursor cell that responds to certain stimuli to acquire the markers of a myofibroblast without undergoing cell division. Precursors may be resident stromal cells such as fibroblasts or airway smooth muscle cells, and there is a recent report that myofibroblasts can be derived from CD34+ circulating fibrocytes [50]. Of note, inhaled steroids used in treatment of asthma may reduce the number of myofibroblasts in the submucosa [51].

A number of investigators have reported changes in the innervation of the airways with remodelling. For example, the loss of nerves containing vasoactive intestinal peptide (VIP) and an increase in fibers containing substance-P has been described [52, 53]. VIP is a bronchodilator, whereas substance P-containing fibers are bronchoconstrictors [54-56]. Cytokines such as interleukin (IL)-4 and IL-6 also appear to have modulatory effect on innervation. IL-4 is increased in the bronchial fluid from asthmatics, and the cytokine modulates the cholinergic control of intestinal smooth muscle [57]. IL-6 stimulates cholinergic differentiation and production of tachykinins by nervous tissue [58].

Physiologic significance of airway remodelling is hard to dissect from the more direct effects that the inflammation has on airway smooth muscle and its response to contractile stimuli in asthma [59]. Of note, some studies have shown that airway hyperresponsiveness can be induced without airway remodelling [60]. Also cytokines increase airway smooth muscle responsiveness to contractile agonists in vivo as well as in vitro [61, 62].

Gap junctions (GJ)

1. GJ – IN TISSUE - FUNCTION:

Intercellular coordination is a basic feature in tissues of multicellular organisms yet diverse unrelated gene families fulfill this function in vertebrate and invertebrate organisms (Figure 2). An important structure ensuring this coordinated signalling between cells are gap junctions (GJ) that couple adjacent cells. GJs provide a direct pathway for cell-cell communication [63, 64]. They are also implicated in regulation of growth, transmission of developmental signals, coordination of muscle contraction, and maintenance of metabolic homeostasis. Gap junctions are complex in terms of both their structure and their activity.

GJ are membrane channels specialized to provide intercellular cytoplasmic communication. These make it possible for small molecules (< 1000 Da) to diffuse and therefore to be exchanged between the cells. Gap junctions allow electrical and biochemical coupling between cells. Signals initiated in one cell can readily propagate to numerous neighbouring cells, perpetuating the response to the initial stimulus. Important examples of molecules that readily pass through GJ include ions [65], cyclic

AMP (329 Da) [66], inositol-1,4,5-triphosphate (420 Da) [67] and nucleotides (250-300 Da) [68].

2. GJ – STRUCTURE - FUNCTION

2.1. Connexins

The protein building blocks of gap junctions are the connexins [63]. Different species of connexin are seen in different organisms and among different tissues within an organism. There are over 20 different connexins described up to date [69], and they range in size from 25 kDa and 60 kDa. Connexins have four transmembrane domains, two extracellular and one intracellular loop, and cytoplasmic amino- and carboxyl-terminal domains. The extracellular and the transmembrane domains are highly conserved as opposed to the cytoplasmic domains that are the sites where regulation by phosphorylation occurs [70] [71].

2.2. Hemichannels

Hemichannels, also called as connexons, are formed out of six connexin subunits. Depending whether the subunits are the same type of the connexin or a mixture of different types of connexins we are talking about homo-oligomeric and hetero-oligomeric hemichannels respectively. After the hemichannels are assembled in the cytoplasm the hemichannels travel towards the plasma membrane where they, based on one of the theories, secondary to high sub plasma membrane calcium levels become closed [72]. They are then randomly inserted into the plasma membrane after which

they migrate to regions where two cells are in contact to form functional GJ [73]. Studies showed that hemichannels in heart are generally in a closed state secondary to normal extracellular calcium concentration because they are phosphorylated at the C-terminus under MAPK signalling pathway regulation [74]. Upon dephosphorylation the hemichannels open allowing extracellular ions to flux into the cell, which can be lethal for the cell.

2.2. GJ structure

Gap junctions are seen under an electron microscope as dense patches of varying size in many excitable tissues (fig. 18) [75]. At the site of GJs the plasma membranes of neighboring cells are separated by a 2-3 nm wide uniform gap. GJ are formed through the interaction of connexons (connexin protein hexamers) from adjacent cells. They form aqueous pores roughly 2 nm in diameter between two cells. Ultrastructural analysis by freeze fracture electron microscopy shows that gap junctions are aggregates of tight channels creating characteristic two-dimensional sheets that are structurally distinct from other clusters of particles also present in the plasma membrane [76]. SDS – fracture labeling under electron microscope provides evidence that the connexin oligomers exist as dispersed entities [76]. This observation is in agreement with the hypothesis that junctions are created by the aggregation of connexons already present in the lipid bilayer [77, 78].

2.3. GJ function

Gap junctions are seen in virtually all cell types in mammals with few exceptions like circulating erythrocytes, spermatozoids and adult innervated skeletal muscle cells [79]. In the regulation of numerous critical physiological processes they play a principal role that can be categorized into two broad functional classifications. First, electrical coupling; gap junctions serving this function are abundant in cardiac and smooth muscle. Depolarization of one group of muscle cells is rapidly spread to adjacent cells, leading to well-coordinated contractions of those muscles [78, 80]. Second, metabolic or "biochemical" coupling; many hormones act by elevating intracellular concentrations of cyclic AMP, which initiates intracellular signalling pathways. Cyclic AMP readily passes through gap junctions and thus, hormonal stimulation of one cell can lead to signal propagation to a cluster of cells.

A key area of study in the field is the identification of the molecules transferred via GJs and the biological processes they influence. In excitable cells, GJs conduct the spread of electrical excitation. The role of gap junctions in non-excitable cells is very unclear. However the evidence of some disease related connexin deficiencies in humans and targeted disruption of connexin genes in mice indicate the importance of these proteins. For example connexin 26 gene mutations are linked to non-syndromic deafness in humans [81-83]. Mutations within the connexin 32 genes are associated with the x-linked peripheral nerve disorder Charcot-Marie-Tooth Syndrome [84-86]. Junctional communication is also important during embryonic development. Connexin 26 [87] and connexin 45 knockout mice die in utero [88], connexin 37 knockout female mice are infertile [89], and connexin 43–deficient mice die shortly after birth from malformation of

the heart [90]. Lack of connexin 46 and connexin 50 function appears to be important in the development of cataracts [91]. Connexins can also have tumor suppressive properties [92].A number of pathologies are known where communication between cells is disrupted by modification of connexins. These proteins of gap junctions thus emerge as therapeutic targets and connexin mimetic peptides, which correspond to specific short sequences in the two extracellular loops of connexins, have been studied recently for relaxing arterial smooth muscle [93].

Cell-to-cell communication has been investigated in many cell types including cardiomyocytes [94], respiratory tract ciliated cells [95, 96], neurons [97], glial cells and cell lines [98-101], smooth muscle cells [102], osteoblastic cells [103], chondrocytes [104], mast cells [105], insulinoma cells [106], PC12 cells [107], lens cells [108], and hepatocytes [109]. Though there has been little investigation of GJs in airway smooth muscle tissue, the role gap junctions have been well described in certain smooth muscle types including the myometrium [110-113], and the gastrointestinal tract [114-117]. Studies looking at GJ in the myometrium showed that Cx expression was dramatically increased during pregnancy leading to increased capacity for synchronous contractions required for childbirth [110-112]. Studies in the GI tract showed the requirement of GJs for coordinated control of intestinal motility [115, 116]. Some studies of GJs in vascular smooth muscle have been reported, and these reveal that the integration and coordination of responses among vascular cells are critical to local modulation of vasomotor tone and to the maintenance of circulatory homeostasis [118]. Moreover there is evidence for an important role of intercellular communication via GJ

to vascular function at all levels of the circulation, from the largest elastic artery to the terminal arterioles [119-121].

3. GJ IN SMOOTH MUSCLE

Earlier GJ were thought to be not an important part of smooth muscle cell communication because without being able to demonstrate the presence of visible GJ in smooth muscle cells there was an obvious electric coupling demonstrated [122]. In recent days its clear that GJ are the structural correlate of electrical coupling and the structure responsible for metabolic coupling in all types of smooth muscle [123-125]. Smooth muscle cells are responsible for wide variety of function that are required for proper functioning of the hollow organs as the airway, digestive tract, blood vessels, urinary and genital tract. In all these cases GJ play an important role in coordinating the proper action (contraction, relaxation) [126]. GJ were previously shown to be present in smooth muscle in intestines [127], bladder [128], corporal smooth muscle [128, 129], uterus [130], and blood vessels [131] just to mention a few. In intestinal smooth muscle the GJ are crucial in maintaining proper peristalsis that propels the nutrients. GJ can be found in different layers in the small intestinal wall (circular muscle cells, between interstitial cells of Cajal of deep muscular plexus and between them and adjacent outer circular muscle). In colon GJ are found between intestinal cells of Cajal and between them and circular muscle cells [127]. In the case of the bladder smooth muscle GJ are the key players in detrusor smooth muscle contraction and secondary the bladder emptying [128]. In the case of corporal smooth muscle the GJ play an important role in penile erectile function [128, 129]. In the uterus there is an increase in GJ number

before delivery and is necessary for normal parturition [130]. GJ are important in maintaining proper tone in blood vessel walls. The major GJ expressed in the blood vessel smooth muscle is Cx43, but Cx 40 was also described to be present and they seem to be more directed towards cell-cell coupling reduction than enhancement [131].

4. GJ IN AIRWAY SMOOTH MUSCLE

There is no report describing gap junctions or the expression of connexins in human airway smooth muscle. Interestingly, early studies using tetraethylamonium (TEA) revealed that TEA significantly increased the distance where the spread of the membrane potential was detectable in cultured canine airway smooth muscle cells [132]. This study indicates that the number of cells stimulated by the same stimulus increased more than 16 times after TEA exposure. In 1978 [132] it was shown by electron microscopy that TEA appears to increase the number of GJ within 1 hour and that this increase could be blocked using cyclohexamide to inhibit *de novo* protein production. Since these observations were reported no other reports further investigating this phenomenon exists [132-134].

5. GJ – PRODUCTION, AND REGULATION (Figure 3)

Both the translocation of proteins (including connexins) across membranes and their intracellular trafficking are basic processes that appear to be nearly identical in all eukaryotic cells [135]. Gap junction channels are oligomeric protein structures. Therefore the connexin subunits have to assemble before they can function. The

integration process of connexins has primarily been investigated using cell free models supplemented with membrane vesicles derived from endoplasmic reticulum [136, 137]. Recent results obtained by studying the assembly and intracellular transport of connexins indicate that assembly in the endoplasmic reticulum may indeed be necessary for the further transport of connexons towards the plasma membrane [138, 139]. Connexons are hexameric structures formed of six connexins. Two connexons of two adjacent cells if joined are called a gap junction.

How gap junction connexons (also termed gap junction hemichannels) are directed to and assembled in the plasma membrane is the topic of intense current research [140-143]. Two different pathways have been proposed. First, the connexons may be transported directly to the site of functional junction formation. Second, they are inserted somewhat randomly into the plasma membrane, and then are transported by lateral movement to the junctional site. Recent results obtained by imaging the assembly of gap junctions in live tissue culture cells support the latter view [138]. This hypothesis is supported by the presence of gap junction connexons in the plasma membranes of cultured cells. How the connexons (also called as hemichannels) in the membranes of apposed cells register with each other is unknown [78], but they are believed to connect via interactions of the extracellular loop domains of the connexin subunits[138]. Assembly of connexins into gap junction channels is complex. Homo-oligomeric connexons (hemichannels) composed of only one connexin isotype are believed to prevail in vivo. Also by studying connexin assembly in cell-free systems it is believed that different connexin isotypes do not assemble in random order, but interact

selectively [136]. It appears that only homo-oligomeric (formed of identical subunits) and distinct sets of hetero-oligomeric connexons (formed of non-identical connexin subunits) assemble to form GJ. This specificity suggests that an assembly signal may be located in the C-terminal portion of the connexin polypeptides. The selectivity signal is located in the amino-terminal (first transmembrane or first extracellular unit) and likely regulates the specific assembly of either homo- or hetero-oligomeric connexons [136].

The diversity of gap junctions is further broadened by the possibility that connexons assembled from divergent connexin isotypes expressed in adjacent cell types can assemble into heterotypic gap junctions (containing of non-identical connexon subunits as opposed to a homotypic GJ that is formed from identical connexon subunits). This has been suggested by both in vitro experiments using culture cells that express different connexin isotypes [144] and by in vivo experiments characterizing gap junctions between different cell types of the central nervous system [145] or the eye [146]. The availability of cDNAs encoding autofluorescent proteins, such as green fluorescent protein, allows observation of the behavior of the expressed proteins in live cells. Tagging connexins with autofluorescent tracer proteins and the use of deconvolution microscopy has allowed studying gap junctions in living cells, their structure, assembly, and degradation [147]. Results suggest that co-expressed connexins sharing the same characteristics assemble into heterotypic channels, while co-expressed connexins with different characteristics arrange only to well separated homotypic channels [138]. Future studies need to elucidate the multiple functions that diverse gap junctions may have.

The degradation and turnover of gap junctions can range between 2 and 5 hours. In cardiac cells as fast as 1.3 hours [148]. Time-lapse recordings demonstrate that gap junctions are highly mobile and dynamic structures. The individual channels are turned over constantly by newly inserted or removed ones [148]. This dynamic change is an adaptation to the function of gap junctions that allows quick response to the changing requirements of cells and tissues [138]. The activity of gap junctions is influenced by posttranslational modification of the connexins. Although phosphorylation is one of the most common modifications, intramolecular disulfide bonds also can be formed [91]. Phosphorylation most commonly occurs on the carboxyl termini of the connexins, which together with the amino termini are located in the cytoplasm of the cells [148-150]. Phosphorylation can also occur on the cytoplasmic loop too as it was shown in the case of Cx56 [151]. Phosphorylation is not the case for all connexins. Cx26 was shown not to be phosphorylated in a couple of experiments [152, 153]. In the case of Cx43 a couple of sites of phosphorylation were identified [150, 154-160]. Immunoblotting is a very good technique to detect various states of phosphorylation, hovever some states of phosphorylation do not show up with this method [161]. Phosphorylation affects the gap junctions in different ways depending on cell type and Cx type [151, 152, 155, 156, 159-166]. Phosphorylation of Cx 43 on serine residues might be responsible for the process of connexin insertion into the plasma membrane [165], degradation, conductance and closure [159, 160, 166]. Phosphorylation of tyrosine residues on Cx43 is associated with the decrease in intercellular coupling [167, 168]. Recent data suggests phosphorylation of serines in the C-terminal intracellular domain of connexin 43 [169] and connexin 45

[170] is a key determinant of the open-closed state of GJs. Furthermore phosphorylation of specific serine sites or a tyrosine site in connexin 43 attenuates gap junction communication by a conformational change in the connexin protein [91].

Elevated intracellular calcium in the vicinity of GJ is established stimuli for rapid closing of connexons [72, 171]. This shows us how much dynamic and how well controlled GJs are. These rapid conformational changes are reversible. This may be of importance when one cell within a group becomes damaged, where extracellular ions are poring into the cell and as a result closing gap junctions of a damaged cell would effectively isolate that cell and prevent spreading of signals triggered by the injury. There are two theories how calcium ion concentration can cause opening and closure of GJ. In the first one as the connexins are formed and are located in the sub plasma membrane region where the concentration of calcium is (~5uM) they assume a closed state that only opens after two hemichannels of two jucstaposed cells dock together and form a micro domain where the calcium concentration is low and more favourable for an open state [172]. In the second theory the constant relatively high calcium concentration in the sub-plasma membrane level favours the closed state of the GJ [72]. In this model and additional protein is associated with regulating the opened and closed state of the gap junction.

The open or closed state of GJ can also depends on the pH, cAMP and voltage.

Many studies aimed at understanding the physiological role of GJs have employed a range of pharmacological agents that appear to have the ability inhibit diffusion of

chemical signals through GJs. As several of these inhibitors are used in experiments of the present project, a list of the most extensively studied gap junction inhibitors is included in Table 1 [93].

TABLE 1: Pharmacological Inhibitors of Gap Junctions

Type of GJ inhibitor:	**Proposed mechanism of action:**	**Reference:**
Aliphatic Alcohols e.g. - Octanol - Heptanol	Disrupts lipids surrounding GJ leading to closure	[173, 174]
Anesthetics e.g. – Halotahane	Disrupts lipids surrounding GJ leading to their closure	[95, 175]
Anadamine	Depletes calcium stores	[95, 175]
18α- Glycirrhetinic acid	Dephosphorylation of connexin 43 and GJ closure	[176-181]
Oleamid	Mechanism is obscure; it may be connected to the chemical structure as a lipid solvent	[174, 182]
Tamoxifen	The mechanism of action of this antitumor drug is unknown	[183, 184]
Ouabain	The mechanism of action of involves dephosphorylation of connexins and perhaps changes in intracellular sodium	[185]
anti-peptide antibodies	An alternative approach involves direct binding of anti-peptide antibodies to exposed connexin sequences	[186-188]
Connexin mimetic peptides	Short synthetic peptides corresponding to chosen sequences in the two extracellular loops of natural connexins. Their proposed mechanism of action is channel gating and/or gap junction assembly	[176, 177, 186-196]
Fatty acids as arachidonic acid, oleic acid and lipoxygenase metabolites	Probably interact with lipid-protein interactions in gap junctions	[197, 198].
Chemical reducing agents	Dislocate connexin extracellular disulphide bridges	[191, 199]

6. SIGNAL PROPAGATION BETWEEN CELLS

There are two different ways a calcium wave can propagate from cell to cell, both of which involve release of inositol triphosphate (IP_3) [67, 200]. In the case of GJ, IP_3 goes through GJ and initiates the intracellular release of calcium from the sarcoplasmic reticulum [201]. The studies in the present project are designed to test the relevance of this model in cell-cell communication in airway smooth muscle. A second model for the propagation of calcium waves between cells involves paracrine activity of secreted ATP on P_2 purinergic receptors [105, 106, 202]. Upon the intracellular release of calcium in one cell ATP is released into the extracellular environment, thereafter the secreted ATP binds purinergic receptors on neighboring cells, thus inducing intracellular calcium mobilization in the target cell [203-205].

RATIONALE, HYPOTHESES & SIGNIFICANCE

According to the 1996-97 National Population Health survey, physicians diagnosed more than 2.2 million Canadians with Asthma. Considerable amounts of money and effort are invested in asthma research and developing new treatments of these patients. Therefore research directed toward understanding the underlying pathophysiology and toward the development of new management and treatment technique is highly warranted. The most dangerous and troublesome part of this chronic inflammatory disease of the airways is the contraction of airway smooth muscle that creates acute airway obstruction known as an "asthma attack". This causes dyspnea, creating distress for the patient, and in severe cases can lead to death. In addition to acute bronchial spasm a marked increase of smooth muscle mass develops in the airway of asthmatics, further accentuating breathing difficulties and underscoring the primary contribution of ASM to disease morbidity.

Gap junctions have the potential to contribute to the development of airways hyperresponsiveness by increasing the number of myocytes that contract in response to stimulation with a contractile against. A well-described example of how changes in GJ activity can affect contractile responses of smooth muscle comes from studies of the myometrium, which provides strong synchronous contractions of the uterus during labour. Increased contractile activity is dependent on electrical coupling of myometrial smooth muscle cells via GJs [110, 206]. The number of GJs in the myometrium increases dramatically in late pregnancy, leading to a functional conversion of the whole muscle organ from a multi-unit to a single unit type [207]. The possibility that GJs could

play an important role in contraction of airway smooth muscle tissue is further supported by observations that innervation to the airway smooth muscle in bronchi is relatively sparse, suggesting that bronchial smooth muscle may exist more-or-less as a single unit muscle (Figure 4) [208].

Our group has reported a novel canine tracheal myocyte primary cell culture system that employs prolonged serum deprivation to induce acquisition of a functionally contractile phenotype in a subset (~15%) of myocytes [21]. Contractile myocytes re-expressed functionally coupled muscarinic M3 receptor (M3R) and mobilized $[Ca2+]_i$ upon exposure to exogenous ACh [21, 23]. These contractile myocytes became organized into 5-10 cell wide bundles coursing through cultures. Of note, Lucifer yellow, a water soluble low molecular weight fluorescent dye, microinjected into a single contractile myocyte diffused into adjacent cells within minutes, suggesting the existence of junctions facilitating cytoplasmic coupling [21]. Further investigation of the nature of these junctions and of their possible role in regulating responses of contractile myocyte to exogenous mediators have not been completed.

Based on these observations we proposed to develop a prolonged serum-free cell culture system with primary cultured human airway smooth muscle cells, and to investigate the nature of cell-cell coupling between contractile myocytes. **Thus, we tested the hypothesis that airway smooth muscle cells express a range of connexins that form gap junctions *in vivo* and *in vitro*, and gap junctions integrate and amplify the response of airway smooth muscle cells to contractile**

agonists. To test this hypothesis we proposed three *Specific Aims: 1)* to establish HASM cell cultures, and characterize the expression pattern of M3R and responsiveness to ACh, 2) to characterize the expression of connexins and distribution of GJs in HASM in vitro, and determine their role in cell-cell coupling and in integrating mobilization of [Ca2+]i in response to contractile agonists, and 3) characterize the expression of connexins in intact airway smooth muscle and determine their functional role in isometric contraction induced by contractile agonists.

The chief questions we will address have received little previous attention despite the fact that all cells are known to express gap junction proteins (connexins), and that there is ample evidence that changes in gap junction number during development or in response to inflammation greatly affects contraction of visceral and vascular smooth muscle [209]. Based on several studies in the late 1970's indicating TEA increase cell-cell in canine tracheal smooth muscle and evidence from electron microscopy studies there is an indication that gap junctions are present in airway smooth muscle [132]. However there are no systematic studies of the connexins expressed by human airway smooth muscle, neither coupling between airway myocytes through GJs *in vitro* or *in vivo* been reported. Moreover, the contribution of GJs to contractile function of intact airway smooth muscle, or whether inflammatory mediators associated with asthma affect function and expression of GJs in airway smooth muscle is unknown. As smooth muscle is not only present in the airways, but is also in many other organs and can play a primary role in disease, our studies have potential for broad impact in understanding disease pathogenesis in organs containing smooth muscle. For example, these

disorders include hypertension akinetic or hypercontractile uterus, hyper- or hypo-motility of the GI, and irritable bowel syndrome.

METHODS

DISSECTION AND TISSUE CULTURE:

PRIMARY CELL CULTURE: Segments of central bronchi of uninvolved lung specimens from patients undergoing partial lung resection for cancer were acquired as per protocols approved by the Human Ethics Committee of the University of Manitoba. A pathologist in the operating room confirmed the disease-free state of the bronchial specimens. Typically bronchial segments were 0.5-1 cm diameter and ~ 0.5 cm long. The samples were stored and transferred to the laboratory in cold (4°C) HBSS (KCl 5.36 mmol/L, KH_2PO_4 0.44 mmol/L, $Na(CO_3)$ 4.17 mmol/L, NaCl 136.9 mmol/L, $K_2H(PO_4)$ 0.336 mmol/L, D-glucose 5.55 mmol/L) kept on ice. Bronchial rings were cut open rinsed in HBSS and pinned down with the epithelial surface facing up to a dissecting dish. The specimens were submersed in HBSS containing penicillin (5 IU/ml)/streptomycin (5 IU/ml) (Pen-Strep) and HBSS was bubbled with 5% carbon dioxide and 95% oxygen. All dissection instruments were rinsed with 70% ethanol. The epithelium was rubbed off gently with a sterile Q-tip. Thereafter the submucosa and bronchial muscle was removed using fine surgical scissors under a binocular dissecting microscope. The smooth muscle strip was then pinned down with the adherent adventitia facing up, and the later was removed by fine dissection. The cleaned muscle sheet was then washed 3x10minutes in HBSS containing 2x Pen-Strep in a sterile hood. Muscle was then minced with sterile scissors and resulted in 4ml of dissociation solution: (600 U/ml Collagenase, 1U/ml Elastase, 2-3 U/ml Protease), for ~1 hours at 37°C with vigorous shaking. Remaining tissue was then disrupted by gentle trituration with a borosilicate Pasteur pipette. The cell suspension was then mixed with

proliferating culture media an equal volume of DMEM containing 20% FBS and Pen-Strep and centrifuged at 600-800 x g for 5 minutes. The cells were resuspended in DMEM/20% FBS/Pen-Strep and were plated at 10,000/cm^2 or in tissue culture treated plates. Culture dishes with cells were placed into a humidified incubator (37°C, 5% CO_2/95% air). After 96 hours media was changed to DMEM/10% FBS/Pen-Strep and thereafter media was changed every 2 days until confluence was reached then serum-containing growth medium was replaced with serum-free media (Ham's F-12 supplemented with insulin (5µg/ml) – transferring (5 µg/ml) - selenium (5 ng/ml) that contained 0.1 mM non-essential amino acids (NEAA) and Pen-Strep. Serum free media was replaced every 2 days. Where necessary cells were passaged at confluence (prior to serum deprivation) by lifting the cells with 0.05% trypsin-0.5 mM EDTA, and replating in new culture dishes in a ratio of 1:5 using DMEM/10% FBS/PenStrep. In all studies cells from passage 3-6 were used. Some cells were stored frozen and stirred before being replated. The freezing procedure consists of lifting the cells with 0.05% trypsin-0.5 mM EDTA, centrifugation (600xg/5 min) to pellet cells, then the cells were resuspended in 90%FBS+10%DMSO using a volume that resulted in a final cell density of 1.8million cells/ml. Cells were than immediately put into cryo-vials and quickly submersed in ice; after 30 minutes the vials were cooled to –70 degrees in a freezer, and after 16-20 hours they transferred to liquid nitrogen for long term storage (up to 1 year). To replate frozen cells in culture, vials were thawed rapidly by warming with hands, the cells were diluted in ~5 volumes of DMEM/10% FBS/Pen-Strep and replated at 10,000 cells/cm^2.

IMMUNOCYTOCHEMISTRY

Cultured cells were grown on coverslips in multiwell culture dishes. At required times the cells were washed three times with warm 37°C phosphate buffered saline (PBS) (2.7 mM KCl, 1.2 mM KH_2PO_4, 138 mM NaCl, 8.1mM Na_2HPO_4, pH 7.4), then fixed with 4°C cold 3% paraformaldehide in PBS (pH 7.6) for 20 minutes cells were then permeabilized with cold 3% paraformaldehyde in PBS + 0.3%Triton X-100 for 5 minutes at 4°C. Coverslips were then rinsed with PBS and stored submerged at 4°C for up to 1 month. Prior to labelling fixed cells they were blocked by incubating in cold cyto-TBS (Tris 20 mM, NaCl 500 mM, EGTA 2mM, MgCl 0.4mM) containing 5% serum (the species of serum was matched to that of the secondary antibody) for 20 minutes. Before applying the primary antibody (Table 2) coverslips were rinsed one time with cyto-TBS. Then coveslips were turned face down onto 20μL of primary antibody diluted appropriately in cyto-TBS containing 0.1% tween-20, that was placed on a piece of hydrophobic parafilm. Cells were incubated with primary antibody overnight at 4°C in a humidified chamber. After incubation cells were washed three times with cyto-TBST then incubated with appropriate secondary antibodies (Table 2) for 2 hours at room temperature in dark humidified chamber. Thereafter, coverslips were rinsed 3 times with cyto-TBS. Some cells were then labeled with 5 μg/mL propidium iodide to stain nuclei. Finally after rinsing in ddH_2O coverslips were mounted cell side down on microscope slides using ProLong Antifade mounting medium (Molecular Probes, Eugene, OR). Slides were stored at room temperature up to 1 month before imaging with an Olympus IX70 inverted confocal microscope with Nomarski DIC optics to evaluate staining.

Images were analyzed with the FluoView software. For all experiments samples were prepared in triplicates from three different cultures.

ANTIBODIES USED IN EXPERIMENTS

	Type	Source	Dilution Cytochemistry	Dilution Western
anti M3R	Rabbit polyclonal	Gift from Dr Jurgen Wess	1:250	
anti Cx43 18A-9	Rabbit	Gift from Dr Jim Nagy	1:500	1:50,000
anti smActin (1A4)	Mouse IgG2a	Sigma	1:100	
anti smMyosin (hSMv) M-7786	Mouse IgG1	Sigma	1:500	
anti B2 Bradykinin BXX820	Mouse		1:100	

SECONDARY ANTIBODY TABLE

Fluorescent dye	Type	Dilution
FITC	Goat-anti-rabbit IgG 0.75 ug/mL	1:100
CY3	conjugated affinitu pure donkey-anti-mouse IgG (H+L)	1:100

MEASURING INTRACELLULAR FREE CALCIUM ($[CA^{2+}]_I$):

Mobilization of free $[Ca^{2+}]_i$ was measured using fura-2 loaded cells grown on glass coverslips that were 25 mm in diameter and No. 1 thickness. Cells were loaded with fura-2 by incubation in HBSS/0.1% BSA/10μM fura-2 AM for 60 minutes at 37°C. Cells were then washed with 37°C HBSS/0.1% BSA and left submerged in the dark at room temperature for a further 30 minutes. Coverslips were then placed into a modified Sykes-Moore chamber and mounted on an Olympus IX70 inverted microscope equipped with an Olympus-LSR Calcium ion digital system, including an Olympix Interline 12-bit CCD camera and UltraView computer software. An Olympus x20/0.75

objective was used for all studies. Cells were alternately exposed to excitation light for 100-400 msec using 340 and 380 nm, with Sutter Filter system; emitted fluorescence (510 nm) was acquired for ~ 400 msec at each excitation wavelength and used to calculate calcium concentrations (nM) from an in vitro calibration curve of known free Ca^{2+} (0 to 1.35 μM) that had been determined for the system. During experiments an equal volume of buffer containing twice the desired concentration was pipetted into the Sykes-Moore chamber to ensure rapid mixing in the chamber. In all experiments, myocytes were exposed to Ach (10^{-6}) and responses were compared in up to 120 (average ~70) individual cells per coverslip.

To make quantitative assessment of data from Ca^{2+} studies, a calibration procedure was used for the calcium system. This allowed for the conversion of light detected by the camera as gray scale ratios into $[Ca^{2+}]_I$ in mM. For calibration the Molecular Probes (F-6774) Fura-2 Calcium Imaging Calibration Kit was used which allowed the measurement of known concentrations of calcium mixed with fura-2. These data were manually imported into the UltraView software thus enabling the calculation of calcium concentration for any given ratio data obtained within the maximum and minimum calibration sample concentrations (fig. 19)

WESTERN BLOT ANALYSIS

CELL LYSATE PREPARATION:

Human airway smooth muscle cells (HASMCs) were grown on 100mm tissue culture dishes. Whole cell or crude membrane and cytosol fractions were obtained using different lysis protocols.

i) WHOLE CELL LYSATES

Cells were washed three times in 5 ml of ice cold HBBS. RIPA lysis buffer (50 mM Tris-HCl, 150 mM NaCl, 1% NP-40, 0.5% sodium deoxycholate, 0.1% SDS, 5mg/ml of pepstatin A, 5mg/ml of PMSF, 5mg/ml leupeptin, 1 mM $NaVO_4$, 10 mM $NaPO_4$ was used to lyse the cells. For each plate 300 μL of lysis buffer was used. Cells were removed from plates by scraping with a cell scraper (on ice). Buffer containing cells and cell debris was transferred to 1.5ml microcentrifuge tube that was sonicated at setting #40 with 3x10s pulses using a probe sonicator. After sonication the sample was centrifuged at 4°C for 15 minutes at 20,000 x g using a microfuge. The supernatant was then transferred into a new centrifuge tube and stored at –70°C up to 2 months.

ii) MEMBRANE AND CYTOSOL FRACTIONATION LYSATE

Cells were washed three times in 5 ml of ice cold HBBS then lysed with 40mM Tris, pH 8.0 with 1 mM $NaVO_4$, 10 mM $NaPO_4$, 5mg/ml of pepstatin A, 5mg/ml of

phenylmethylsulfonyl fluoride (PMSF), 5mg/ml leupeptin. For each 100 mm plate 300 µl of lysis buffer was used. Cells were removed from plates by scraping with a cell scraper (on ice). Buffer containing cells and cell debris was transferred to 1.5ml micro centrifuge tube. Cell lysates were sonicated on ice with 2 pulses for 10 seconds each using a probe sonicator (setting #40). Sonicated lysates were centrifuged at 4°C for 15 minutes at 20,000 x g using a microfuge and the supernatant containing the cytosolic fraction was transferred to a new 1.5ml micro centrifuge tube. The pellet was lysed with RIPA (pH 8.0) containing 1 mM $NaVO_4$, 10 mM $NaPO_4$, 5mg/ml of Pepstatin A, 5mg/ml of PMSF, 5mg/ml Leupeptin. A volume of 300 µl per pellet (representing one 100 mm plate) was used. Samples were than sonicated 4°C with 2 pulses for 10 seconds each using a probe sonicator (setting #40). Sonicated lysate was then centrifuged at 4°C for 15 minutes at 20,000 x g and the supernatant containing the membrane fraction was transferred to a new 1.5ml micro centrifuge tube and stored at –70°C up to 2 months.

PROTEIN ASSAY

Protein was measured using the BioRad DC Protein Assay based on Lowry Method. Absorbance at 750nm was measured using an Ultraspec 3000 spectrophotometer. Bovine serum albumin (Fischer CAS 9048/46/8) was used as a relative protein standard for all assays. Calculated concentrations were used to calculate the dilution required to bring all samples to the same concentration for use in subsequent Western Blot analyses.

PROTEIN ELECTROPHORESIS: SDS-PAGE + WESTERN BLOTTING

The BioRad Protean II minigel vertical electrophoresis apparatus was used for all applications. The gels measured 8 x 10 x 1 cm. Because the proteins investigated were in the range of ~26-47kd, 12.5% acrylamide separating gel and 3.5% acrylamide stacking gels were used. The buffer system described by Laemmeli [210] was used. Separating gels contained 375mM Tris, pH 8.8, 0.1% sodium dodecyl sulphate (SDS). Stacking gel buffer was 125mM Tris, pH 6.8, 0.1% SDS. The amount of protein loaded into each well was 10-40 μg. Proteins were fractionated at constant voltage of 200V for 60 minutes at room temperature. The running buffer used was of the following composition: Tris (25 mM), Glycine (0.192 M), SDS (0.1%). The transfer of proteins from the gel onto nitrocellulose paper was done at constant voltage of 100 V for 80 minutes at 4-8°C. The transfer buffer composition was the following: Tris (25mM), Glycine (192mM), SDS (0.05%), Methanol (20%). After transfer, blots were immediately placed into TBST. To confirm transfer efficiency and equal loading of samples in each lane after transfer blots were stained for total protein. India Ink or Ponceau S were used. For India ink staining TBS containing 0.1% India Ink and 0.1% Tween-20 was used staining was performed for 1 hour at room temperature, then blots were rinsed in distilled water and incubated in fresh water for 30 minutes before air drying. India Ink staining was only used for western blot analyses were complete. For staining blots after but before labeling with antibodies Ponceau S staining was used immediately after transfer. The composition of the stain was: 0.15% trichloroacetic acid (TCA), 100 mg/ml Ponceau S. Stain was applied for 15 minutes then blots were rinsed with distilled water until bands were clear. Blots were then washed further until no color remained. Blots

were then incubated in fresh TBST for at least 30 minutes before being used for immunostaining.

BLOT IMMUNOSTAINING

Blots were blocked overnight at 4°C in TBST with 5% skim milk powder then were placed into TBST/1% skim milk powder with diluted primary antibody (Table 2) overnight with constant shaking the antibody containing solution. Blots were then rinsed 3 times with TBST and incubated for one hour with horseradish peroxidase conjugated secondary antibody (Table 2) appropriately diluted in TBST/1% of skim milk powder. Blots were then rinsed with TBST three times. To detect the protein of interest a chemiluminescence techniques were used, with ECL reagents (Amersham) as specified by the manufacturer. Chemiluminograms were captured on Kodak biomax light film. The film was exposed for 10 – 300 seconds. Densitometry was performed using a page scanner with the MCID M4 (3.0 Rev. 1.2) software.

ISOMETRIC FORCE MEASUREMENT IN EQUINE TRACHEAL SMOOTH MUSCLE STRIPS

Equine trachea was obtained from a regional abattoir. Trachea were placed into Kreb's-Herseleit solution of the following composition: 118 mM NaCl, 4.75 mM KCl, 2.54 mM $CaCl_2$, 1.03 mM KH_2PO_4, 23 mM $NaHCO_3$, and 11 mM glucose. A sheet of trachealis muscle was dissected from trachea rings after removing the serosal and epithelial layers. Thin parallel strips of tracheal smooth muscle (TSM) (n=16 strips from three animals) were separated and tethered vertically with 3-O surgical silk. One end of the

muscle was fastened to a rigidly clamped glass hook in a 10 ml jacketed organ bath (37°C). The other end was tied to a Grass FT 0.03 force transducer on a rack and pinion to allow the length of the muscle to be adjusted. The organ bath was filled with Krebs buffer at 37°C and was bubbled gently with 95% O_2 and 5% CO_2 gas mixture to maintain a pH of ~7.4. Tissues were equilibrated by repeated exposures to 47mM KCl substituted Kreb's bicarbonate solution. In preliminary concentration response studies, 47mM KCl elicited maximal contractile responses. During this time (approximately 90 minutes and 4 exposures to KCl) muscle length was adjusted to elicit maximum isometric force i.e. optimal length. Thereafter strips were stimulated by electrical field stimulation (EFS) (12Vx15secs; current density 400 mA/cm^2) every 10 minutes for the duration of the experimental protocol. Maximum contractile responses to EFS were ~130% of maximum response to KCl. Isometric force was recorded using Chart 4 software and a PC computer. To determine the role of GJ in EFS-induced contractile responses after adjusting strips to optimal length, 300 mM octanol or 100 mM Glycirrhetinic acid was added to some baths. Thereafter responses to EFS for up to 1 hour was recorded and compared to time-matched untreated controls. To confirm the viability of muscle strips at the end of each experiment, strips were again exposed to 47 mM KCl, and data was only accepted in the force generated was +/- 20% of the KCl responses induced at the beginning of the protocol. All experiments were completed in triplicate using strips from at least 3 different animals.

LY DIFFUSION - 0M EXTRA CELLULAR CALCIUM ($[Ca^{2+}]_e$) LOADING

To determine whether functional hemichannels were expressed by confluent or subconfluent HASMCs grown on #1, 25 mm diameter coverslips were bathed in Ca^{2+} and Mg^{2+}-defficient HBSS containing 1% LY at 37°C. After 5 minutes of incubation cultures were washed with HBSS containing calcium and magnesium. Images of dye loading were taken with a confocal microscope as described above. In some studies either octanol (300mM) or GRA (100mM) were included to confirm that dye loading occurred through hemichannels.

LUCIFER YELLOW (LY) DIFFUSION - SCRAPE LOADING [211]

To measure functional coupling between cells multilayered confluent HASMCs on 25 mm diameter coverslips were scraped with a surgical disposable scalpel while submerged in HBSS containing 2% Lucifer Yellow (LY) and 1% Alexa568 dextran conjugate at room temperature. A single linear cut was introduced across the coverslip and the cells remained in LY for 5 minutes thereafter. Then cells were washed with fresh HBSS. Microscopic images of dye spread were taken by confocal microscopy as described above in "Immunocytochemistry". Images were then further analyzed with the software Fluoview and Adobe Photoshop as described below to enable quantification of the distance of LY and dextran conjugated Alexa 568 diffusion into coupled myocytes adjacent to the wound. In some studies either octanol (300mM) or GRA (100mM) was also included to confirm dye spread occurred through GJs.

LY DIFFUSION – SCRAPE LOADING ANALYSIS

Twenty four-bit grayscale pictures from the confocal microscope were converted to 8-bit grayscale with the Fluoview software (Figure 5A). This picture was converted with UltraView software to a 246-color spectral image (Figure 5B) (red color represented the highest fluorescence intensity and violet the lowest) and implemented an edge detection algorithm that formed an artificial edge of black color couple of pixels wide. In this manner the edge of the scrape wound could be identified (seen in red in Figure 5C). Thereafter on top of this image a graphical mask was applied 4 pixels wide which appears as a solid line demarking the wound edge border in the 246 color spectral image (Figure 5D). This picture was then imported back to UltraView and lines drawn perpendicular to the wound edge were applied every 3 pixels along the wound edge (Figure 5E) to yield a set of data representing the fluorescent intensity along the line moving away from the wound edge (Figure 5F). The edge was chosen, because it shows up as 0 intensity on the data sheet (Figure 5G). 200 lines were collected and averaged out to obtain a final curve that graphically represents the distance from the wound edge that LY diffused into intact cells.

RT – PCR

RNA ISOLATION FROM CULTURED HASMC

HASMC were grown on 100mm tissue culture dishes to confluence in DMEM/10%FS then were maintained in serum free Ham's F12 for 7 days. RNA was isolated from cells at 70% confluence, 100% confluence (serum fed) and 7-day serum deprived cultures.

To isolate RNA cells were washed 2x with HBSS then the Qiagen RNA isolation Kit was used to isolate the RNA.

RNA ISOLATION FROM HUMAN BRONCHIAL SMOOTH MUSCLE TISSUE

Segments of central bronchi were obtained from uninvolved lung specimens from patients undergoing partial lung resection for cancer as described above for preparation of protein lysates. On ice, bronchial smooth muscle was rapidly dissected free from bronchial rings as described for preparation of primary cultures then total RNA was isolated using the Qiagen RNA isolation kit following manufacturer's instructions. RNA was stored in ddH_2O at –20 until used for PCR reactions.

RT- PCR REACTION

To run the reverse transcriptase and PCR amplification reaction the one step Qiagen taq PCR kit was used with the following cycling temperature regime: 1) 72° for 3 min, 2) 3 min on ice, 3) 50° for 30 min 4) 95 °C for 4 min, 5) 55 °C for 1min (annealing), 6) 72 °C for 1½ min (extension), 7) 95 °C for 1min (denaturation), 8) 55 °C 1min, then 9) 72 °C for 10min. Steps 2-4 were repeated 40 times completing the PCR reaction with steps 5 and 6.

Then the sample is run on a 0.8% agarose gel of the following composition: 0.4g agarose, 50ml TAE buffer, and 1μL of ethidium bromide. The sample is run at 100V. The product identity was confirmed by comparing the molecular mass seen with that predicted based on the primers that were used using New England BioLab marker.

PRIMERS USED

Primer	Type	Source	Sequence
Sense Cx43	Rat	Gift from Dr Jim Nagy	5'-ATG GGT GAC TGG AGT GCC TTG-3'
Antisense Cx43	Rat	Gift from Dr Jim Nagy	5'-TTA AAT CTC CAG GTC ATC AGG-3'
Sense Cx57	mouse	Gift from Dr Jim Nagy	5'-GGT TGC AAC AAT ATC TGT TAC GA-3'
Antisense Cx57	mouse	Gift from Dr Jim Nagy	5'-TCT GTG GGC CTG GAA ACA AAG CA-3'
Sense Cx47	mouse	Gift from Dr Jim Nagy	5'-ATG AGC TGG AGC TTC CTG ACG CGG CTG-3'
Antisense Cx47	mouse	Gift from Dr Jim Nagy	5'-TCA GAT CCA CAC GGT GGC CTT GCC GTC-3'
Sense Cx40	human	Gift from Dr Jim Nagy	5'-TTG GAG CTT CCT GGG AAA TT-3'
Antisense Cx40	human	Gift from Dr Jim Nagy	5'-TAG GTC ATC TGA CCT TGC CTT-3'

MATERIALS

All cell culture reagents were purchased from Life Technologies, Grand Island, NY unless otherwise stated. Penicillin and Streptomycin was purchased from Sigma. The fluorescent calcium indicator fura-2 was purchased from Molecular Probes, Inc. (Eugene, OR). Gap junction inhibitors: Octanol was purchased from Sigma Chemicals Co. (St. Louis, MO) and 18β-Glycyrrhetinic acid from Aldrich Chemical Company, Inc. (Milwaukee, WE). Enzymes for digestion solutions: Protease and Elastase were purchased from Sigma.

RESULTS AND DISCUSSION

Specific Aim #1: *To establish HASM cell cultures, and characterize the expression pattern of M3R and responsiveness to ACh.*

1.1 THE HASMC CULTURE

Cells were acquired and cultured using conditions described in Methods. For most studies the cells were grown from vials of primary myocytes that has been stored frozen after reaching confluence (passage 2 or 3). Shortly after re-plating cells from frozen vials (~1 hour), evidence for the attachment and spreading of individual myocytes was seen by phase contract microscopy (Figure 6A). Approximately 80% of all cells became attached; unattached cells were removed by aspiration 48 hours after initial plating. About 5 days after seeding at ~10,000 cells/cm^2 the cultures reached confluence. Myocytes were spindle shaped with a large central nucleus and organized in a hill-and-valley pattern at confluence (Figure 6B). Post-confluent cultures tended to form multi-layers, thus contact inhibition was not absolute. Confluent cultures that were maintained in serum-free condition for up to 20 days developed organized bundles of phase-dense elongate myocytes similar to the pattern previously described for canine tracheal myocyte primary cultures [21] (Figure 6C). By 20 days of serum deprivation, bundles of contractile myocyte covered approximately 20% of the cell culture growth surface.

1.2 EXPRESSION OF PHENOTYPE MARKERS BY HASMC

Immunocytochemistry was used to demonstrate expression pattern of smooth muscle actin (sm-α–Actin), smooth muscle myosin heavy chain (sm-myosin), muscarinic type 3

receptor (M3R) and the bradykinin BK2 receptor after serum deprivation of D5–D7 cultured P4-P6 HASMCs. Antibodies used and dilutions are listed in the methods section. The experiment was performed in triplicate each of three different primary cultures. Microscopic analyses revealed that a fraction of five-to-seven day serum deprived P4-P6 HASMCs (~20-30% as determined by counting cell nuclei) acquire an elongate morphology and accumulate abundant contractile proteins (sm-α–actin and sm-myosin) (Figure 7). Of note, in a manner similar to our previousli published observations using primary cultured canine airway SMC, only myocytes that accumulated contractile proteins also exhibited aggregates of cell surface M3R (Figure 7). In contrast, the BK2 receptor appeared to be somewhat ubiquitously expressed, and appeared as large aggregates near the nucleus of each cell. Multi-nucleation was rarely seen in serum-deprived human airway smooth muscle cell cultures.

1.3 HASMC RESPONSIVENESS TO ACh and BK

M3R is a Gαq-coupled seven transmembrane receptor that mediates ACh-induced mobilization of $[Ca2+]_i$ required for eliciting airway smooth muscle contraction. We measured changes in $[Ca2+]_i$ in cultured human airway myocytes loaded with the ratiometric Ca^{2+}-sensitive dye, fura-2 by fluorescent microscopy using a high speed computer controlled digital camera and UltraView software. For these studies 4^{th}-to-6^{th} passage (P4-P6) HASMC cultures that had been grown to confluence then maintained in serum-free conditions for 5-to-7 days (D5-D7). These conditions were similar to those used for the immunocytochemistry experiments described in Section 1.2. Serum-deprived HASMC were stimulated with 10^{-6} M ACh and cell response was recorded for

up to 300s thereafter. More than 95% of the cells mobilized intracellular calcium (Figure 8A).

These studies revealed a temporal disparity between the time-to-peak $[Ca^{2+}]_i$ in response to ACh (10^{-6}M), with some cells reaching peak values within ~5 seconds whereas other cells did not reach peak $[Ca^{2+}]_i$ until ~45 sec after agonist was added. Of note, this disparity was not the result of differences in the rate of increase to peak $[Ca^{2+}]_i$, rather it appeared to result from differences in the time for initiation of a response after agonist was added (Figure 8A). The disparity in response time was unique to studies using ACh to provoke a response, as similar studies using BK (10^{-6} M) produced temporally synchronous cellular responses (Figure 8A and B). These functional measurements appear to correlate well with our prior observations using immunohistochemistry to assess expression and distribution of M3R and BK receptors on the primary cultured HASMC studies (Figure 7); these studies revealed that M3R was expressed by only ~20% of all cells, whereas BK2 receptor was expressed homogeneously. Thus, since almost all myocytes were able to respond to ACh, our observations are consistent with the existence of cell-cell coupling between myocytes expressing M3R and those that do not express M3R. Moreover, the temporal disparity we noted in time-to-peak $[Ca^{2+}]_i$ may reflect time required for transmission of intracellular signals between coupled myocytes. Therefore, for Specific Aim#2 of our project, we designed experiments to more directly characterize the nature of cell-cell coupling between HASMC in vitro, and to assess the role of cell-cell coupling and in integrating mobilization of $[Ca^{2+}]$i in response to contractile agonists.

Specific Aim #2: *To characterize the expression of connexins and distribution of GJs in HASM in vitro, and determine their role in cell-cell coupling and in integrating mobilization of [Ca2+]i in response to contractile agonists.*

2.1 SCRAPE WOUND TEST

We first investigated the existence of functional of intercellular cytoplasmic communication in primary cultured HASM cells, and used selective chemical inhibitors to determine if cell-cell coupling occurred via gap junctions. We used an assay in which confluent myocytes cultures receive a "scrape wound" creating a clean cut across the monolayer. The wound is inflicted while cells are bathed in physiological saline containing a low molecular weight green fluorescent dye (Lucifer yellow, 2%, Mol. Wt. 457 Da) and a high molecular weight dextran-conjugated red fluorescence dye (dextran-Alexa 568, 1%, Mol. Wt. >10,000 Da). Though both dyes rapidly diffuse into damaged cells, only Lucifer Yellow is able to pass through GJ to adjacent cells. By confocal fluorescence microscopic analysis of the wound area (see Methods for details) after the scrape wound is made, we quantified the diffusion distance of Lucifer yellow through GJs. For these studies we used serum deprived P4-6 D2-6 HASMCs.

Figure 9 shows typical confocal images showing the diffusion of Lucifer yellow and dextran-Alexa 568 five minutes after making a scrape wound. These studies clearly indicated that LY (green) was able to diffuse into cell adjacent myocytes at the wound margin, whereas high molecular weight dextran-Alexa568 (red) loading was limited only to those cells at the wound margin. To more specifically investigate the role of GJs in

the diffusion of LY between adjacent HASM cells we next measured the effects of selective GJ inhibitors on diffusion of LY after preparing a scrape wound. We employed two well-described inhibitors that appear to inhibit diffusion of low molecular weight molecules through GJs by different mechanisms [212, 213] (Table 2). We performed scrape wound assays using P4-P6 HASMC (D2 serum deprivation) in the presence and absence of the GJ inhibitors octanol (300mM) and β-glycirrhetinic acid (100 mM). As summarized in Figure 10, both octanol and β-glycirrhetinic acid abrogated the diffusion of LY between adjacent myocytes after scrape loading. These data strongly suggest that diffusion of low molecular weight, water soluble molecules between HASMC after scrape loading in primary culture is entirely mediated via GJs. Moreover, these data are the first to demonstrate the existence of functional GJs in cultured human airway smooth muscle cells.

2.2 FUNCTIONAL HEMICHANNELS

As many cells are known to express connexins that are organized into hemi-channels that may be important for juxtacrine signalling between cells we next tested whether functional hemichannels were present on sub-confluent and confluent cultured HASMC. For these studies we used a standard method [78, 214, 215] in which hemi-channels are gated transiently by maintaining cells in Ca^{2+}-deficient physiologic saline by metabolic inhibition [216, 217] and by membrane depolarisation [218]. HASMCs P4-P6 2-day serum-deprived and P4-P6 subconfluent serum-fed were equilibrated in HBSS and then the bathing media was rapidly changed to Ca^{2+}-, Mg^{2+}-deficient HBSS containing 2% LY to cause opening of hemi-channels. Cells were incubated for 5

minutes at room temperature. Thereafter, the bathing medium was rapidly removed and replaced with LY-free, complete HBSS, leading to closure of hemi-channels and the trapping of any LY that has entered the cells when they were incubated in Ca^{2+}-, Mg^{2+}-deficient HBSS. In some studies, to block connexon opening octanol (300mM) or β-Glycirrhetinic acid (100mM) was included in all bathing solutions. The diffusion of LY into myocytes via hemi-channels was quantified by confocal microscopy as described in Methods.

Lucifer yellow diffused into >95% of the myocytes in sub-confluent cultures when incubated in Ca2+-deficient media (Figure 11). In control experiments in which cells were incubated in complete medium containing LY, virtually no LY diffusion was detected during the time course of the experiment, indicating that LY-loading was inhibited by the presence of extracellular Ca^{2+}; this behaviour is consistent with the presumption that LY-loading in Ca^{2+}-free condition occurs through hemichannels (Figure 11C). Confluent cultures were resistant to LY-loading in response to removal of extracellular Ca^{2+} (Figure 11 and Figure 15F); this is of note, as the open/closed state of intact GJs (consisting of two hemichannels in register) is not affected rapidly by changes in extracellular Ca^{2+}. These data suggest that hemichannels are rare in confluent HASM cell cultures. An exception to this pattern was seen near the edge of cultures grown on glass coverslips where areas of subconfluence occurred in which prominent LY-loading was observed as a result of incubation in Ca^{2+}-deficient medium (Figure 15 E). In all experiments both octanol and β-glycirrhetinic acid significantly

reduced diffusion of LY into HASM cells, confirming diffusion likely occurred though hemichannels on the surface of cells in areas of subconfluence (Figure 11D).

2.3 CELL-CELL COUPLING: REGULATION OF THE RESPONSE OF HASMC TO CONTRACTILE AGONISTS.

To test whether the temporal disparity in time-to-peak $[Ca^{2+}]_i$ response we observed for cultured HASMC was the result of differences in the time constant for M3R-deficient myocytes coupled to M3R-expressing myocytes we investigated the effects of GJ blockers, octanol and β-glycirrhetinic acid on the response of myocytes to ACh and BK. Experiments were completed using fura-2 loaded, confluent 5-7 day serum-deprived HASMC (P4-P6), as described in Section 1.3 (Results). Changes in $[Ca^{2+}]_i$ elicited by ACh (10^{-6} M) in individual myocytes were measured before and 30 minutes after cells were incubated with either 300 mM octanol or 100 mM β-glycirrhetinic acid. To confirm the viability of each cell studied, and to determine the effects of gap junction inhibition on the response elicited by a homogeneously expressed agonist receptor, the response to BK (10^{-6} M) was also measured for each field of myocytes studied; these measurements were obtained ~4 minutes after acquiring ACh-induced responses in the presence of octanol or β-glycirrhetinic acid. Prior to measuring the response to BK, cells were washed twice with HBSS containing either 300mM octanol or 100mM β-glycirrhetinic acid to remove residual ACh and ensure $[Ca^{2+}]_i$ returned to a stable baseline. Time-matched control studies were also performed for comparison in all treatment groups.

The results of our studies investigating the effects of inhibitors of gap junctions on the response of HASMC to contractile agonist stimulation are summarized in Figures 8B, 8C, and 12. Based on prior studies by Dr. Halayko [23], on average the peak response of cultured canine airway myocytes to serial treatments with ACh becomes reduced to ~85% of the initial response after 30 minutes; therefore, for analytical purposes, we considered any myocyte unable to mount a 2nd response that was ≥ 80% of the 1st response to be inhibited. For these studies the mean peak $[Ca^{2+}]_i$ induced by ACh was reduced by 33.08% and 39.87% after treatment with octanol or β-glycirrhetinic acid respectively (Figures 8B, 8C and 12A). In contrast, for control HASMC the mean peak $[Ca^{2+}]_i$ measured in the second response to ACh was equal to or greater (126 ±9%) than that recorded during the first exposure to ACh in the same myocytes. Interestingly, our control data indicate that, unlike cultured canine tracheal smooth muscle cells [23], there does not appear to be a time-associated decline in ACh-elicited peak $[Ca^{2+}]_i$ in HASMC.

Though prior to treatment with octanol or β-glycirrhetinic acid virtually all myocytes exhibited the ability to mobilize intracellular Ca^{2+} in response to ACh (10^{-6} M), only 32.27 ± 12% and 31.14 ± 14% of these myocytes retained the capacity to mount a similar response after inhibition of gap junctions with octanol or β-glycirrhetinic acid respectively (Figures 8A,B and 12B). In contrast, for control cultures where myocytes were twice treated with ACh with 30 minutes between exposures, 91.21 ± 5% of the myocytes were able to mount a 2nd response of equal magnitude to that we recorded after the 1st exposure to ACh. In striking contrast to our observations examining

responses to ACh, both peak $[Ca^{2+}]_i$ and the fraction of responsive HASMC to BK (10^{-6} M) was unaffected by treatment with octanol or β-glycirrhetinic acid. Based on our studies using ACh to induce intracellular Ca^{2+} mobilization, our results suggest the existence of two distinct subpopulations of HASMC in confluent primary culture, one group (~30% of total cell number) that exhibits GJ-independent responses to ACh, and another group (~80% of total cell number) characterized by GJ-dependent responses to ACh. Though our experimental design does not allow confirmation that only those myocytes that express M3R are capable of responding to ACh stimulation after GJ inhibitor treatment, it may be of note that the fraction of cells that express functional M3R (~20%) is the same as the fraction of myocytes that exhibit GJ-independent responses to ACh. This suggests a cause-effect relationship, which is further corroborated by the observation that GJ inhibitors had no effect on mobilization of intracellular Ca^{2+} in response to BK, a ligand that stimulates signalling via the homogeneously expressed BK2 receptor.

2.4 CONNEXIN EXPRESSION AND DISTRIBUTION IN HASMC.

As our experiments using pharmacological inhibitors of GJs provided evidence for functional myocyte-myocyte coupling in HASMC cultures, we next investigated the expression profile of connexins in HASMC and lung tissue obtained from human donors. We first performed Western blot analyses (12.5% separating gel) on cytoplasmic and plasma membrane-associated protein lysates prepared from cultured myocytes at different stages of confluence and at different times after serum withdrawal to characterize the abundance of ubiquitously expressed Cx43 (Figure 13). Monomeric

Cx43, which appears as a cluster of bands ~43 kDa, was enriched in the membrane fraction of 50% subconfluent and 100% confluent cultured HASMC in serum-fed conditions, and in confluent cultures after 2 and 7 days serum deprivation. The upper 2 or 3 bands that make up the 43 kDa cluster are likely differentially phosphorylated forms of monomeric Cx43, whereas the lowest band is non-phosphorylated Cx43 [219, 220]. For all Western analyses, whole cell lysates from a C6 glioma cell line stably transfected with Cx43 was used as a positive control. Over the course of the culture time the total abundance of monomeric Cx43 was stable. Multiple oligomeric forms of Cx43 were clearly visible in membrane-enriched protein lysates; these oligomers were absent in cytosolic fractions and, likely due to the diluting effect of including the cytoplasm with the membrane fraction in whole cell lysates, the relative abundance of oligomeric Cx43 complexes was greatly decreased in whole cell lysates (Figure 13). A unique band ~65 kDa was also seen in cytoplasmic and whole cell lysates obtained from serum-fed cultures (50% and 100% confluent); due to its molecular mass the identity of this band is not known. One can speculate that it might be a conjugate of Cx43 with an unknown protein that keeps this fraction of Cx43 in the cytosol.

To confirm that Cx43 was not expressed exclusively in primary cultured HASMC we also examined the abundance of Cx43 in lysates prepared from intact human bronchial smooth muscle by immunoblotting. Bronchial smooth muscle tissue was dissected from 5-10mm diameter human bronchi obtained from non-diseased portions of lungs from patients undergoing lung resection at the Winnipeg Health Sciences Centre (in accordance with a human ethics protocol approved by the U of Manitoba HREB). The

dissection was performed for samples from three different patients using fine instruments under a binocular dissecting microscope at 4°C; thereafter, whole tissue lysates were prepared as described in Methods. Abundant Cx43 was detected in all 3 samples analyzed (Figure 14). Interestingly, Cx43 from each sample appeared to exist almost exclusively in a phosphorylated state, suggesting that the activity of connexins and GJs in human bronchial smooth muscle tissue may be subject to rigorous regulation (Figure 14).

Our Western blot studies (Figure 13) and experiments investigating functional loading of Lucifer yellow via hemichannels (Figures 15D-F) were giving us a slight hint that the cytosol *vs.* membrane-associated distribution of Cx43 changed as cultured HASMC reached confluence, we used immunocytochemistry to more thoroughly characterize the cellular distribution of Cx43 in these cells. Myocytes were fixed and immunolabelled for Cx43 at 25% and 50% confluence (serum-fed), and at 100% confluence (5 days serum deprived) then Cx43 distribution was captured by confocal microscopy as described in Methods (Figure 15A-C). In HASMC from subconfluent cultures Cx43 appeared to be principally localized to perinuclear intracellular regions, and also occurred in dense clusters of punctate staining in more peripheral regions of each myocyte. This pattern was dramatically different in confluent cultures, where perinuclear labeling was greatly diminished and Cx43 was present principally in arrays or clusters of punctate labeling that frequently appeared to demarcate sites of cell-cell contact.

Specific Aim #3: *To characterize the expression of connexins in intact airway smooth muscle and determine their functional role in isometric contraction induced by contractile agonists.*

3.1 CONNEXIN EXPRESSION IN HUMAN BRONCHIAL SMOOTH MUSCLE TISSUE AND CELLS

Based on previous reports describing connexin expression in various smooth muscle-containing organs, we used RT-PCR to more fully characterize the profile of connexin genes expressed by human bronchial smooth muscle tissue and primary cultured HASMC (Figure16). The preparation of mRNA and conditions used for RT-PCR was completed as described in Methods. Though the profile of connexins expressed by primary cultured HASMC was similar to that observed for human bronchial smooth muscle tissue, our analyses revealed that the pattern observed in situ was not fully reconstituted in confluent, serum-deprived cultures. Abundant mRNA for Cx40, Cx43 was evident for both cultured HASMC and intact human bronchial smooth muscle, however mRNA for Cx57, which is abundant in bronchial smooth muscle tissues was not expressed by cultured HASMC. In addition, Cx47, which was not present in lysates from bronchial smooth muscle tissue, was significantly induced in cultured HASMC. The presence of mRNA however does not mean that the protein is expressed. So in the cases of connexins other than Cx43 where western blot analysis were not performed we cannot assume that the protein is made, we know only that there is a potential of the above mentioned protein formation. Though our studies do not address the functional significance of a change in connexin expression in airway smooth muscle, neither do

they address the possibility of in-culture selection of a subset of HASMCs with a specific connexin pattern, but they do indicate that airway myocytes have the capacity to modulate connexin expression, suggesting a mechanism to change the nature of myocyte-myocyte coupling leading to altered tissue and/or cell function. Of note, phenotype plasticity of airway myocytes between a contractile and proliferative state has been well described using primary cell culture systems; the relationship of the changes that occur in expression of phenotype markers with changes we have observes in connexin expression has not yet been investigated.

3.2 FUNCTIONAL ROLE OF GAP JUNCTIONS IN AGONIST-INDUCED CONTRACTION OF AIRWASY SMOOTH MUSCLE

As our functional evidence for the existence of GJs in airway smooth muscle had been derived exclusively from studies using primary cultured airway myocytes, we designed experiments to determine whether GJs regulate the contractile response of intact airway smooth muscle. It was technically unfeasible to acquire adequate human bronchial segments for these studies; therefore we measured the effects of GJ inhibitors on active isometric force generated by strips of equine tracheal smooth muscle in response to electrical field stimulation (EFS). Previous work form our group shows that EFS-induced contractions of tracheal smooth muscle strips are abrogated by atropine, a competitive inhibitor of ACh, confirming that EFS mediated contraction by inducing release of ACh from varicosities of parasympathetic nerves that innervate the muscle tissue. Details of tissue preparation and a complete description of the isometric force lever system used are provided in Methods.

After mounting and equilibration, tracheal smooth muscle strips were subjected to repeated EFS at 8 minute intervals over ~70 minutes and active force was recorded. For all strips the response to 47mM KCl was measured at the beginning and end of each experiment to confirm that muscle viability was not compromised (data from strips that demonstrated >20% drop in KCl-induced active force generation during the experiment were not included for further analysis). To study the effects of GJ inhibition on contractile responses, in some strips after equilibration and measurement of initial contractile responses, octanol (300 mM) or β-glycirrhetinic acid (100 mM) was added to the muscle baths and contractile responses to EFS were recorded thereafter for 60 minutes. At the end of the treatment period GJ inhibitors were removed with multiple washes and contractile responses to EFS were monitored for an addition 20 minutes. In addition, at the end of each experiment the force generated by each strip in response to muscarinic receptor stimulation by exogenous ACh (10^{-6} M) was measured to determine if contraction relative to KCl stimulation was affected by GJ inhibitor treatment. The results of these studies are summarized in Figure 17.

Inhibition of GJ activity by octanol or β-glycirrhetinic acid decreased EFS-mediated active isometric force by as much as 27.2 ± 2.5% and 59.4 ± 18.6% respectively, compared to time-matched control strips (N=3, $p>0.05$, one-way ANOVA with Tukey-Kramer Multiple Comparison Test). Maximum inhibition with octanol occurred after 40 minutes treatment and the reduced isometric force was maintained until the inhibitor was removed. Treatment with β-glycirrhetinic acid resulted in steady decline in active

isometric force over the duration of the experiment, with maximum inhibition recorded after 60 minutes. The inhibitory effects of octanol on isometric force were reversible, as 20 minutes after washing the inhibitor away maximum EFS-induced force returned to 95 ± 3.1% of control strips. Moreover, at the end of the experiment (~30 min after octanol was removed), contraction induced by exogenous ACh relative to that induced by 47mM KCl was the same for control strips and those that had been treated with octanol (142.2 ± 20.3% for controls, and 132.2 ± 22.8% for octanol-treated). The inhibitory effects of GJ blockade with β-glycirrhetinic acid on contraction were not reversible within 20 minutes, as maximum EFS-induced force fell to 34.2 ± 4.9% of control strips even after removing the inhibitor. Maximum isometric force generation of β-glycirrhetinic acid-treated strips in response to 47mM KCl stimulation was only reduced by 14.2 ± 4.4% compared to time-matched controls. However, exogenous ACh-induced isometric force normalized to force induced by 47mM KCl was significantly lower than that measured in time matched controls (142.2 ± 20.3% for controls, and 43.2 ± 7.1% for β-glycirrhetinic acid treated). These data suggest that β-glycirrhetinic acid produces the irreversible blockade of GJs in tracheal smooth muscle strips, whereas recovery of myocyte-myocyte coupling can occur after octanol exposure. Moreover, these data provide conclusive evidence that the degree of myocyte-myocyte coupling in intact tracheal smooth muscle tissue is a key determinant of contractile function.

FIGURES AND LEGENDS

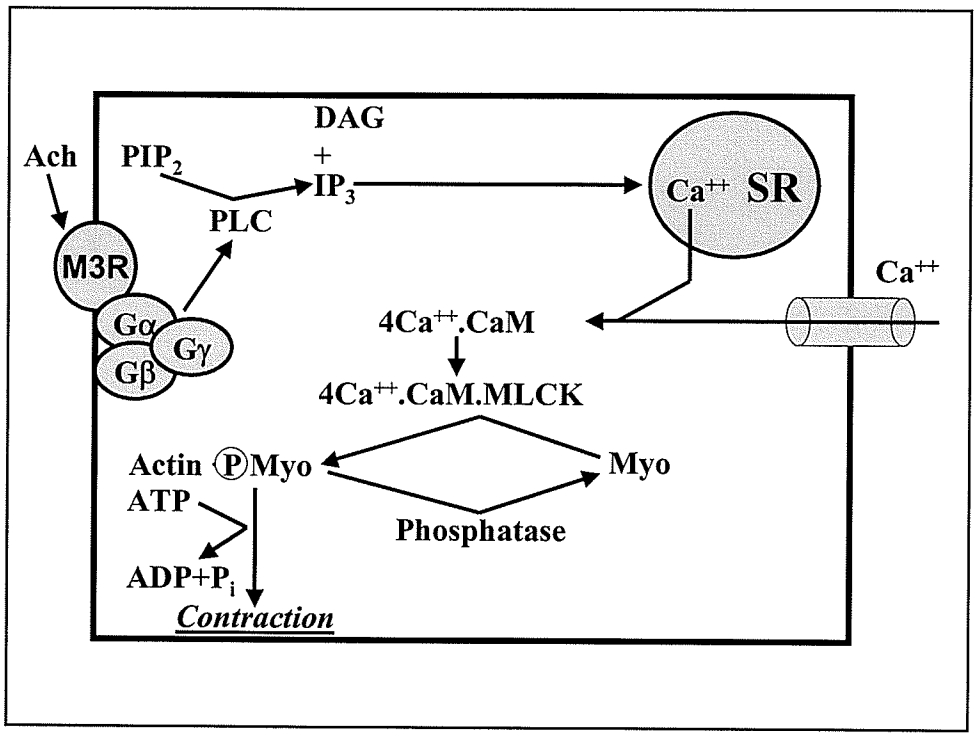

Figure 1.

Smooth muscle contraction.

Primary signaling pathways and proteins involved in the regulation of smooth muscle contraction. Interaction between actin and myosin with the subsequent hydrolysis of ATP by the myosin head is the basic chemical reaction leading to muscle contraction.

Ach – acetylcholine, M3R – muscarinic 3 receptor, PIP_2 – phosphatidylinositol 4,5 biphosphate, PLC – phospholipase C, IP_3 - Inositol-1,4,5-triphosphate, Ca^{++} - free calcium, SR – sarcoplasmic reticulum, CaM – calmodulin, MLCK – myosin light chain kinase, Myo – myosin, ATP – adenosine triphosphate, ADP – adenosine diphosphate, Pi – phosphate.

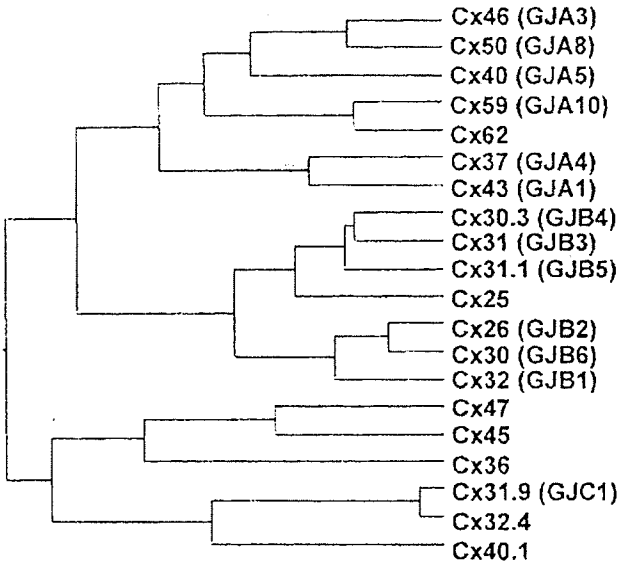

Figure 2.

Dendrogram of human connexin protein sequences.

Unrelated gene families with similar functional properties encode gap junctions in vertebrates. Dendrogram of human connexin protein sequences. Connexin genes are distributed into 3 subgroups recognized by the Human Genome Nomenclature Committee (i.e., GJA, GJB, and GJC). Note that connexins display high homology across vertebrate species. [48]

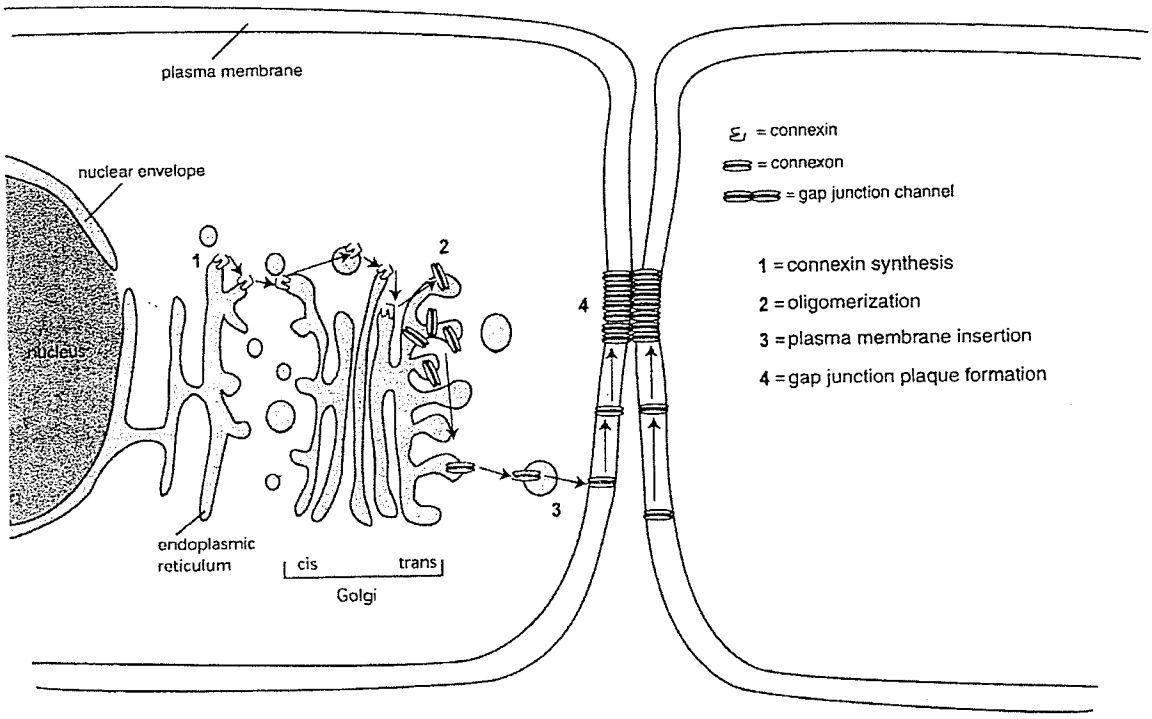

Figure 3.
Connexin 43 assembly.
Schematic representation of the steps involved in the assembly of connexin (Cx) 43 gap junctions based on current literature. Step 1: connexins are synthesized in the endoplasmic reticulum. Step 2: oligomerization of Cx43 into connexons occurs in the trans-Golgi network. Step 3: connexon-containing transport vesicles travel along microtubules to the nonjunctional plasma membrane, where they fuse. Step 4: the connexons that are delivered to the plasma membrane can reach the outer margins of the gap junction plaques by lateral diffusion. [101]

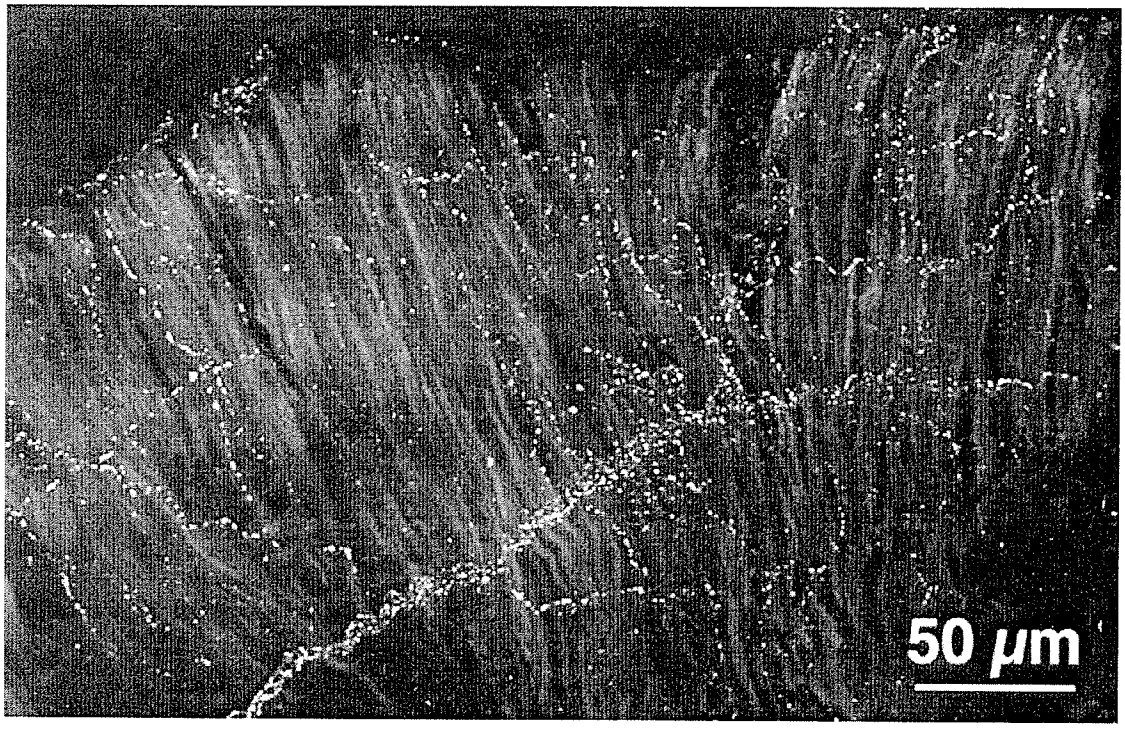

Figure 4

Sparse parasympathetic nerve varicosities with active Ach release in pig bronchus.

Parasympathetic nerve varicosities in pig bronchus section immunostained with anti SV2 antibody (white vesicles) to identify sites of active Ach release. This image illustrates the considerable areas of smooth muscle, where there is no active release of acetylcholine suggesting that bronchial smooth muscle may exist more-or-less as a single unit muscle. [142]

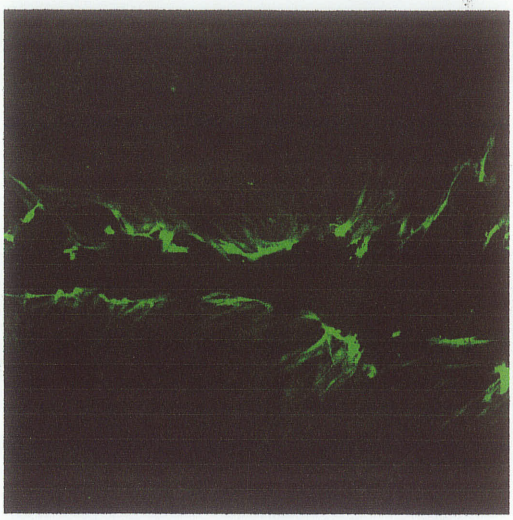

Fig. 5A

Fig. 5A
HASMC scratch wound analysis steps.
10X gray scale image of D7 serum deprived human airway smooth muscle cell culture grown on a 25mm glass coverslip 5 minutes after the scratch wound is applied with a scalpel blade across the coverslip. The culture was scratched in the presence of Lucifer yellow (LY) in the medium after which it was washed away. The cells loaded with Lucifer yellow a green fluorescent dye. This is the raw picture that we got directly from the confocal microscope.

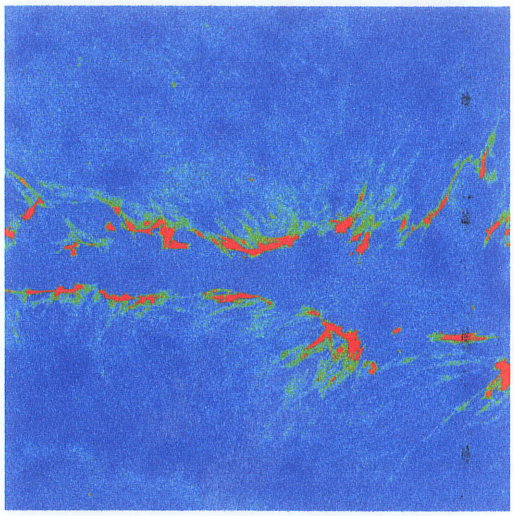

Fig. 5B

Fig. 5B
HASMC scratch wound analysis steps.
This is the same view area as in Figure 5A. The grayscale image was changed to a 246-color image, where the highest light intensity corresponds to the red color and the lowest intensity corresponds to dark blue. To create this image is necessary for analysis purposes, because the Ultraview software cannot convert the light intensity i.e. to convert the color differences to numbers in pictures with more colors than 256.

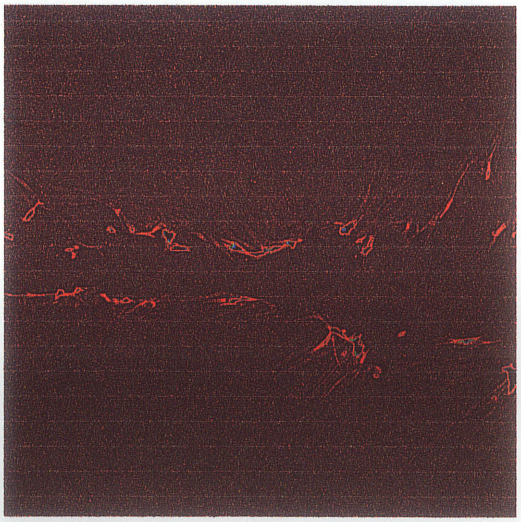

Fig. 5C

Fig. 5C
HASMC scratch wound analysis steps.
This is again the same view area as in figure 2. This image was created using an edge detection algorithm that is one of the functions of the Ultraview software. This was necessary to determine, where is the wound edge located and where to start analyzing the data i.e. the spread distance of Lucifer yellow.

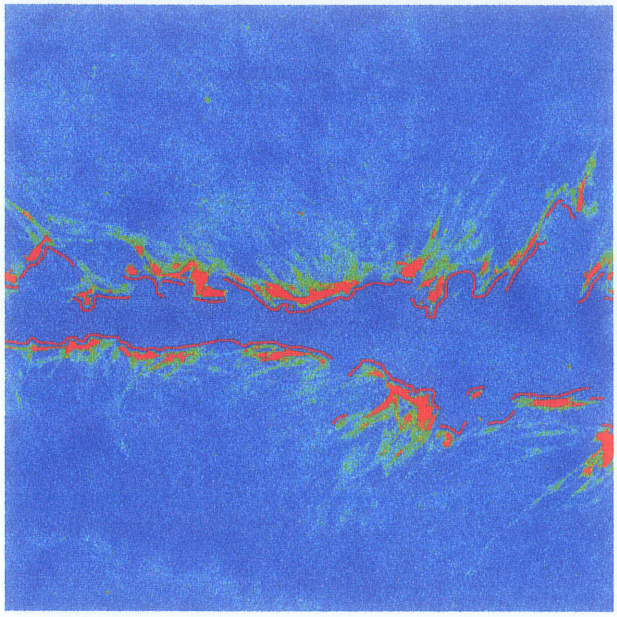

Fig. 5D

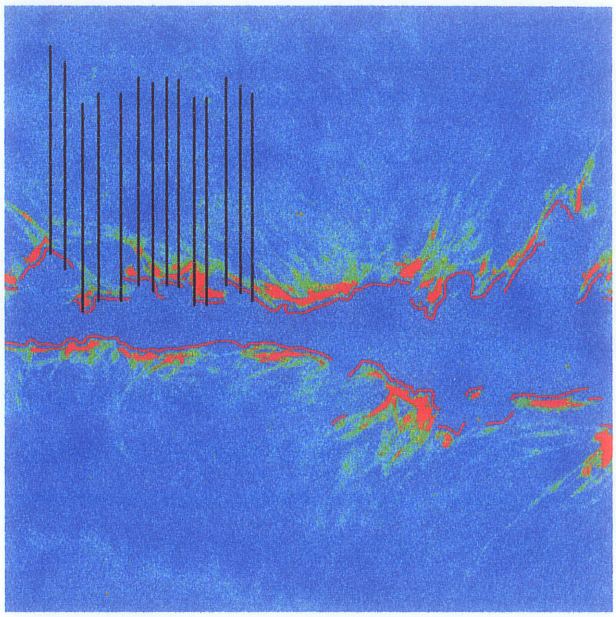

Fig. 5E

Distance In pixels From wound edge	LY fluorescence intensity (grey scale units)
0	12
1	44
1.4142	0
2.2361	0
3.1623	0
4.1231	0
5.099	4
6.0828	23
7.0711	174
8.0623	241
9.0554	241
10.0499	241
11.0454	241

Fig. 5F

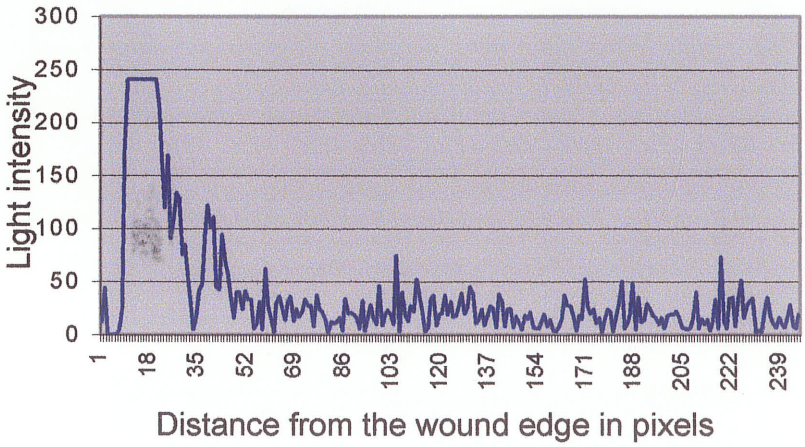

Fig. 5G

Fig. 5D

HASMC scratch wound analysis steps.

Using a translucent mask on the top of the image from 5C we can draw a line along the edge of the scratch wound. The translucent mask with the edge drawn onto it is than placed on top of image 5B. These two images, 5B and the mask with the edge, are then merged into one image that is shown here. We end up with a 246-color image with a detected edge 4-5 pixels wide of pink color. The pink color was chosen on purpose as it represents the number zero for the computer's analysis software.

Fig. 5E

HASMC scratch wound analysis steps.

Analysis lines (shown in black) are drown perpendicularly to the scratch wound. The computer extracts data based on the color of the background above which the analysis line lies for every single pixel it covers.

Fig. 5F

HASMC scratch wound analysis steps.

The computer provides the data along the analysis line in a spreadsheet format. The first column shows the distance from the beginning of the analysis line (which is placed close to the scratch wound edge). The second column shows the light intensity at a given distance from the beginning of the analysis line. When the line crosses the wound edge, that we colored to pink, as mentioned above, the data in the spreadsheet shows up as a sequence of zeros (shown with black arrows). This is the point where we start to analyze the data.

Fig. 5G

HASMC scratch wound analysis steps.

Graphical representation of the data described in figure 5F. Light density versus distance from the wound edge in pixels. Note the rough saw like appearance of the curve. This appearance smoothens out after averaging out more lines as shown in figure 10B where 200 lines were analyzed and averaged out.

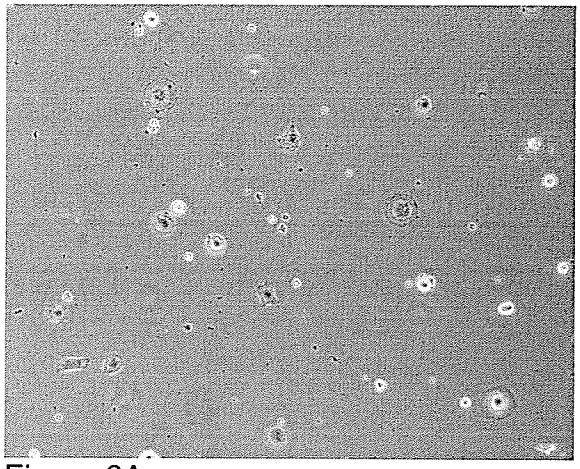

Figure 6A

Figure 6A
Freshly isolated HASMC 1 hour in DMEM.
20X phase contrast image of P4 HASMC 1 hour after plating in serum containing DMEM media. A cytoplasmic halo is apparent around the cells as they attach and start spreading on the bottom of the culture plate.

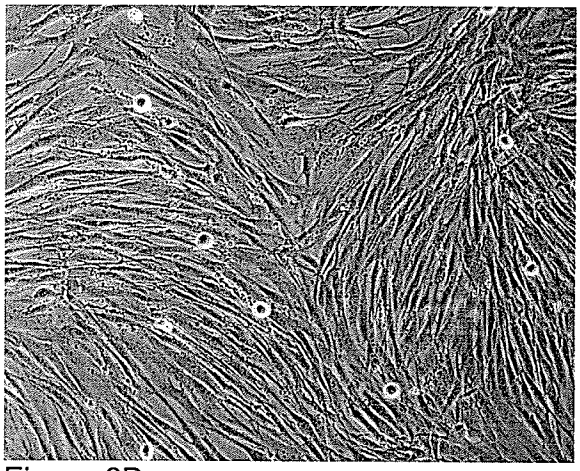

Figure 6B

Figure 6B
"Hill and valley" appearance of HASMC
20X phase contrast image of P4 HASMC soon after reaching confluence in serum containing DMEM and forming a so called "hill and valley" appearance.

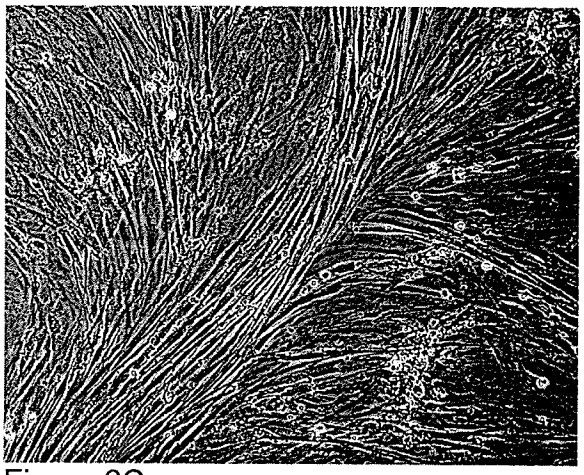

Figure 6C

Figure 6C
HASMC forming bundles after serum deprivation
20X phase contrast image of P4 HASMC 7 days after reaching confluence in the serum deprived F12 culture. There is a tendency of bundle formation. Note the evolution of the cell shape, alignment, and general organization through images 6A, 6B and 6C.

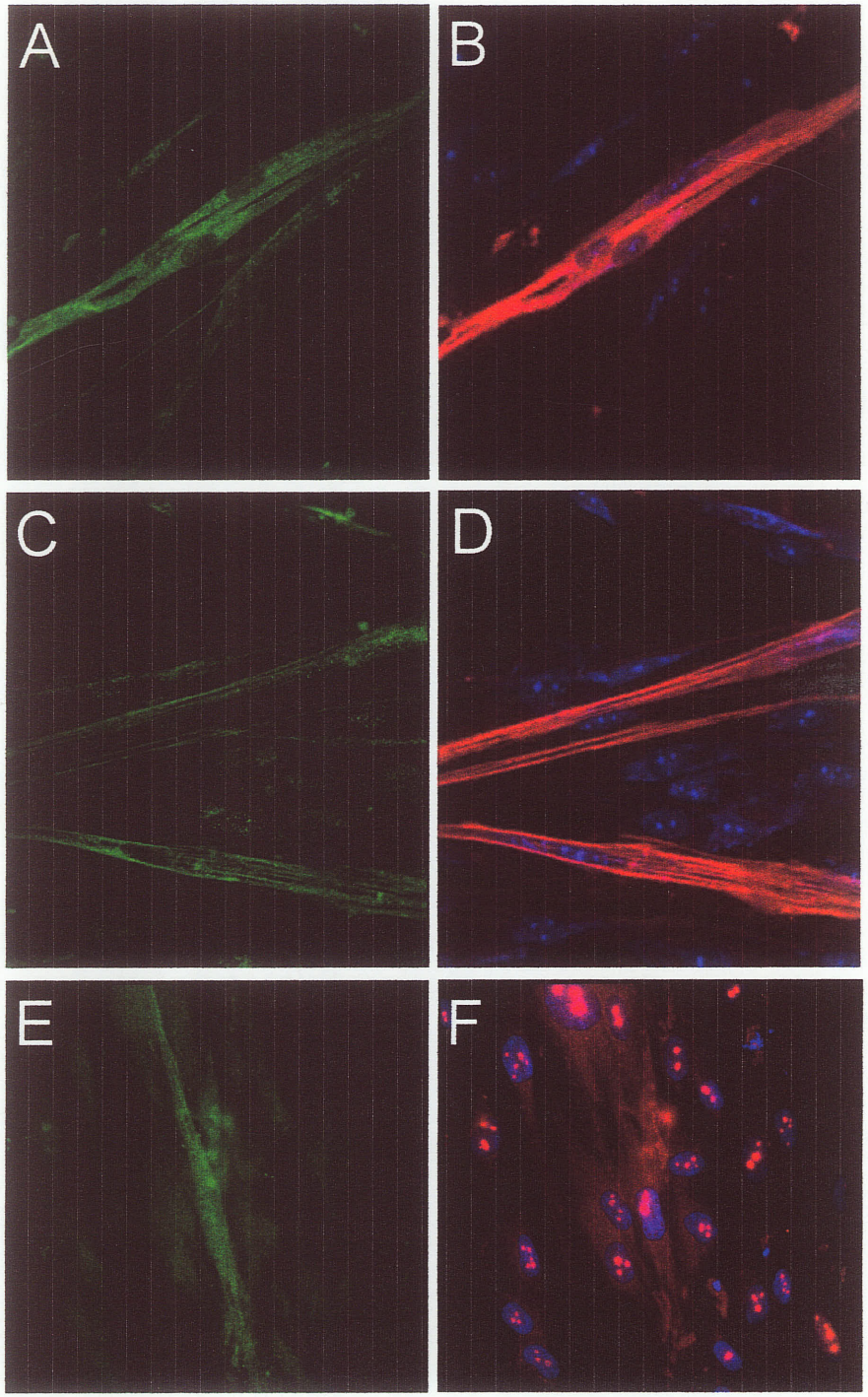
A
B
C
D
E
F

Figure 7

Expression of phenotype markers by cultured human airway smooth muscle cells.

40X immunofluorescent image taken with a confocal microscope. There are 3 matching panels showing the same field of serum deprived P4 HASMC after reaching confluence. The top panel (A and B) shows a green immuno staining for M3R and red for sm-myosin. The middle panel (C and D) shows a green immuno staining for M3R and in this case a red for immuno staining for sm-α-actin. There is an apparent apparent colocalization in both cases i.e. cells expressing M3R are the ones that are also expressing actin and myosin. The bottom panel (E and F) shows green immuno staining for M3R and red immuno staining for BK that is present in every cell. The nuclei were stained using TOTO3 to blue.

P4 – passage 4, HASMC – human airway smooth muscle cells, M3R- muscarinic 3 receptor, sm – smooth muscle, BK – bradykinin, TOTO3 – blue nuclear stain.

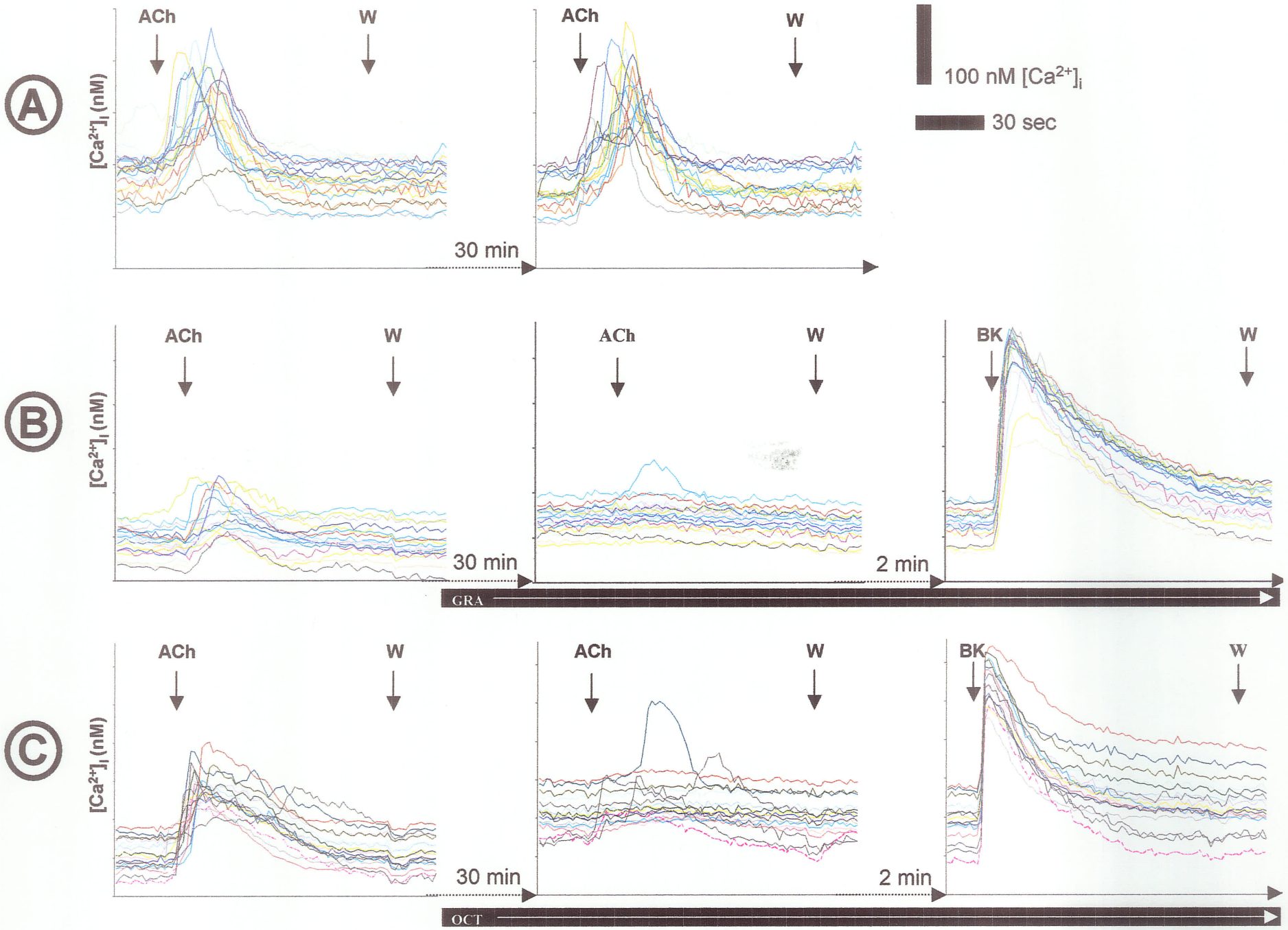
A
ACh
W
ACh
W
100 nM [Ca2+]i
30 sec
[Ca2+]i (nM)
30 min
B
ACh
W
ACh
W
BK
W
[Ca2+]i (nM)
30 min
2 min
GRA
C
ACh
W
ACh
W
BK
W
[Ca2+]i (nM)
30 min
2 min
OCT

Figure 8.

Human airway smooth muscle cell (HASMC) responsiveness to ACh and BK

Images are measurements of intracellular free calcium levels versus time using fura-2 fluorescent dye and ratiometric analysis. Each colored line represents free calcium concentration within a single cell.

8A. Usual response of P4-P6 serum deprived confluent D7 HASMC to repetitive exposure of 10^{-6} Ach. Note that after the first response to Ach the second response is approximately of the same height and occurs approximately with the same delay after exposing the cells to 10^{-6} Ach. Also note the slight temporal shift in both, cells starting to respond and cells reaching peak free intracellular calcium concentration.

8B. After the initial response to 10^{-6} Ach we washed away Ach as in 8A and we incubated the cells for 30 minutes in 100 mM β-glycirrhetinic acid. The same cells in the same analysis field are then exposed to 10^{-6} Ach again. Note the decrease in free intracellular calcium level peak. To prove that the cells are alive we exposed the cells to 10^{-6} BK. BK was picked because all the HASMC in our culture system express BK receptors. Note the brisk and synchronous response to 10^{-6} BK. The synchronicity is likely due to the ubiquitous presence of the BK receptors as opposed to M3R receptors for Ach that are only expressed in ~20% of cells.

8C. The same experiment as in 8B but using 300 mM octanol as GJ blocker. Note the similar effect as in the case of β-glycirrhetinic acid.

Ach – acetylcholine, BK – bradykinin, M3R – muscarinic 3 receptor, W – wash, OCT – octanol, GRA - β-glycirrhetinic acid

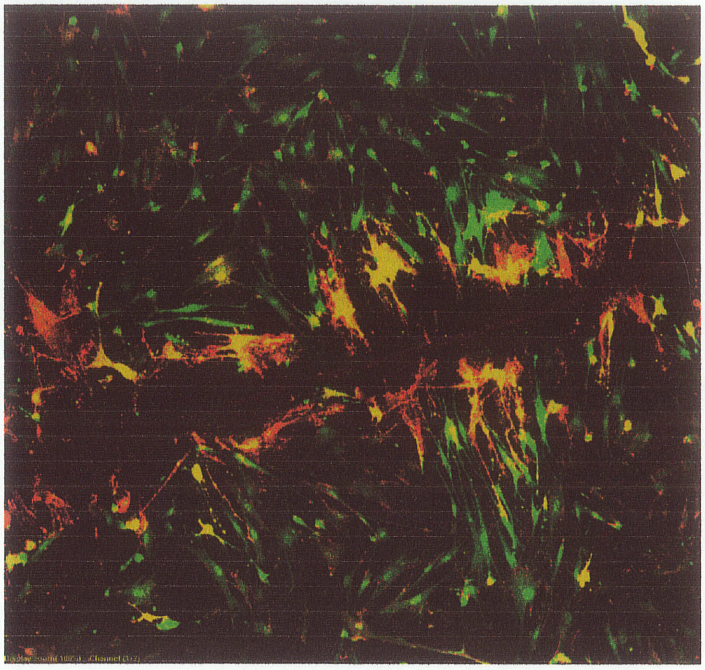

Figure 9.
Scratch wound test on a human airway smooth muscle culture (HASMC).
20X confocal microscope image of P4 confluent serum-deprived HASMC being damaged with a cut through the culture with a scalpel blade while LY and Alexa568 were present in the buffer. The small molecular weight LY was able to enter the damaged cells and diffuse further through intercellular channels from cell to cell. The shape of the cells that got the fluorescence by diffusion is preserved. Alexa568, a large molecular weight fluorescent dye, was only able to enter the cells that were directly damaged by the scalpel. The color of the cells that have both the green LY and the red Alexa568 appears orange colored. The shape of cells with the orange color is distorted i.e. only the directly damaged cells picked up the red fluorescent dye that was unable to diffuse to other undamaged cells through diffusion via intercellular channels.

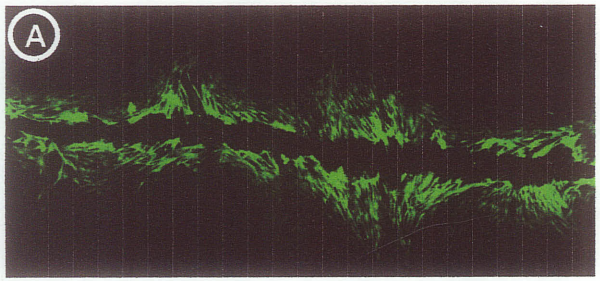
A

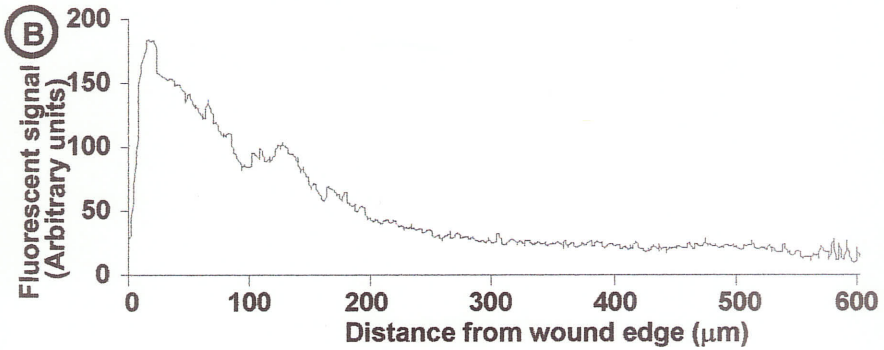
B
Fluorescent signal (Arbitrary units)
200
150
100
50
0
0
100
200
300
400
500
600
Distance from wound edge (μm)

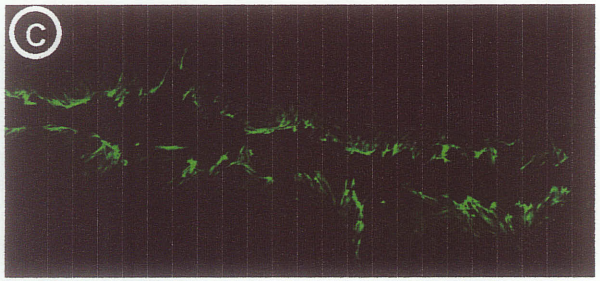
C

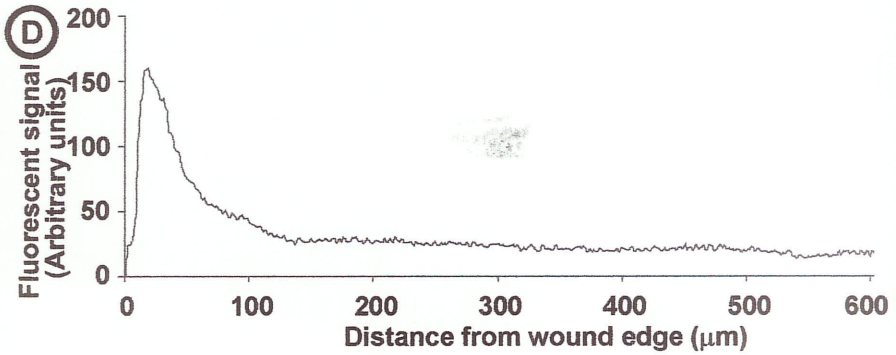
D
Fluorescent signal (Arbitrary units)
200
150
100
50
0
0
100
200
300
400
500
600
Distance from wound edge (μm)

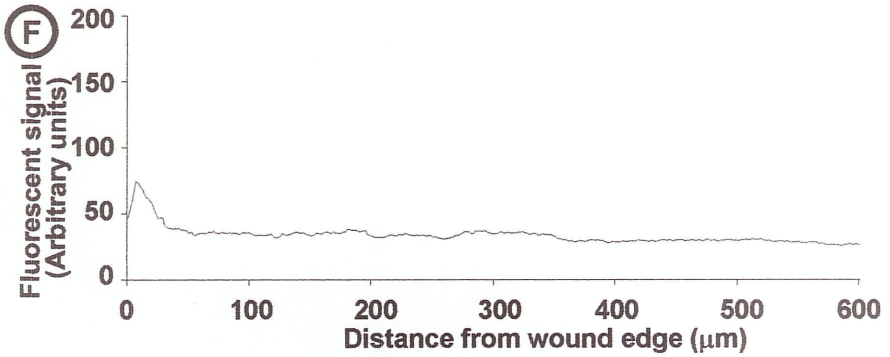
F
Fluorescent signal (Arbitrary units)
200
150
100
50
0
0
100
200
300
400
500
600
Distance from wound edge (μm)

Figure 10.

Scratch wound induced diffusion of Lucifer yellow (LY) in human airway smooth muscle cell (HASMC) culture is inhibited by octanol and β-glycirrhetinic acid.

A: 20X confocal microscopy image of P4 confluent serum deprived HASMC in culture after scraping the culture with a scalpel in the presence of LY. LY diffused from the point of initial line of cell injury towards the periphery. There were no GJ inhibitors in the media, so this is the maximum achievable diffusion in the culture system that was used. (n=3)

B: Graphical representation of the fluorescence intensity versus distance from the scrape wound shown in figure A. Note the high fluorescence intensity (peak of the curve) and long distance the fluorescence dye LY was able to spread. This image is an average of 200 analysis lines as described in methods.

C: 20X confocal microscopy image of P4 confluent serum deprived HASMC in culture after scraping the culture with a scalpel in the presence of LY and octanol. LY diffused from the point of initial line of cell injury towards the periphery. There is a visible marked reduction in diffusion distance because octanol, a GJ inhibitor. (n=3)

D: Graphical representation of the fluorescence intensity versus distance from the scrape wound shown in figure C. Note the lower fluorescence intensity (peak of the curve) and shorter distance the fluorescent dye LY was able to spread than in panel B. This image is an average of 200 analysis lines as described in methods.

E: 20X confocal microscopy image of P4 confluent serum deprived HASMC in culture after scraping the culture with a scalpel in the presence of LY and β-glycirrhetinic acid. LY diffused from the point of initial line of cell injury towards the periphery. There is a visible marked reduction in diffusion distance because β-glycirrhetinic acid, a GJ inhibitor. (n=3)

F: Graphical representation of the fluorescence intensity versus distance from the scrape wound shown in figure E. Note the lower fluorescence intensity (peak of the curve) and shorter distance the fluorescent dye LY was able to spread than in panel B. This image is an average of 200 analysis lines as described in methods.

All fluorescent images are composed of a multitude of smaller 20X confocal images attached to each other giving us a view along the whole scratch wound.

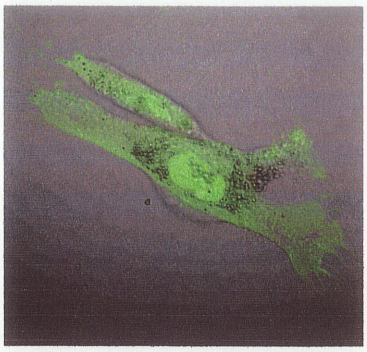

11A

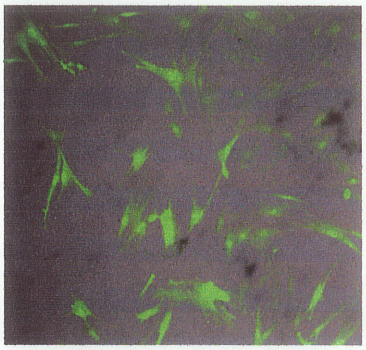

11B

11C

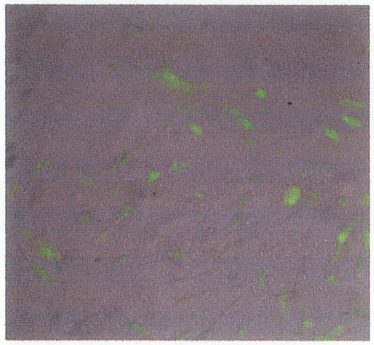

11D

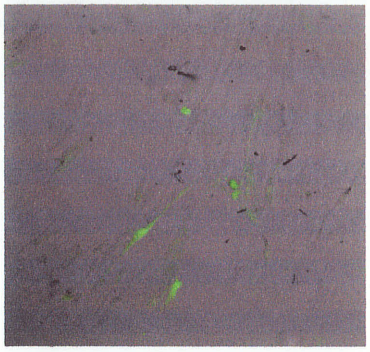

11E

Figure 11

Assessing the presence and functionality of hemichannels in subconfluent human airway smooth muscle cultures (HASMC).

P4 subconfluent serum-fed HASMC in culture were exposed for 5 minutes to LY under different conditions i.e. with or without extracellular calcium and/or with or without a GJ inhibitor that was either octanol or β-glycirrhetinic acid.

11A: 60X confocal image of a HASM cell loaded with LY (green fluorescent dye) within 5 minutes of exposure to a buffer containing LY and no extracellular calcium. Note the detailed visualization of the cytoplasmic distribution of LY.

11B: The same experiment as in 11A at lower magnification. 20x confocal image of P4 HASMC loaded with LY (green fluorescent dye) within 5 minutes of exposure to a buffer containing LY and no extracellular calcium. Note that almost all cells loaded with LY. We assume that all cells at the subconfluent level have functional hemichannels on their surfaces.

11C: 20X confocal image of P4subconfluent serum fed HASMC with extracellular calcium and LY in the buffer solution at the same time. No LY was able to enter the cells, because calcium kept the hemichannels in a closed position.

11D, E: 20X confocal images of P4 subconfluent serum fed HASMC in the presence of no extracellular calcium, which should cause the hemichannels to open, but we added GJ inhibitors, such as β-glycirrhetinic acid (11D) and octanol (11E) to the buffer solution and a marked inhibition in LY diffusion into the cells was noticed.

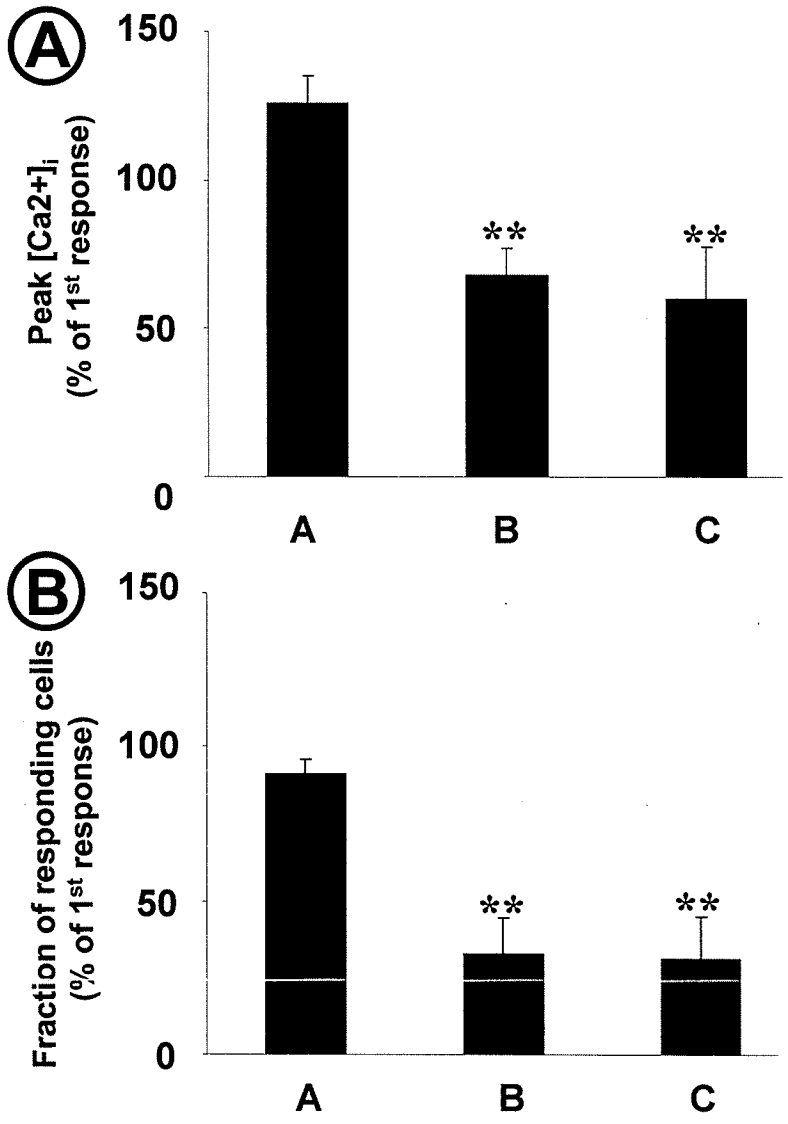
A
150
100
50
0
Peak [Ca2+]i
(% of 1st response)
**
**
A
B
C
B
150
100
50
0
Fraction of responding cells
(% of 1st response)
**
**
A
B
C

Figure 12

Effect of gap junction blockers, octanol and β-glycirrhetinic acid, on human airway smooth muscle cell responsiveness to Ach.

12A.

Column A compares the peak free intracellular calcium levels in P4-P6 confluent serum deprived HASMC after repeated exposure to 10^{-6} Ach. The two exposures were 30 mins apart. Column A represents the second response to 10^{-6} Ach compared to the first one. Note that cells in average have higher peak free intracellular calcium levels. We do not have explanation for this phenomenon, but it is consistently observed in our HASMC experiments.

Column B compares the peak free intracellular calcium levels in P4-P6 confluent serum deprived HASMC after repeated exposure to 10^{-6} Ach. The cells were incubated with 100 mM of β–glycirrhetinic acid for 30 minutes between the two exposures. Note the significantly ($p<0.01$) decreased average peak free intracellular calcium level.

Column C repeats the experiment in Column C but using 300 mM octanol instead of β–glycirrhetinic acid. Note the significantly ($p<0.01$) decreased average peak free intracellular calcium level.

12B

Column A compares the number of P4-P6 confluent serum deprived HASMC response after repeated exposure to 10^{-6} Ach. The two exposures were 30 mins apart. Column A represents the second response to 10^{-6} Ach compared to the first one. Note that only about 90% of cells responded. We do not have explanation for this phenomenon, but it is consistently observed in our HASMC experiments.

Column B compares the number of P4-P6 confluent serum deprived HASMC after repeated exposure to 10^{-6} Ach. The cells were incubated with 100 mM of β–glycirrhetinic acid for 30 minutes between the two exposures. Note the significantly ($p<0.01$) decreased number of responding cells. The cutoff for a cell to be normal second responder was to have at least 80% peak free intracellular calcium level of the first response. This experiment revealed the presence of a subset of HASMC whose response upon 10^{-6} Ach stimulation is gap junction dependent.

Column C repeats the experiment in Column C but using 300 mM octanol instead of β–glycirrhetinic acid. Note the significantly ($p<0.01$) decreased number of responding cells. This experiment also confirmed the presence of a subset of HASMC whose response upon 10^{-6} Ach stimulation is gap junction dependent.

The results were statistically analyzed with one-way ANOVA with Tukey-Kramer Multiple Comparison Test.

** - $p<0.01$

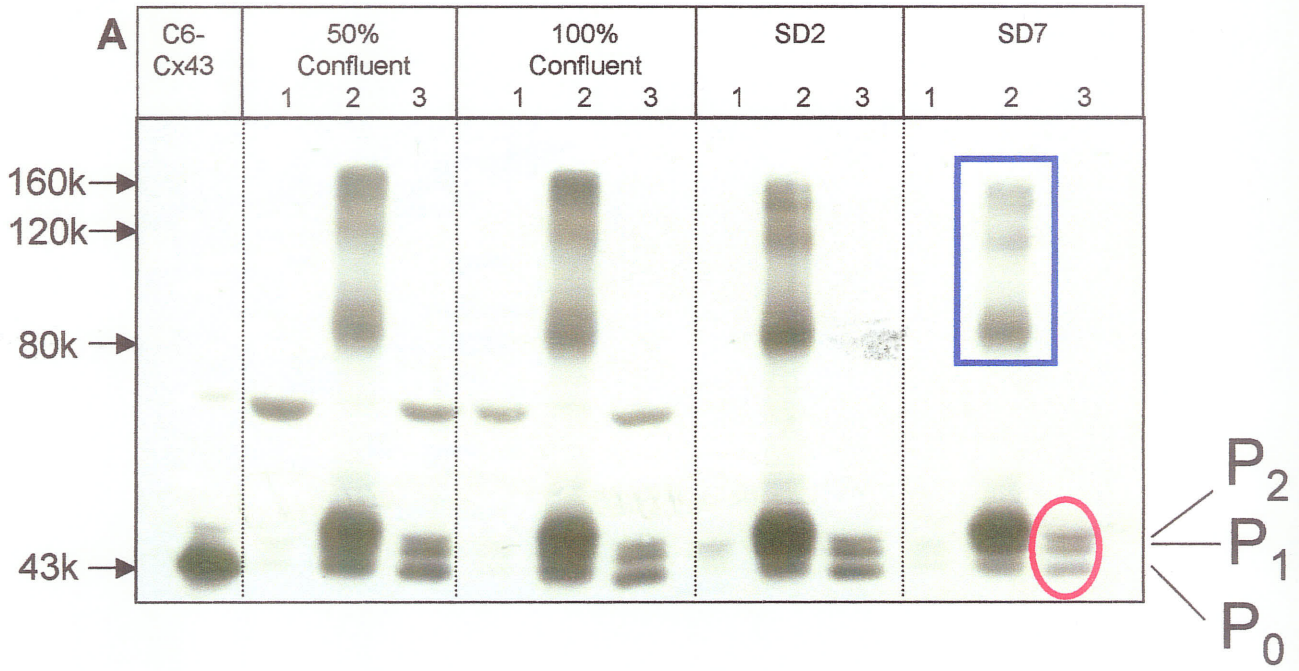
A
C6-Cx43
50% Confluent
1 2 3
100% Confluent
1 2 3
SD2
1 2 3
SD7
1 2 3
160k
120k
80k
43k
P2
P1
P0

Figure 13.

Connexin 43 western blot analysis.

Western blot analysis image that shows the pattern of distribution of Cx43 in cultured HASMC at 50% and 100% of confluence in serum and serum deprived (SD), day 2 and day 7 state. Lane 1 indicates the cytoplasmic fraction of the cells, lane 2 indicates the membrane fraction of the cells and lane 3 is the whole cell lysate. Cx43 is mainly found in the membrane fraction of the cells in all stages of confluence and serum deprivation. The red circle indicates the unphosphorylated (bottom band), less- and more-extensively-phosphorylated Cx43 (middle and top band respectively). On the gel also bands appeared that we believe to be multimeres of Cx43 (dimers, trimers...) as they are binding the primary antibody for Cx43 and are found to be at molecular weights that are multiples of the monomere. These are indicated by a blue square on the image. The first lane contains the C6 glioma cell line that expresses Cx43 in high abundance which was used as a control.

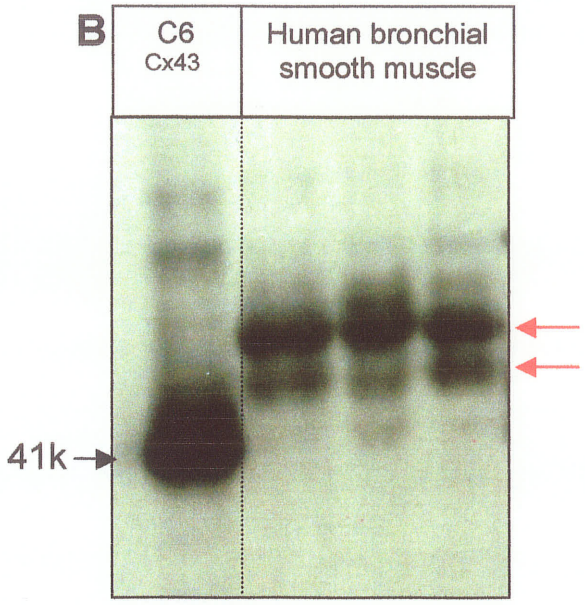

Figure 14.
Human airway smooth muscle tissue western blot analysis.
Western blot analysis performed on fresh human airway smooth muscle tissue that was collected from patients undergoing partial lung resection. C6Cx43 is used as control. All three samples from three different patients demonstrated the presence of Cx43 mainly in the phosphorylated state shown by red arrows. (n=3)

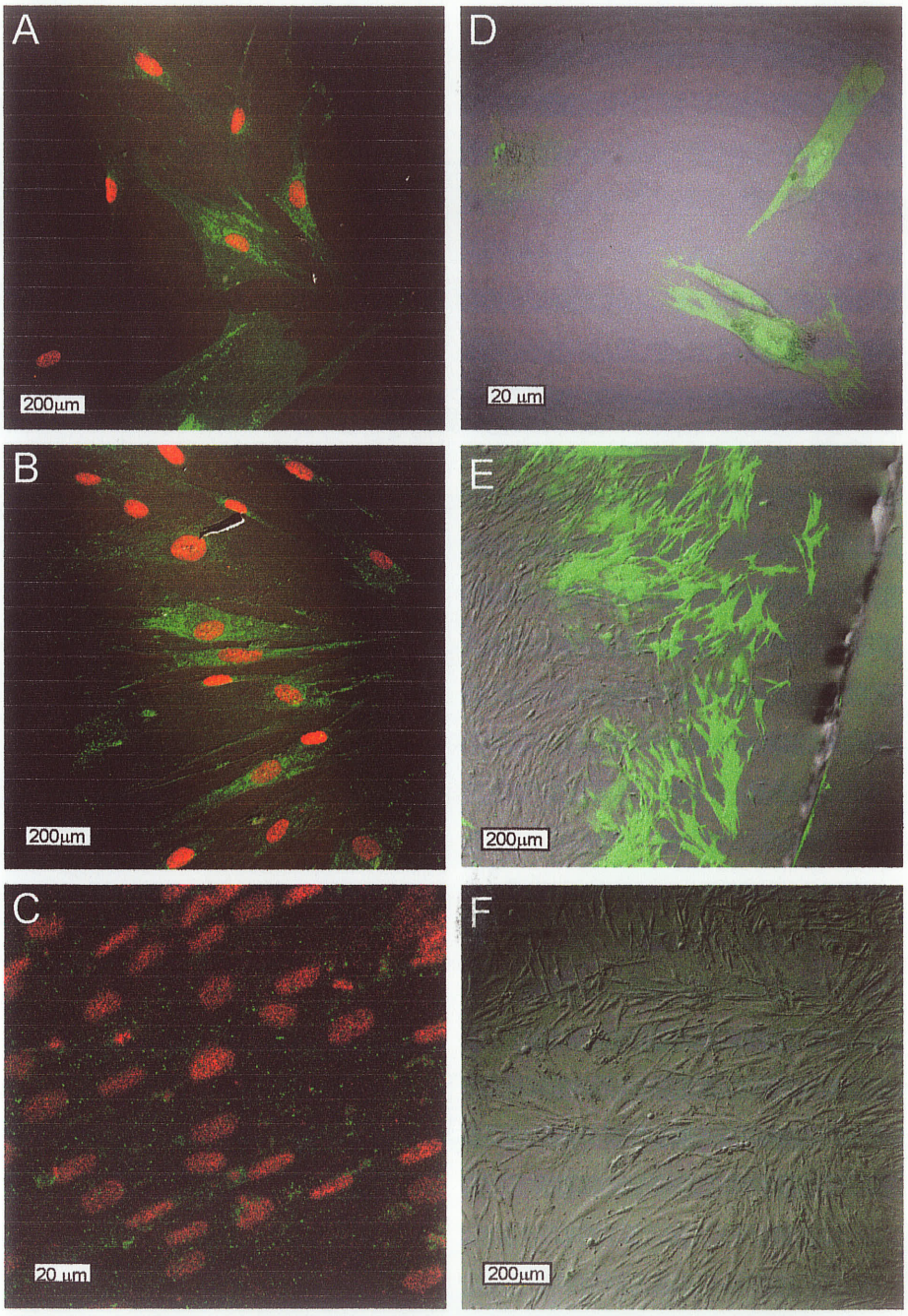

Figure 15.

Figure 15.

Characterization of connexin 43 (Cx43) expression and GJ/hemi channel function in cultured human airway smooth muscle cells (HASMC) depending on the state of confluence.

Pattern of distribution of Cx43 in P4 HASMC in different stages of confluence: A – 25%, B - 75%, C – confluent, serum deprived. Cx43 is stained green and the nuclei are stained red. The patchy distribution (A) gradually changes to punctate, even distribution (C) as the cells become confluent.

In the calcium free environment >95% of the cells loaded with LY (D) (see also figure 11B) in subconfluent state. In the presence of Ca^{2+} none of the cells loaded with LY (Figure 11C) in subconfluent or confluent state. In the calcium free environment confluent cultures did not load with LY presumably because there were no hemichannels available for the dye entry because all hemichannels were "used up" to form GJ with neighboring cells (F). Confluent cultures in calcium free environment loaded on the edges of the culture as there are no neighboring cells to form complete GJ and hemichannels are freely available for dye diffusion (E).

One could argue that the increased LY uptake is due to the loss of viability and secondary increased permeability in the cells once they are exposed to calcium deprivation. This is however unlikely as in figure 15E only the subconfluent part of the culture is loaded with LY and the confluent part is not.

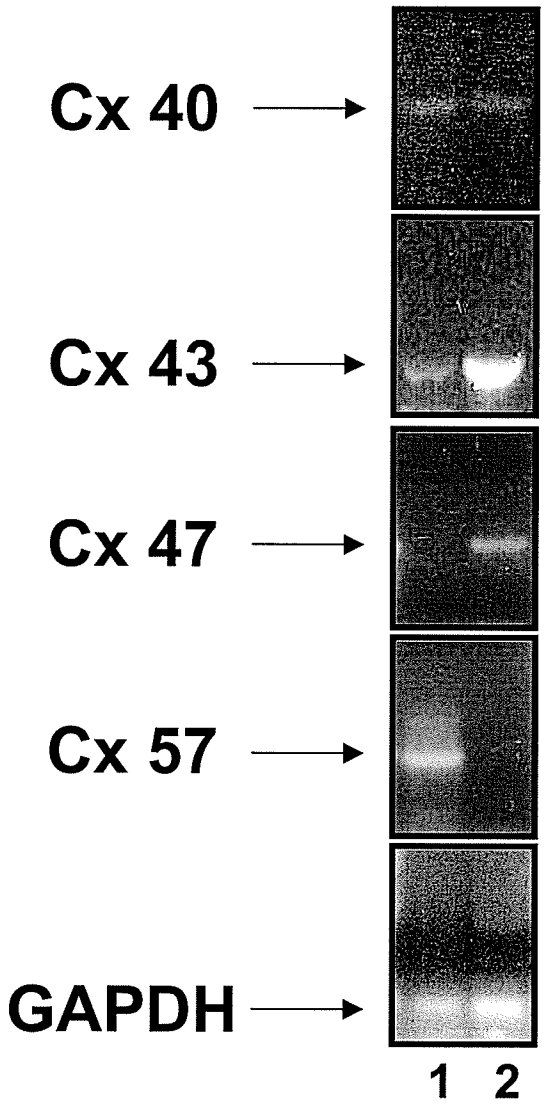

Figure 16.

Screening for connexins in cultured human airway smooth muscle cells using rt-PCR.

rt-PCR results showing expression of connexins 40, 43, 47 and 57 in human airway smooth muscle tissue (lane 1) and in cultured confluent D7 HASMC (lane2). The results confirmed the presence of Cx43 in cultured HASMCs and showed the presence of Cx40, Cx47 and Cx57 with different level of expression depending on whether we tested cells from whole tissue or cells from tissue culture systems. Connexin 40 and 43 are expressed both in human airway smooth muscle tissue and also in cultured HASMC. Connexin 47 is present only in cultured HASMC and connexin 57 is present only in human airway smooth muscle tissue. (n=3)

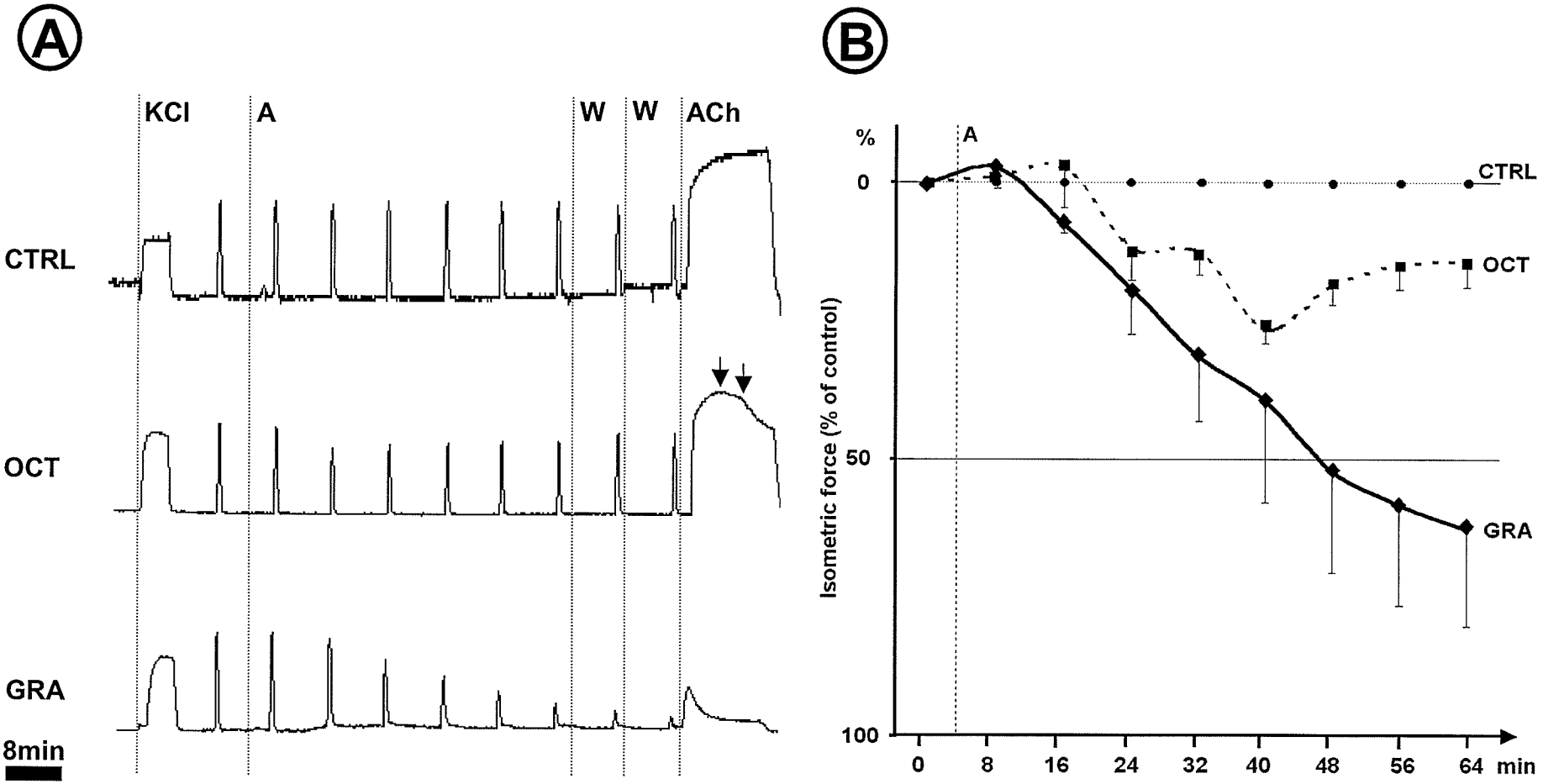
A
KCl
A
W
W
ACh
CTRL
OCT
GRA
8min
B
%
A
0
50
100
CTRL
OCT
GRA
Isometric force (% of control)
0
8
16
24
32
40
48
56
64
min

Figure 17.

Effect of gap junction blockers on electrical field stimulated equine smooth muscle strip contraction.

A: Active isometric force generation in equine tracheal smooth muscle (ETSM) with electrical field stimulation generated peaks on the time/force curves that in the control group (CTRL) were equal in height indicating that over the time of the experiment the muscle remains viable and no significant change in force generation occurs (interval from the time when antagonists octanol (OCT) and β-glycirrhetinic (GRA) acid were added (A) to the first washing (W)). In the group where octanol was added to the bath, there was a decrease in isometric force that is represented by smaller peaks. A much more profound decrease in isometric force was noticed in samples treated with β-glycirrhetinic acid that is represented also by smaller peaks than in the control. After the cells were washed 2 times to remove the GJ inhibitors Ach was added to the baths which triggered a contraction in all the groups. In the octanol group we tried to add back octanol to the bath (represented by black arrows) that resulted in decreased force generation represented by the blunting of the Ach curve upon each addition of octanol. In the β-glycirrhetinic acid group the curve upon Ach introduction started to rise and then started to fall back towards baseline but baseline was not reached until Ach was removed from the bath. We hypothesized that this is probably due to the population of the cells that have Ach receptors and can contract independently without GJ and they stopped to contract after Ach was removed from the bath. (n=3)

B: Chart representation of the above-described experiments in time versus % of inhibition compared to the control. Note the marked inhibition that in the case of GRA is more than 50% of the control. The results were statistically analyzed with one-way ANOVA with Tukey-Kramer Multiple Comparison Test. (n=3)

CTRL – control, OCT – octanol, GRA – glycirrhetinic acid, W – wash, Ach – acetylcholine, A – time when gap junction blockers were added to the bath.

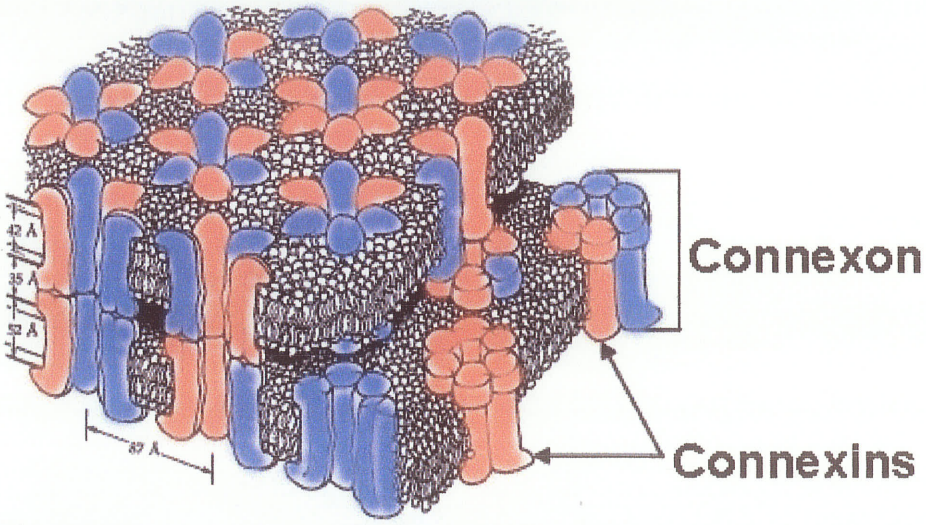

Figure 18

Schematic representation of the gap junctions.

Gap junction proteins (connexins) in hexameric configuration. Two connexons from neighboring cells in close contact dock and begin to gate between the open and closed state of the gap junction channel. The figure shows two connexons associated with one another. Connexin protein in a connexon can vary (as an example both Cx40 and Cx43 can be in the same connexon as indicated in the figure above by different colors [blue = Cx40 while pink = Cx43]). Note the different proportion of Cx40 and Cx43 in the same connexon.

(Picture by David Kurjiaka, PhD, Pennsylvania State University)

a

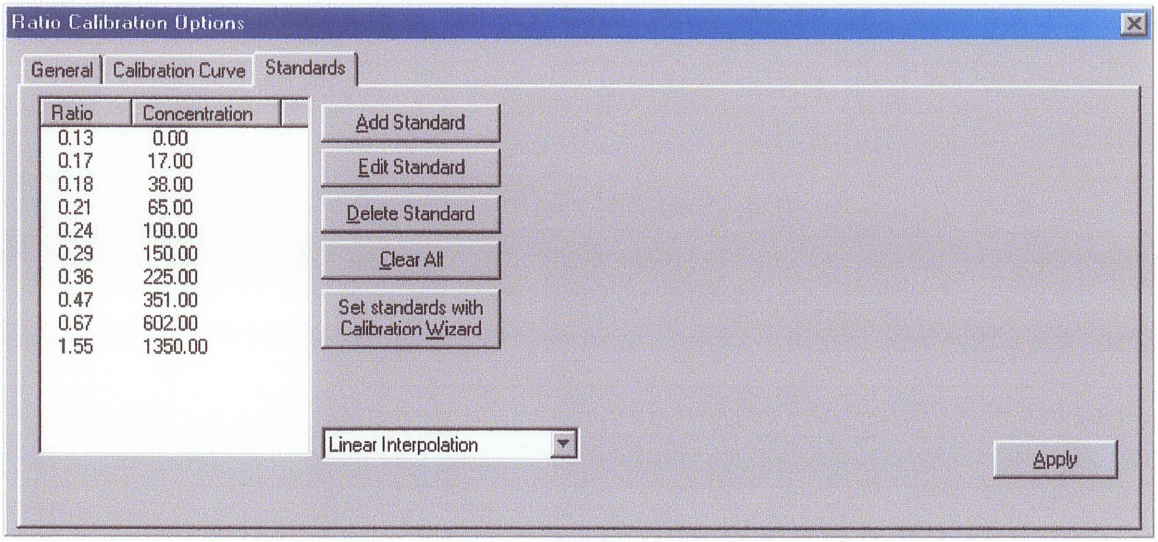

b

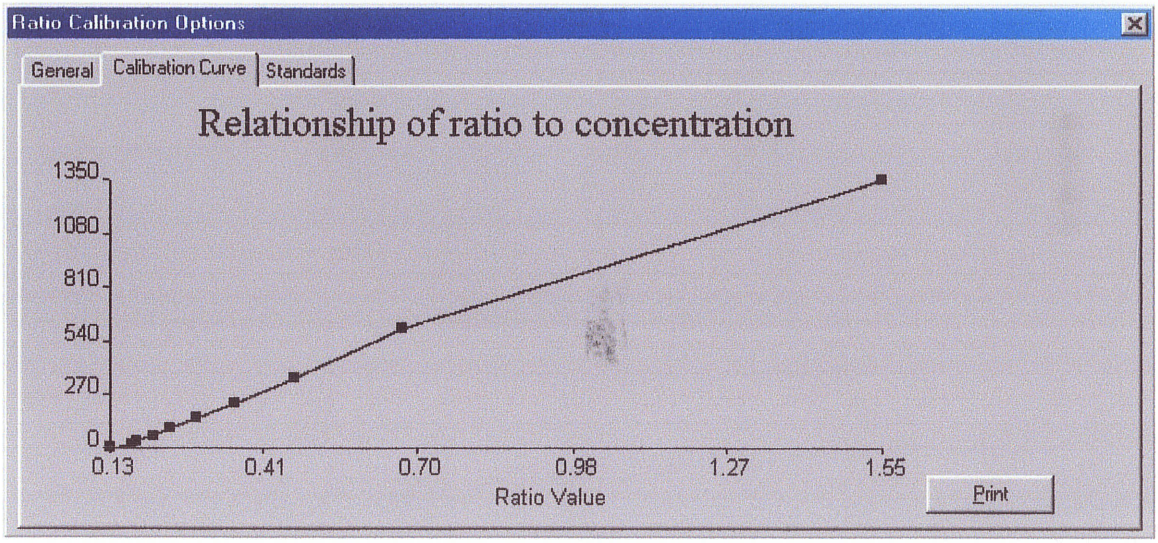

Figure 19 a, b
CALIBRATION CURVE CONSTRUCTION

Figure 19 a, b

CALIBRATION CURVE CONSTRUCTION

a. The UltraView software interface, where we enter the data (ratio and concentration) acquired during the sequential calibration measurements of solutions with known calcium concentrations using Molecular Probes (F-6774) Fura-2 Calcium Imaging Calibration Kit.
b. Using the above-mentioned data the software draws a calibration curve. This curve is used by the computer to convert gray scale data acquired during measurements to levels of free calcium.

Leaf inserted to correct page numbering

DISCUSSION

(Significance and Future Directions)

Our studies show that human airway smooth muscle cells in culture and fresh tissue lysates express functional gap junctions. Because of the scarce availability of human airway smooth muscle tissue, in situ experiments were not performed. Further our studies have characterized for the first time the expression pattern and distribution of connexin proteins in airway smooth muscle cells and tissues. Specifically we observed that in situ human bronchial smooth muscle cells express abundant Cx43, Cx40, and Cx57, and that though primary cultured HASMC also express Cx43 and Cx40, they are deficient in Cx57 mRNA and express Cx47, which was absent in myocytes from intact airway smooth muscle tissue. The presence of mRNA however does not mean that the protein is expressed. So in the cases of connexins other than Cx43 where western blot analysis were not performed we cannot assume that the protein is made, we know only that there is a potential of the above mentioned protein formation. We used immunocytochemistry, Western Blot, and RT-PCR to detect connexin expression and cellular distribution in cultured HASMC and human bronchial smooth muscles. Our studies were limited to the analysis of connexins that had been previously published reported in various smooth muscle tissues [221-223]. Undoubtedly a more thorough survey of the full range of connexins described in all tissues will reveal that airway smooth muscle cells also express other connexins. In addition, other than to compare connexin expression in tissue and cultured cells, we have not investigated how the profile of connexins expressed by airway smooth muscle cells might be altered during

development and in disease states such as asthma that affect the function and abundance of airway smooth muscle. Based on our studies that showed GJs play a significant role in determining contractile function of airway smooth muscle changes in expression of connexins and/or in regulation of GJ opening that could occur associated with disease states may play a critical role in disease morbidity and pathophysiology. As dramatic remodeling or the airways that occurs in asthma and is associated development of hypercontractile properties of airway smooth muscle, clearly the studies described in this report should be extended to determine if changes in connexin expression and GJ function occurs in parallel with disease progression.

We performed a series of studies using primary cultured HASMC and intact equine tracheal smooth muscle that provided functional evidence for the presence of GJs. Using a scrape-loading assay and Lucifer Yellow loading in Ca^{2+}-deficient buffer, our experiments showed not just the presence, but also how the functional competence of gap junctions in primary cultured human airway smooth muscle cells was affected by cell density. Though the abundance of Cx43 protein appeared to be stable in all cell culture conditions, the cellular distribution was greatly affected by the proximity of other cells. In subconfluent culture airway myocytes appear to have a large number of functional hemichannels that served as an effective conduit to load Lucifer Yellow. The physiological relevance of these channels is not clear, though hemichannels have been shown to play a critical role in juxtacrine and paracrine signal transduction for molecules such as adenosine and ATP between some cell types. As these mediators in particular play a role in controlling contraction, proliferation and migration of cultures airway

myocytes, clearly our results suggest that future studies of the precise role for GJs in mechanisms that determine the role of these mediators in controlling airway smooth function are warranted. Our experiments using scrape loading and Lucifer Yellow loading in Ca^{2+}-deficient buffer also revealed the effectiveness of using two general GJ inhibitors, octanol and β-glycirrhetinic acid, to investigate the role of GJs in airway myocyte cell physiology, and suggests that mediators such as these will be extremely useful tools for future investigations.

In addition to studies to determine whether functional GJs were present in primary cultured HASMC we also used chemical inhibitors of GJs to assess the role of myocyte-myocyte coupling in intracellular signalling in response to contractile agonists. The unique cell culture system we employed possessed several key characteristics that contributed to the extent of the conclusions we were able to derive. First, in serum deprived cultures at least two phenotypically disparate myocyte cell populations developed, and importantly our immunocytochemical analyses demonstrated that a unique population, comprising only ~20% of all cells, express the Gαq-coupled M3R that mediate ACh-induced mobilization of IP3-sensitive intracellular Ca^{2+} stores into the cytosol. Second, despite the fact that only a relatively small subgroup of myocytes express M3R, our experiments using fura-2 loaded myocytes revealed virtually all cells could be induced to mobilize intracellular Ca^{2+} after ACh exposure. This observation suggested that the myocytes in confluent primary cultures were capable of cell-cell communication, and our experiments using octanol and β-glycirrhetinic acid confirmed that in ~80% of myocytes, Ca^{2+} mobilization after ACh exposure was GJ-dependent.

Third, despite the heterogeneity we observed in M3R expression, virtually all myocytes in confluent serum-deprived HASMC cultures appeared to express the Gαq-coupled BK2 receptor for bradykinin and mobilized intracellular Ca^{2+} in a temporally synchronous manner. This character provided an internal control mechanism for us to confirm that the GJ inhibitors we used had little effect of receptor mediated signal transduction, rather their effects were exclusively associated with the open/close state of GJs in our myocyte culture model.

We also performed a series of studies using intact airway smooth muscle that were an extension of our experiments using primary cultured HASMC. These experiments demonstrated for the first time that GJs, which, based on electron microscopy, have previously been reported to exist in airway smooth muscle, play a significant functional role in controlling contraction of airway smooth muscle tissues in response physiologically relevant stimulation via parasympathetic neurons. As noted in an early comment, this observation as potential to provide new insight to mechanisms that might control altered airway smooth muscle contractility in disease states such as asthma. Though hyperresponsiveness of the airways to allergic and non-allergic stimuli is a key feature of bronchial asthma that is linked with local inflammation and structural remodelling (i.e. airway smooth muscle hypertrophy), the cellular and molecular mechanisms that contribute directly to the hypercontractile response of airway smooth muscle are not well understood. Our studies suggest that GJs have the potential to contribute to changes in contractile properties of airway smooth muscle, thus GJs could

represent novel mechanism for altered contractile function in asthma; on this basis future studies to investigate this possibility are warranted.

In addition to our studies of GJs and their presence in airway smooth muscle, a cause-effect role for GJs in physiology and pathophysiology associated with smooth muscle containing organs in humans have been reported. Perhaps the best-studied system is the myometrium during pregnancy. Near the end of the third trimester prior to labour the number of GJ, and abundance of connexin protein and mRNA exhibit a multi-fold increase in uterine smooth muscle cells [112]. This dramatic increase in GJ number leads coverts the uterine smooth muscle from that of a multiunit type (i.e. few GJ) to that of a single unit type (i.e a highly coupled syncitium), a process that is essential to ensure precise coordination of contractions so that sufficient force can be generated to facilitate successful birth of the baby. The dramatic increase in connexin expression and GJ number appears to be controlled by programmed changes in hormone levels (ie. estrogen and progesterone) during the latter stages of pregnancy [112]. It is not known whether connexin expression and GJ number in lung cells may also be controlled dynamically by such factors as changes in hormonal status in women and men. However, a potential association between normal physiologic fluctuation in hormonal levels and lung function has been described for a condition that has been termed "premenstrual asthma" [224]. In some women the condition is characterized by the frequent occurrence of asthma exacerbation immediately preceding the onset of menses. Though there is no evidence linking GJ number in airway smooth muscle to these episodes, it is intriguing to speculate that normal fluctuations in progesterone and

estrogen occur as in the menstrual cycle may induce transient changes in GJ function that could contribute to the disorder. As this hypothesis is entirely speculative, clearly a definitive studies investigating the effects of progesterone and/or estrogen on connexin expression and GJ function in airway smooth muscle cells in vitro, in situ and in vivo need to be completed. As excessive contraction of airway smooth muscle is the principal factor that contributes to acute asthma exacerbations, the most troublesome aspect of the disease, it is worth speculating in general about the possibility that changes in GJ number of function might in some way modulate disease pathophysiology. Therefore, the results of our project suggest that future studies examining the effects of asthma-associated pro-inflammatory mediators may be insightful. Many questions relating the effects of inflammation on GJ in airway smooth muscle could be addressed using the in vitro and in vivo sytems, cells and compounds we have employed in our current project. A number of studies examining the effects of inflammation during sepsis on GJ number in vascular smooth muscle indicate that some inflammatory mediators are capable of affecting connexin expression and functional GJ-associated parameters [225].

The usual goal of a medical research project is to get new discoveries from the bench to the bedside. There are a number of reasons why our project has the potential to be used as a springboard leading to new approaches to treat people with airway reactive diseases (eg. asthma and COPD). There is good evidence that only a subset of bronchial smooth muscle cells in pig airway is innervated directly by parasympathetic neurons (Figure 4)[208]. As porcine and human lung physiology and structure is known to be quite similar, it would seem reasonable to expect a similar organization of

myocytes and neurons in human airway smooth muscle tissue. Of note, preliminary studies from Dr. Halayko's using confocal microscopy (not shown) indicate that M3R expressed by human bronchial smooth muscle are almost exclusively localized to sites of parasympathetic varicosities (sites of active ACh release). Thus it seems likely that not all myocytes in intact bronchial smooth muscle, and in particular those that are not in the immediate vicinity of parasympathetic nerve varicosities, respond directly to ACh released from nerves that innervate the tissue. This implies that signals to induce contraction of entire bronchial smooth muscle segments rely upon effective signal transduction between coupled myocytes, and that changes in functional competence may modulate contractile responses. On this basis, the delivery if of a therapeutic agent that inhibits myocyte-myocyte coupling would have potential to dampen airway constriction. To avoid systemic effect on the body as a whole an inhaler form could be utilised to have just limited local action as in the case of commonly used of inhaled corticosteroids, leukotrien inhibitors, beta agonists, and acetylcholine receptor blockers these days. The compounds employed for our studies, octanol and β-glycirrhetinic acid, are widely used by GJ investigators to modulate the open/close state of these channels. Octanol is commonly used in the perfume industry, and β-glycirrhetinic acid accumulates in the blood after consuming licorice. One study examined the effects of licorice consumption on human pulmonary function and the results revealed that licorice consumption lead to a moderate improvement in selected lung function parameters of some patients in the study [226]. Octanol and β-glycirrhetinic acid are relatively non-toxic, thus potentially could be used as agents to try in whole animal experiments to test their potential effectiveness to inhibit airway constriction in vivo. Hypothetically, a good

GJ blocker inhaler could be another way to fight airway reactive diseases such as asthma and COPD either alone or in combination with other agents and this way alleviate the severity and duration of an asthmatic attack.

References

1. McIntyre, B.A., et al., *Glomulin is predominantly expressed in vascular smooth muscle cells in the embryonic and adult mouse.* Gene Expr Patterns, 2004. **4**(3): p. 351-8.
2. Fredberg, J.J., *Bronchospasm and its biophysical basis in airway smooth muscle.* Respir Res, 2004. **5**(1): p. 2.
3. Suzuki, R. and S. Kobayashi, *Effects of divalent cations on the spontaneous synchronization in mammalian iris sphincter muscle cells.* Exp Eye Res, 1986. **42**(5): p. 407-15.
4. Bitar, K.N., *Function of gastrointestinal smooth muscle: from signaling to contractile proteins.* Am J Med, 2003. **115 Suppl 3A**: p. 15S-23S.
5. Kippelen, P., et al., *Asthma and exercise-induced bronchoconstriction in amateur endurance-trained athletes.* Int J Sports Med, 2004. **25**(2): p. 130-2.
6. Goldman, Y.E. and A.F. Huxley, *Actin compliance: are you pulling my chain?* Biophys J, 1994. **67**(6): p. 2131-3.
7. Huxley, H.E., et al., *X-ray diffraction measurements of the extensibility of actin and myosin filaments in contracting muscle.* Biophys J, 1994. **67**(6): p. 2411-21.
8. Mijailovich, S.M., J.J. Fredberg, and J.P. Butler, *On the theory of muscle contraction: filament extensibility and the development of isometric force and stiffness.* Biophys J, 1996. **71**(3): p. 1475-84.
9. Wakabayashi, K., et al., *X-ray diffraction evidence for the extensibility of actin and myosin filaments during muscle contraction.* Biophys J, 1994. **67**(6): p. 2422-35.
10. Gunst, S.J., et al., *Mechanisms for the mechanical plasticity of tracheal smooth muscle.* Am J Physiol, 1995. **268**(5 Pt 1): p. C1267-76.
11. Gunst, S.J., M.F. Wu, and D.D. Smith, *Contraction history modulates isotonic shortening velocity in smooth muscle.* Am J Physiol, 1993. **265**(2 Pt 1): p. C467-76.
12. Mehta, D. and S.J. Gunst, *Actin polymerization stimulated by contractile activation regulates force development in canine tracheal smooth muscle.* J Physiol, 1999. **519 Pt 3**: p. 829-40.
13. Mehta, D., et al., *Role of Rho in Ca(2+)-insensitive contraction and paxillin tyrosine phosphorylation in smooth muscle.* Am J Physiol Cell Physiol, 2000. **279**(2): p. C308-18.
14. Pratusevich, V.R., C.Y. Seow, and L.E. Ford, *Plasticity in canine airway smooth muscle.* J Gen Physiol, 1995. **105**(1): p. 73-94.
15. Seow, C.Y., V.R. Pratusevich, and L.E. Ford, *Series-to-parallel transition in the filament lattice of airway smooth muscle.* J Appl Physiol, 2000. **89**(3): p. 869-76.
16. Fredberg, J.J., *Frozen objects: small airways, big breaths, and asthma.* J Allergy Clin Immunol, 2000. **106**(4): p. 615-24.
17. Fredberg, J.J., et al., *Perturbed equilibrium of myosin binding in airway smooth muscle and its implications in bronchospasm.* Am J Respir Crit Care Med, 1999. **159**(3): p. 959-67.
18. Gunst, S.J., J.Q. Stropp, and J. Service, *Mechanical modulation of pressure-volume characteristics of contracted canine airways in vitro.* J Appl Physiol, 1990. **68**(5): p. 2223-9.
19. King, G.G., et al., *Time course of increased airway narrowing caused by inhibition of deep inspiration during methacholine challenge.* Am J Respir Crit Care Med, 1999. **160**(2): p. 454-7.

20. Stephens, N.L., et al., *The biophysics and biochemistry of smooth muscle contraction.* Can J Physiol Pharmacol, 1992. **70**(4): p. 515-31.
21. Halayko, A.J., et al., *Divergent differentiation paths in airway smooth muscle culture: induction of functionally contractile myocytes.* Am J Physiol, 1999. **276**(1 Pt 1): p. L197-206.
22. Roux, E., et al., *Muscarinic stimulation of airway smooth muscle cells.* Gen Pharmacol, 1998. **31**(3): p. 349-56.
23. Mitchell, R.W., et al., *Selective restoration of calcium coupling to muscarinic M(3) receptors in contractile cultured airway myocytes.* Am J Physiol Lung Cell Mol Physiol, 2000. **278**(5): p. L1091-100.
24. Stephens, N.L., *Airway smooth muscle.* Lung, 2001. **179**(6): p. 333-73.
25. Stephens, N.L., et al., *The contractile apparatus of airway smooth muscle. Biophysics and biochemistry.* Am J Respir Crit Care Med, 1998. **158**(5 Pt 3): p. S80-94.
26. Huxley, H.E., *The mechanism of muscular contraction.* Science, 1969. **164**(886): p. 1356-65.
27. Statistics, C., *National Population Health Survey: Asthma Supplementary Survey.* 1997. **http://www.hc-sc.gc.ca/hpb/lcdc/brch/measuring/mu_r_e.html**.
28. Conference, *Canadian Asthma Consensus.* http://www.pulsus.com/Respir/03_02/erns_ed.htm, 1996.
29. Baldwin, L. and W.R. Roche, *Does remodelling of the airway wall precede asthma?* Paediatr Respir Rev, 2002. **3**(4): p. 315-20.
30. Halayko, A.J. and N.L. Stephens, *Potential role for phenotypic modulation of bronchial smooth muscle cells in chronic asthma.* Can J Physiol Pharmacol, 1994. **72**(11): p. 1448-57.
31. Davies, D.E., et al., *Airway remodeling in asthma: new insights.* J Allergy Clin Immunol, 2003. **111**(2): p. 215-25; quiz 226.
32. Foster, P.S., et al., *CD4(+) T-lymphocytes regulate airway remodeling and hyper-reactivity in a mouse model of chronic asthma.* Lab Invest, 2002. **82**(4): p. 455-62.
33. Little, S.A., et al., *High resolution computed tomographic assessment of airway wall thickness in chronic asthma: reproducibility and relationship with lung function and severity.* Thorax, 2002. **57**(3): p. 247-53.
34. Kasahara, K., et al., *Correlation between the bronchial subepithelial layer and whole airway wall thickness in patients with asthma.* Thorax, 2002. **57**(3): p. 242-6.
35. Krymskaya, V.P., et al., *Activation of class IA PI3K stimulates DNA synthesis in human airway smooth muscle cells.* Am J Physiol Lung Cell Mol Physiol, 2001. **280**(5): p. L1009-18.
36. Panettieri, R.A., Jr., et al., *Repeated allergen inhalations induce DNA synthesis in airway smooth muscle and epithelial cells in vivo.* Am J Physiol, 1998. **274**(3 Pt 1): p. L417-24.
37. Panettieri, R.A., et al., *Histamine stimulates proliferation of airway smooth muscle and induces c-fos expression.* Am J Physiol, 1990. **259**(6 Pt 1): p. L365-71.
38. Sommerhoff, C.P., *Mast cell tryptases and airway remodeling.* Am J Respir Crit Care Med, 2001. **164**(10 Pt 2): p. S52-8.
39. van der Velden, V.H. and A.R. Hulsmann, *Autonomic innervation of human airways: structure, function, and pathophysiology in asthma.* Neuroimmunomodulation, 1999. **6**(3): p. 145-59.

40. Kaliner, M., et al., *Autonomic nervous system abnormalities and allergy.* Ann Intern Med, 1982. **96**(3): p. 349-57.
41. Hossain, S., *Quantitative measurement of bronchial muscle in men with asthma.* Am Rev Respir Dis, 1973. **107**(1): p. 99-109.
42. Ebina, M., et al., *Cellular hypertrophy and hyperplasia of airway smooth muscles underlying bronchial asthma. A 3-D morphometric study.* Am Rev Respir Dis, 1993. **148**(3): p. 720-6.
43. Tomas, J.J., et al., *Beta-galactosidase-tagged adventitial myofibroblasts tracked to the neointima in healing rat vein grafts.* J Vasc Res, 2003. **40**(3): p. 266-75.
44. Medrado, A.R., et al., *Influence of low level laser therapy on wound healing and its biological action upon myofibroblasts.* Lasers Surg Med, 2003. **32**(3): p. 239-44.
45. Cheng, B., et al., *[The effect of basic fibroblast growth factor on myofibroblasts and its significance on wound healing].* Zhonghua Yi Xue Za Zhi, 2002. **82**(17): p. 1187-91.
46. Hoshino, M., et al., *Bronchial subepithelial fibrosis and expression of matrix metalloproteinase-9 in asthmatic airway inflammation.* J Allergy Clin Immunol, 1998. **102**(5): p. 783-8.
47. Brewster, C.E., et al., *Myofibroblasts and subepithelial fibrosis in bronchial asthma.* Am J Respir Cell Mol Biol, 1990. **3**(5): p. 507-11.
48. Gizycki, M.J., et al., *Myofibroblast involvement in the allergen-induced late response in mild atopic asthma.* Am J Respir Cell Mol Biol, 1997. **16**(6): p. 664-73.
49. Phipps, S., et al., *The relationship between allergen-induced tissue eosinophilia and markers of repair and remodeling in human atopic skin.* J Immunol, 2002. **169**(8): p. 4604-12.
50. Schmidt, M., et al., *Identification of circulating fibrocytes as precursors of bronchial myofibroblasts in asthma.* J Immunol, 2003. **171**(1): p. 380-9.
51. Hoshino, M., et al., *Inhaled corticosteroid reduced lamina reticularis of the basement membrane by modulation of insulin-like growth factor (IGF)-I expression in bronchial asthma.* Clin Exp Allergy, 1998. **28**(5): p. 568-77.
52. Ollerenshaw, S.L., et al., *Substance P immunoreactive nerves in airways from asthmatics and nonasthmatics.* Eur Respir J, 1991. **4**(6): p. 673-82.
53. Ollerenshaw, S., et al., *Absence of immunoreactive vasoactive intestinal polypeptide in tissue from the lungs of patients with asthma.* N Engl J Med, 1989. **320**(19): p. 1244-8.
54. Howarth, P.H., et al., *Neuropeptide-containing nerves in endobronchial biopsies from asthmatic and nonasthmatic subjects.* Am J Respir Cell Mol Biol, 1995. **13**(3): p. 288-96.
55. Ollerenshaw S, W.A., *Quantification and location of vasoactive intestinal peptide immunoreactive nerves in bronchial biopsies from subjects with mild asthma.* Am Rev Respir Dis, 1993. **147**: p. A285.
56. Sharma R, J.P., *Airway VIP receptor number is reduced in cystic fibrosis but not in asthma.* Am Rev Respir Dis, 1990. **141**: p. A726.
57. Goldhill, J., et al., *Interleukin-4 modulates cholinergic neural control of mouse small intestinal longitudinal muscle.* Am J Physiol, 1997. **272**(5 Pt 1): p. G1135-40.
58. Nawa, H., S. Nakanishi, and P.H. Patterson, *Recombinant cholinergic differentiation factor (leukemia inhibitory factor) regulates sympathetic neuron phenotype by alterations in the size and amounts of neuropeptide mRNAs.* J Neurochem, 1991. **56**(6): p. 2147-50.
59. Haley, K.J. and J.M. Drazen, *Inflammation and airway function in asthma: what you see is not necessarily what you get.* Am J Respir Crit Care Med, 1998. **157**(1): p. 1-3.

60. Cohn, L., J.S. Tepper, and K. Bottomly, *IL-4-independent induction of airway hyperresponsiveness by Th2, but not Th1, cells.* J Immunol, 1998. **161**(8): p. 3813-6.
61. Amrani, Y. and R.A. Panettieri, Jr., *Cytokines induce airway smooth muscle cell hyperresponsiveness to contractile agonists.* Thorax, 1998. **53**(8): p. 713-6.
62. Einarsson, O., et al., *Interleukin-11: stimulation in vivo and in vitro by respiratory viruses and induction of airways hyperresponsiveness.* J Clin Invest, 1996. **97**(4): p. 915-24.
63. Bruzzone, R., T.W. White, and D.L. Paul, *Connections with connexins: the molecular basis of direct intercellular signaling.* Eur J Biochem, 1996. **238**(1): p. 1-27.
64. Evans, W.H. and P.E. Martin, *Gap junctions: structure and function (Review).* Mol Membr Biol, 2002. **19**(2): p. 121-36.
65. Beblo, D.A. and R.D. Veenstra, *Monovalent cation permeation through the connexin40 gap junction channel. Cs, Rb, K, Na, Li, TEA, TMA, TBA, and effects of anions Br, Cl, F, acetate, aspartate, glutamate, and NO3.* J Gen Physiol, 1997. **109**(4): p. 509-22.
66. Murray, S.A. and W.H. Fletcher, *Hormone-induced intercellular signal transfer dissociates cyclic AMP-dependent protein kinase.* J Cell Biol, 1984. **98**(5): p. 1710-9.
67. Saez, J.C., et al., *Hepatocyte gap junctions are permeable to the second messenger, inositol 1,4,5-trisphosphate, and to calcium ions.* Proc Natl Acad Sci U S A, 1989. **86**(8): p. 2708-12.
68. Pitts, J.D. and J.W. Simms, *Permeability of junctions between animal cells. Intercellular transfer of nucleotides but not of macromolecules.* Exp Cell Res, 1977. **104**(1): p. 153-63.
69. White, T.W., *Nonredundant gap junction functions.* News Physiol Sci, 2003. **18**: p. 95-9.
70. Musil, L.S., et al., *Differential phosphorylation of the gap junction protein connexin43 in junctional communication-competent and -deficient cell lines.* J Cell Biol, 1990. **111**(5 Pt 1): p. 2077-88.
71. Trosko, J.E. and R.J. Ruch, *Cell-cell communication in carcinogenesis.* Front Biosci, 1998. **3**: p. D208-36.
72. Rose, B. and W.R. Loewenstein, *Calcium ion distribution in cytoplasm visualised by aequorin: diffusion in cytosol restricted by energized sequestering.* Science, 1975. **190**(4220): p. 1204-6.
73. John, S., D. Cesario, and J.N. Weiss, *Gap junctional hemichannels in the heart.* Acta Physiol Scand, 2003. **179**(1): p. 23-31.
74. Garcia-Dorado, D., et al., *Gap junction-mediated intercellular communication in ischemic preconditioning.* Cardiovasc Res, 2002. **55**(3): p. 456-65.
75. Cascio, M., et al., *Physical characterization of gap junction membrane connexons (hemi-channels) isolated from rat liver.* J Biol Chem, 1995. **270**(31): p. 18643-8.
76. Benedetti, E.L., et al., *Structural organization of gap junctions as revealed by freeze-fracture and SDS fracture-labeling.* Eur J Cell Biol, 2000. **79**(8): p. 575-82.
77. Bukauskas, F.F., et al., *Clustering of connexin 43-enhanced green fluorescent protein gap junction channels and functional coupling in living cells.* Proc Natl Acad Sci U S A, 2000. **97**(6): p. 2556-61.
78. Quist, A.P., et al., *Physiological role of gap-junctional hemichannels. Extracellular calcium-dependent isosmotic volume regulation.* J Cell Biol, 2000. **148**(5): p. 1063-74.
79. Rozental, R., C. Giaume, and D.C. Spray, *Gap junctions in the nervous system.* Brain Res Brain Res Rev, 2000. **32**(1): p. 11-5.

80. Toyofuku, T., et al., *[Functional role and molecular mechanism of intercellular signaling via gap junction].* Tanpakushitsu Kakusan Koso, 2001. **46**(10): p. 1367-73.
81. Toth, T., et al., *[Frequency of the Connexin26/35delG mutation and its characteristic phenotype in patients with hearing impairment and controls in Northeastern Hungary].* Orv Hetil, 2002. **143**(40): p. 2285-9.
82. Iliades, T., et al., *Prelingual nonsyndromic hearing loss in Greece. Molecular and clinical findings.* ORL J Otorhinolaryngol Relat Spec, 2002. **64**(5): p. 321-3.
83. Ferraris, A., et al., *Pyrosequencing for detection of mutations in the connexin 26 (GJB2) and mitochondrial 12S RNA (MTRNR1) genes associated with hereditary hearing loss.* Hum Mutat, 2002. **20**(4): p. 312-20.
84. Numakura, C., et al., *Molecular analysis in Japanese patients with Charcot-Marie-Tooth disease: DGGE analysis for PMP22, MPZ, and Cx32/GJB1 mutations.* Hum Mutat, 2002. **20**(5): p. 392-8.
85. Luo, W., et al., *[A new mutation in the connexin 32 gene of a Chinese family with Charcot-Marie-Tooth disease associated with central conduction slowing].* Zhonghua Yi Xue Yi Chuan Xue Za Zhi, 2002. **19**(5): p. 367-9.
86. Street, V.A., et al., *Charcot-Marie-Tooth neuropathy: clinical phenotypes of four novel mutations in the MPZ and Cx 32 genes.* Neuromuscul Disord, 2002. **12**(7-8): p. 643-50.
87. Gabriel, H.D., et al., *Transplacental uptake of glucose is decreased in embryonic lethal connexin26-deficient mice.* J Cell Biol, 1998. **140**(6): p. 1453-61.
88. Kruger, O., et al., *Defective vascular development in connexin 45-deficient mice.* Development, 2000. **127**(19): p. 4179-93.
89. Simon, A.M., et al., *Female infertility in mice lacking connexin 37.* Nature, 1997. **385**(6616): p. 525-9.
90. Li, W.E., et al., *An essential role for connexin43 gap junctions in mouse coronary artery development.* Development, 2002. **129**(8): p. 2031-42.
91. Lampe, P.D. and A.F. Lau, *Regulation of gap junctions by phosphorylation of connexins.* Arch Biochem Biophys, 2000. **384**(2): p. 205-15.
92. Qin, H., et al., *Retroviral delivery of connexin genes to human breast tumor cells inhibits in vivo tumor growth by a mechanism that is independent of significant gap junctional intercellular communication.* J Biol Chem, 2002. **277**(32): p. 29132-8.
93. Evans, W.H. and S. Boitano, *Connexin mimetic peptides: specific inhibitors of gap-junctional intercellular communication.* Biochem Soc Trans, 2001. **29**(Pt 4): p. 606-12.
94. Oyamada, M., et al., *Abnormalities in gap junctions and Ca2+ dynamics in cardiomyocytes at the border zone of myocardial infarcts.* Cell Commun Adhes, 2001. **8**(4-6): p. 335-8.
95. Boitano, S., E.R. Dirksen, and M.J. Sanderson, *Intercellular propagation of calcium waves mediated by inositol trisphosphate.* Science, 1992. **258**(5080): p. 292-5.
96. Hansen, M., et al., *Intercellular calcium signaling induced by extracellular adenosine 5'-triphosphate and mechanical stimulation in airway epithelial cells.* J Cell Sci, 1993. **106 (Pt 4)**: p. 995-1004.
97. Charles, A.C., S.K. Kodali, and R.F. Tyndale, *Intercellular calcium waves in neurons.* Mol Cell Neurosci, 1996. **7**(5): p. 337-53.
98. Charles, A.C., et al., *Intercellular signaling in glial cells: calcium waves and oscillations in response to mechanical stimulation and glutamate.* Neuron, 1991. **6**(6): p. 983-92.

99. Charles, A.C., et al., *Intercellular calcium signaling via gap junctions in glioma cells.* J Cell Biol, 1992. **118**(1): p. 195-201.
100. Enkvist, M.O. and K.D. McCarthy, *Activation of protein kinase C blocks astroglial gap junction communication and inhibits the spread of calcium waves.* J Neurochem, 1992. **59**(2): p. 519-26.
101. Venance, L., et al., *Inhibition by anandamide of gap junctions and intercellular calcium signalling in striatal astrocytes.* Nature, 1995. **376**(6541): p. 590-4.
102. Young, S.H., H.S. Ennes, and E.A. Mayer, *Propagation of calcium waves between colonic smooth muscle cells in culture.* Cell Calcium, 1996. **20**(3): p. 257-71.
103. Xia, S.L. and J. Ferrier, *Propagation of a calcium pulse between osteoblastic cells.* Biochem Biophys Res Commun, 1992. **186**(3): p. 1212-9.
104. D'Andrea, P. and F. Vittur, *Gap junctions mediate intercellular calcium signalling in cultured articular chondrocytes.* Cell Calcium, 1996. **20**(5): p. 389-97.
105. Osipchuk, Y. and M. Cahalan, *Cell-to-cell spread of calcium signals mediated by ATP receptors in mast cells.* Nature, 1992. **359**(6392): p. 241-4.
106. Cao, D., et al., *Mechanisms for the coordination of intercellular calcium signaling in insulin-secreting cells.* J Cell Sci, 1997. **110 (Pt 4)**: p. 497-504.
107. Lynn, B.D., C.A. Marotta, and J.I. Nagy, *Propagation of intercellular calcium waves in PC12 cells overexpressing a carboxy-terminal fragment of amyloid precursor protein.* Neurosci Lett, 1995. **199**(1): p. 21-4.
108. Churchill, G.C., M.M. Atkinson, and C.F. Louis, *Mechanical stimulation initiates cell-to-cell calcium signaling in ovine lens epithelial cells.* J Cell Sci, 1996. **109 (Pt 2)**: p. 355-65.
109. Schlosser, S.F., A.D. Burgstahler, and M.H. Nathanson, *Isolated rat hepatocytes can signal to other hepatocytes and bile duct cells by release of nucleotides.* Proc Natl Acad Sci U S A, 1996. **93**(18): p. 9948-53.
110. Garfield, R.E., et al., *Possible role of gap junctions in activation of myometrium during parturition.* Am J Physiol, 1978. **235**(5): p. C168-79.
111. Pierce, B.T., et al., *Connexin 43 expression in normal versus dysfunctional labor.* Am J Obstet Gynecol, 2002. **186**(3): p. 504-11.
112. Carbillon, L., N. Seince, and M. Uzan, *Myometrial maturation and labour.* Ann Med, 2001. **33**(9): p. 571-8.
113. Kilarski, W.M., et al., *Multiple connexins localized to individual gap-junctional plaques in human myometrial smooth muscle.* Microsc Res Tech, 2001. **54**(2): p. 114-22.
114. Daniel, E.E. and Y.F. Wang, *Control systems of gastrointestinal motility are immature at birth in dogs.* Neurogastroenterol Motil, 1999. **11**(5): p. 375-92.
115. Suzuki, H., *Cellular mechanisms of myogenic activity in gastric smooth muscle.* Jpn J Physiol, 2000. **50**(3): p. 289-301.
116. Thuneberg, L. and S. Peters, *Toward a concept of stretch-coupling in smooth muscle. I. Anatomy of intestinal segmentation and sleeve contractions.* Anat Rec, 2001. **262**(1): p. 110-24.
117. Shinohara, K., et al., *Effects of gap junction blocker on vasopressin and vasoactive intestinal polypeptide rhythms in the rat suprachiasmatic nucleus in vitro.* Neurosci Res, 2000. **38**(1): p. 43-7.
118. Christ, G.J., et al., *Gap junctions in vascular tissues. Evaluating the role of intercellular communication in the modulation of vasomotor tone.* Circ Res, 1996. **79**(4): p. 631-46.

119. Hill, C.E., et al., *Heterogeneity in the distribution of vascular gap junctions and connexins: implications for function.* Clin Exp Pharmacol Physiol, 2002. **29**(7): p. 620-5.
120. Kruger, O., et al., *Altered dye diffusion and upregulation of connexin37 in mouse aortic endothelium deficient in connexin40.* J Vasc Res, 2002. **39**(2): p. 160-72.
121. Hortovanyi, E., et al., *Connexin 43 expression in rat aortic smooth muscle after ovariectomy and hormonal replacement.* Pathol Res Pract, 2001. **197**(2): p. 109-12.
122. Daniel, E.E., *Is the nexus necessary for cell-to-cell coupling of smooth muscle?* J. Membr. Biol, 1976. **28**: p. 207-239.
123. Peracchia, C., *Structural correlates of gap junction permeation.* Int. Rev. Cytol., 1980. **66**: p. 81-146.
124. Loewenstein, W.R., *Junctional intercellular communication in the cell-to-cell membrane channel.* Physiol. Rev., 1981. **61**: p. 829-913.
125. Spray, D.C., *Physiology and pharmacology of gap junctions.* Am J Physiol, 1985. **47**: p. 281-303.
126. Lagaud, G., et al., *The physiology, pathophysiology and therapeutic potential of gap junctions in smooth muscle.* Curr Drug Targets, 2002. **3**(6): p. 427-40.
127. Daniel, E.E. and Y.F. Wang, *Gap junctions in intestinal smooth muscle and interstitial cells of Cajal.* Microsc Res Tech, 1999. **47**(5): p. 309-20.
128. Karicheti, V. and G.J. Christ, *Physiological roles for K+ channels and gap junctions in urogenital smooth muscle: implications for improved understanding of urogenital function, disease and therapy.* Curr Drug Targets, 2001. **2**(1): p. 1-20.
129. Duan, Y.F. and J.H. Liu, *[Intercellular gap junctions in corporal smooth muscle].* Zhonghua Nan Ke Xue, 2002. **8**(2): p. 136-8.
130. Garfield, R.E., et al., *Are gap junctions necessary for cell-to-cell coupling of smooth muscle?: An update.* Can J Physiol Pharmacol, 1992. **70**(4): p. 481-90.
131. Brink, P.R., *Gap junctions in vascular smooth muscle.* Acta Physiol Scand, 1998. **164**(4): p. 349-56.
132. Kannan, M.S. and E.E. Daniel, *Formation of gap junctions by treatment in vitro with potassium conductance blockers.* J Cell Biol, 1978. **78**(2): p. 338-48.
133. Daniel, E.E., et al., *The nature of control over coupling between smooth muscle cells and layers; its contribution to the synchrony of smooth muscle contraction.* Nippon Heikatsukin Gakkai Zasshi, 1978. **14 Suppl**: p. 37-8.
134. Daniel, E.E., et al., *Structure and function of smooth muscle, role of cell-to-cell coupling.* Nippon Heikatsukin Gakkai Zasshi, 1980. **16**(3): p. 125-32.
135. Hurtley, S.M. and A. Helenius, *Protein oligomerization in the endoplasmic reticulum.* Annu Rev Cell Biol, 1989. **5**: p. 277-307.
136. Falk, M.M., *Cell-free synthesis for analyzing the membrane integration, oligomerization, and assembly characteristics of gap junction connexins.* Methods, 2000. **20**(2): p. 165-79.
137. Falk, M.M., *Connexins/connexons. Cell-free expression.* Methods Mol Biol, 2001. **154**: p. 91-116.
138. Falk, M.M., *Biosynthesis and structural composition of gap junction intercellular membrane channels.* Eur J Cell Biol, 2000. **79**(8): p. 564-74.
139. Yeager, M., V.M. Unger, and M.M. Falk, *Synthesis, assembly and structure of gap junction intercellular channels.* Curr Opin Struct Biol, 1998. **8**(4): p. 517-24.

140. Oshima, A., et al., *Roles of Met-34, Cys-64, and Arg-75 in the assembly of human connexin 26. Implication for key amino acid residues for channel formation and function.* J Biol Chem, 2003. **278**(3): p. 1807-16.
141. Cooper, C.D. and P.D. Lampe, *Casein kinase 1 regulates connexin-43 gap junction assembly.* J Biol Chem, 2002. **277**(47): p. 44962-8.
142. Martin, P.E., R.J. Errington, and W.H. Evans, *Gap junction assembly: multiple connexin fluorophores identify complex trafficking pathways.* Cell Commun Adhes, 2001. **8**(4-6): p. 243-8.
143. Ahmad, S. and W.H. Evans, *Post-translational integration and oligomerization of connexin 26 in plasma membranes and evidence of formation of membrane pores: implications for the assembly of gap junctions.* Biochem J, 2002. **365**(Pt 3): p. 693-9.
144. Valiunas, V., R. Weingart, and P.R. Brink, *Formation of heterotypic gap junction channels by connexins 40 and 43.* Circ Res, 2000. **86**(2): p. E42-9.
145. Nagy, J.I. and J.E. Rash, *Connexins and gap junctions of astrocytes and oligodendrocytes in the CNS.* Brain Res Brain Res Rev, 2000. **32**(1): p. 29-44.
146. Vaney, D.I. and R. Weiler, *Gap junctions in the eye: evidence for heteromeric, heterotypic and mixed-homotypic interactions.* Brain Res Brain Res Rev, 2000. **32**(1): p. 115-20.
147. Jordan, K., et al., *Trafficking, assembly, and function of a connexin43-green fluorescent protein chimera in live mammalian cells.* Mol Biol Cell, 1999. **10**(6): p. 2033-50.
148. Saffitz, J.E., J.G. Laing, and K.A. Yamada, *Connexin expression and turnover : implications for cardiac excitability.* Circ Res, 2000. **86**(7): p. 723-8.
149. Hertzberg, E.L., et al., *Topology of the Mr 27,000 liver gap junction protein. Cytoplasmic localization of amino- and carboxyl termini and a hydrophilic domain which is protease-hypersensitive.* J Biol Chem, 1988. **263**(35): p. 19105-11.
150. Yancey, S.B., et al., *The 43-kD polypeptide of heart gap junctions: immunolocalization, topology, and functional domains.* J Cell Biol, 1989. **108**(6): p. 2241-54.
151. Berthoud, V.M., et al., *The gap-junction protein connexin 56 is phosphorylated in the intracellular loop and the carboxy-terminal region.* Eur J Biochem, 1997. **244**(1): p. 89-97.
152. Saez, J.C., et al., *Phosphorylation of connexin 32, a hepatocyte gap-junction protein, by cAMP-dependent protein kinase, protein kinase C and Ca2+/calmodulin-dependent protein kinase II.* Eur J Biochem, 1990. **192**(2): p. 263-73.
153. Traub, O., et al., *Comparative characterization of the 21-kD and 26-kD gap junction proteins in murine liver and cultured hepatocytes.* J Cell Biol, 1989. **108**(3): p. 1039-51.
154. Traub, O., et al., *Immunochemical and electrophysiological characterization of murine connexin40 and -43 in mouse tissues and transfected human cells.* Eur J Cell Biol, 1994. **64**(1): p. 101-12.
155. Warn-Cramer, B.J., et al., *Characterization of the mitogen-activated protein kinase phosphorylation sites on the connexin-43 gap junction protein.* J Biol Chem, 1996. **271**(7): p. 3779-86.
156. Berthoud, V.M., et al., *Connexin43 in MDCK cells: regulation by a tumor-promoting phorbol ester and Ca2+.* Eur J Cell Biol, 1992. **57**(1): p. 40-50.
157. Jongen, W.M., et al., *Regulation of connexin 43-mediated gap junctional intercellular communication by Ca2+ in mouse epidermal cells is controlled by E-cadherin.* J Cell Biol, 1991. **114**(3): p. 545-55.

158. Laird, D.W., K.L. Puranam, and J.P. Revel, *Turnover and phosphorylation dynamics of connexin43 gap junction protein in cultured cardiac myocytes.* Biochem J, 1991. **273(Pt 1)**: p. 67-72.
159. Moreno, A.P., G.I. Fishman, and D.C. Spray, *Phosphorylation shifts unitary conductance and modifies voltage dependent kinetics of human connexin43 gap junction channels.* Biophys J, 1992. **62**(1): p. 51-3.
160. Kwak, B.R., et al., *Effects of cGMP-dependent phosphorylation on rat and human connexin43 gap junction channels.* Pflugers Arch, 1995. **430**(5): p. 770-8.
161. Saez, J.C., *The functional state of gap junctions between neonatal rat cardiac myocytes is directly related to changes in the state of phosphorylation of connexin43.* Journal of Molecular and Cellular Cardiology, 1997. **29**: p. 2131-2145.
162. Oh, S.Y., C.G. Grupen, and A.W. Murray, *Phorbol ester induces phosphorylation and down-regulation of connexin 43 in WB cells.* Biochim Biophys Acta, 1991. **1094**(2): p. 243-5.
163. Reynhout, J.K., P.D. Lampe, and R.G. Johnson, *An activator of protein kinase C inhibits gap junction communication between cultured bovine lens cells.* Exp Cell Res, 1992. **198**(2): p. 337-42.
164. Chanson, M., et al., *Cell uncoupling and protein kinase C: correlation in a cell line but not in a differentiated tissue.* Am J Physiol, 1988. **255**(5 Pt 1): p. C699-704.
165. Lampe, P.D., *Analyzing phorbol ester effects on gap junctional communication: a dramatic inhibition of assembly.* J Cell Biol, 1994. **127**(6 Pt 2): p. 1895-905.
166. Burt, J.M. and D.C. Spray, *Inotropic agents modulate gap junctional conductance between cardiac myocytes.* Am J Physiol, 1988. **254**(6 Pt 2): p. H1206-10.
167. Crow, D.S., et al., *Phosphorylation of connexin43 gap junction protein in uninfected and Rous sarcoma virus-transformed mammalian fibroblasts.* Mol Cell Biol, 1990. **10**(4): p. 1754-63.
168. Swenson, K.I., et al., *Tyrosine phosphorylation of the gap junction protein connexin43 is required for the pp60v-src-induced inhibition of communication.* Cell Regul, 1990. **1**(13): p. 989-1002.
169. Lampe, P.D., et al., *Phosphorylation of connexin43 on serine368 by protein kinase C regulates gap junctional communication.* J Cell Biol, 2000. **149**(7): p. 1503-12.
170. van Veen, T.A., H.V. van Rijen, and H.J. Jongsma, *Electrical conductance of mouse connexin45 gap junction channels is modulated by phosphorylation.* Cardiovasc Res, 2000. **46**(3): p. 496-510.
171. Lazrak, A. and C. Peracchia, *Gap junction gating sensitivity to physiological internal calcium regardless of pH in Novikoff hepatoma cells.* Biophys J, 1993. **65**(5): p. 2002-12.
172. Li, H., et al., *Properties and regulation of gap junctional hemichannels in the plasma membranes of cultured cells.* J Cell Biol, 1996. **134**(4): p. 1019-30.
173. Cotrina, M.L., et al., *Connexins regulate calcium signaling by controlling ATP release.* Proc Natl Acad Sci U S A, 1998. **95**(26): p. 15735-40.
174. Guan, X., et al., *The sleep-inducing lipid oleamide deconvolutes gap junction communication and calcium wave transmission in glial cells.* J Cell Biol, 1997. **139**(7): p. 1785-92.
175. Venance, L., S. Sagan, and C. Giaume, *(R)-methanandamide inhibits receptor-induced calcium responses by depleting internal calcium stores in cultured astrocytes.* Pflugers Arch, 1997. **434**(1): p. 147-9.

176. Chaytor, A.T., et al., *The endothelial component of cannabinoid-induced relaxation in rabbit mesenteric artery depends on gap junctional communication.* J Physiol, 1999. **520 Pt 2**: p. 539-50.
177. Mambetisaeva, E.T., V. Gire, and W.H. Evans, *Multiple connexin expression in peripheral nerve, Schwann cells, and Schwannoma cells.* J Neurosci Res, 1999. **57**(2): p. 166-75.
178. Boitano, S. and W.H. Evans, *Connexin mimetic peptides reversibly inhibit Ca(2+) signaling through gap junctions in airway cells.* Am J Physiol Lung Cell Mol Physiol, 2000. **279**(4): p. L623-30.
179. Takens-Kwak, B.R., et al., *Mechanism of heptanol-induced uncoupling of cardiac gap junctions: a perforated patch-clamp study.* Am J Physiol, 1992. **262**(6 Pt 1): p. C1531-8.
180. Taylor, H.J., et al., *Inhibition of the gap junctional component of endothelium-dependent relaxations in rabbit iliac artery by 18-alpha glycyrrhetinic acid.* Br J Pharmacol, 1998. **125**(1): p. 1-3.
181. Guan, X., et al., *Gap-junction disassembly and connexin 43 dephosphorylation induced by 18 beta-glycyrrhetinic acid.* Mol Carcinog, 1996. **16**(3): p. 157-64.
182. Boger, D.L., et al., *Arachidonic acid amide inhibitors of gap junction cell-cell communication.* Bioorg Med Chem Lett, 1999. **9**(8): p. 1151-4.
183. Zhang, W., et al., *Tamoxifen-induced enhancement of calcium signaling in glioma and MCF-7 breast cancer cells.* Cancer Res, 2000. **60**(19): p. 5395-400.
184. Verrecchia, F. and J. Herve, *Reversible inhibition of gap junctional communication by tamoxifen in cultured cardiac myocytes.* Pflugers Arch, 1997. **434**(1): p. 113-6.
185. Harris, D., et al., *Role of gap junctions in endothelium-derived hyperpolarizing factor responses and mechanisms of K(+)-relaxation.* Eur J Pharmacol, 2000. **402**(1-2): p. 119-28.
186. Boitano, S., E.R. Dirksen, and W.H. Evans, *Sequence-specific antibodies to connexins block intercellular calcium signaling through gap junctions.* Cell Calcium, 1998. **23**(1): p. 1-9.
187. Becker, D.L., et al., *Functional analysis of amino acid sequences in connexin43 involved in intercellular communication through gap junctions.* J Cell Sci, 1995. **108 (Pt 4)**: p. 1455-67.
188. Meyer, R.A., et al., *Inhibition of gap junction and adherens junction assembly by connexin and A-CAM antibodies.* J Cell Biol, 1992. **119**(1): p. 179-89.
189. Isakson, B.E., W.H. Evans, and S. Boitano, *Intercellular Ca2+ signaling in alveolar epithelial cells through gap junctions and by extracellular ATP.* Am J Physiol Lung Cell Mol Physiol, 2001. **280**(2): p. L221-8.
190. Warner, A., et al., *Specific motifs in the external loops of connexin proteins can determine gap junction formation between chick heart myocytes.* J Physiol, 1995. **488 (Pt 3)**: p. 721-8.
191. Dahl, G., W. Nonner, and R. Werner, *Attempts to define functional domains of gap junction proteins with synthetic peptides.* Biophys J, 1994. **67**(5): p. 1816-22.
192. Chaytor, A.T., W.H. Evans, and T.M. Griffith, *Peptides homologous to extracellular loop motifs of connexin 43 reversibly abolish rhythmic contractile activity in rabbit arteries.* J Physiol, 1997. **503 (Pt 1)**: p. 99-110.

193. Chaytor, A.T., W.H. Evans, and T.M. Griffith, *Central role of heterocellular gap junctional communication in endothelium-dependent relaxations of rabbit arteries.* J Physiol, 1998. **508 (Pt 2)**: p. 561-73.
194. Hutcheson, I.R., et al., *Nitric oxide-independent relaxations to acetylcholine and A23187 involve different routes of heterocellular communication. Role of Gap junctions and phospholipase A2.* Circ Res, 1999. **84**(1): p. 53-63.
195. Oviedo-Orta, E., T. Hoy, and W.H. Evans, *Intercellular communication in the immune system: differential expression of connexin40 and 43, and perturbation of gap junction channel functions in peripheral blood and tonsil human lymphocyte subpopulations.* Immunology, 2000. **99**(4): p. 578-90.
196. Oviedo-Orta, E., P. Gasque, and W.H. Evans, *Immunoglobulin and cytokine expression in mixed lymphocyte cultures is reduced by disruption of gap junction intercellular communication.* Faseb J, 2001. **15**(3): p. 768-74.
197. Burt, J.M., K.D. Massey, and B.N. Minnich, *Uncoupling of cardiac cells by fatty acids: structure-activity relationships.* Am J Physiol, 1991. **260**(3 Pt 1): p. C439-48.
198. Lavado, E., et al., *Oleic acid inhibits gap junction permeability and increases glucose uptake in cultured rat astrocytes.* J Neurochem, 1997. **69**(2): p. 721-8.
199. Dahl, G., et al., *Cell/cell channel formation involves disulfide exchange.* Eur J Biochem, 1991. **197**(1): p. 141-4.
200. Sanderson, M.J., A.C. Charles, and E.R. Dirksen, *Mechanical stimulation and intercellular communication increases intracellular Ca2+ in epithelial cells.* Cell Regul, 1990. **1**(8): p. 585-96.
201. Sanderson, M.J., et al., *Mechanisms and function of intercellular calcium signaling.* Mol Cell Endocrinol, 1994. **98**(2): p. 173-87.
202. Harden, T.K., J.L. Boyer, and R.A. Nicholas, *P2-purinergic receptors: subtype-associated signaling responses and structure.* Annu Rev Pharmacol Toxicol, 1995. **35**: p. 541-79.
203. Pearson, R., et al., *Purinergic and muscarinic modulation of the cell cycle and calcium signaling in the chick retinal ventricular zone.* J Neurosci, 2002. **22**(17): p. 7569-79.
204. Kaiser, R.A., et al., *Functional compartmentation of endothelial P2Y receptor signaling.* Circ Res, 2002. **91**(4): p. 292-9.
205. Moccia, F., et al., *P2y1 and P2y2 receptor-operated Ca2+ signals in primary cultures of cardiac microvascular endothelial cells.* Microvasc Res, 2001. **61**(3): p. 240-52.
206. Ou, C.W., A. Orsino, and S.J. Lye, *Expression of connexin-43 and connexin-26 in the rat myometrium during pregnancy and labor is differentially regulated by mechanical and hormonal signals.* Endocrinology, 1997. **138**(12): p. 5398-407.
207. Geimonen, E., et al., *Activation of protein kinase C in human uterine smooth muscle induces connexin-43 gene transcription through an AP-1 site in the promoter sequence.* J Biol Chem, 1996. **271**(39): p. 23667-74.
208. Weichselbaum, M., A.W. Everett, and M.P. Sparrow, *Mapping the innervation of the bronchial tree in fetal and postnatal pig lung using antibodies to PGP 9.5 and SV2.* Am J Respir Cell Mol Biol, 1996. **15**(6): p. 703-10.
209. Akiho, H., et al., *Role of IL-4, IL-13, and STAT6 in inflammation-induced hypercontractility of murine smooth muscle cells.* Am J Physiol Gastrointest Liver Physiol, 2002. **282**(2): p. G226-32.

210. Laemmli, U.K., *Cleavage of structural proteins during the assembly of the head of bacteriophage T4.* Nature, 1970. **227**(259): p. 680-5.
211. McNeil, P.L., et al., *A method for incorporating macromolecules into adherent cells.* J Cell Biol, 1984. **98**(4): p. 1556-64.
212. Goldberg, G.S., et al., *Evidence that disruption of connexon particle arrangements in gap junction plaques is associated with inhibition of gap junctional communication by a glycyrrhetinic acid derivative.* Exp Cell Res, 1996. **222**(1): p. 48-53.
213. Kolomytkin, O.V., et al., *IL-1beta-induced production of metalloproteinases by synovial cells depends on gap junction conductance.* Am J Physiol Cell Physiol, 2002. **282**(6): p. C1254-60.
214. Muller, D.J., et al., *Conformational changes in surface structures of isolated connexin 26 gap junctions.* Embo J, 2002. **21**(14): p. 3598-607.
215. Pfahnl, A. and G. Dahl, *Gating of cx46 gap junction hemichannels by calcium and voltage.* Pflugers Arch, 1999. **437**(3): p. 345-53.
216. Cortina, M.L., *Astrocytic gap junctions remain open during ischemic conditions.* J. Neurosci., 1998. **18**: p. 2520-2537.
217. John, S.A., et al., *Connexin-43 hemichannels opened by metabolic inhibition.* J Biol Chem, 1999. **274**(1): p. 236-40.
218. DeVries, S.H. and E.A. Schwartz, *Hemi-gap-junction channels in solitary horizontal cells of the catfish retina.* J Physiol, 1992. **445**: p. 201-30.
219. Guo, Y., et al., *Inhibition of gap junction communication in alveolar epithelial cells by 18alpha-glycyrrhetinic acid.* Am J Physiol, 1999. **276**(6 Pt 1): p. L1018-26.
220. Shimada, M., T. Maeda, and T. Terada, *Dynamic changes of connexin-43, gap junctional protein, in outer layers of cumulus cells are regulated by PKC and PI 3-kinase during meiotic resumption in porcine oocytes.* Biol Reprod, 2001. **64**(4): p. 1255-63.
221. John, H., et al., *[Gap junctions in the human urinary bladder].* Aktuelle Urol, 2003. **34**(5): p. 328-32.
222. Young, R.C., R. Schumann, and P. Zhang, *The signaling mechanisms of long distance intercellular calcium waves (far waves) in cultured human uterine myocytes.* J Muscle Res Cell Motil, 2002. **23**(4): p. 279-84.
223. Jimenez, M., et al., *Slow waves in circular muscle of porcine ileum: structural and electrophysiological studies.* Am J Physiol, 1999. **276**(2 Pt 1): p. G393-406.
224. Gibbs, C.J., et al., *Premenstrual exacerbation of asthma.* Thorax, 1984. **39**(11): p. 833-6.
225. Hu, J. and I.A. Cotgreave, *Differential regulation of gap junctions by proinflammatory mediators in vitro.* J Clin Invest, 1997. **99**(10): p. 2312-6.
226. Wang, H., B. Chang, and B. Wang, *[The effect of herbal medicine including astragalus membranaceus (fisch) bge, codonpsis pilosula and glycyrrhiza uralensis fisch on airway responsiveness].* Zhonghua Jie He He Hu Xi Za Zhi, 1998. **21**(5): p. 287-8.